

EFFECT OF BASE IMPURITY DISTRIBUTION
ON THE FIGURE OF MERIT OF TRANSISTORS

A THESIS

SUBMITTED IN PARTIAL FULFILMENT OF
THE REQUIREMENTS FOR THE DEGREE OF

DOCTOR OF PHILOSOPHY

IN THE
FACULTY OF ENGINEERING AND TECHNOLOGY

BY

Laxmi Kant Maheshwari

Department of Electrical and Electronics Engineering
BIRLA INSTITUTE OF TECHNOLOGY AND SCIENCE
PILANI (RAJASTHAN)
1971

CERTIFICATE

The study and work on 'Effect of Base Impurity Distribution on the Figure of Merit of Transistors', carried out and presented herein, by Mr. L.K. Maheshwari, embodies original investigations. It is recommended that the thesis be accepted in partial fulfilment of the requirements for the degree of Doctor of Philosophy in the Department of Electrical and Electronics Engineering of the Faculty of Engineering and Technology of the Birla Institute of Technology and Science, Pilani.

Supervisor of Thesis :

K.V. Ramanan
(K.V. Ramanan)
Professor and Head,
E.E.E. Department,
B.I.T.S., Pilani.

ACKNOWLEDGEMENTS

The author wishes to express his sincere gratitude to his thesis supervisor Prof. K.V. Ramanan, Head, Department of Electrical and Electronics Engineering, Birla Institute of Technology and Science, Pilani, for his excellent guidance and continuous interest in this work.

This work was supported by a full time research fellowship of the Birla Institute of Technology and Science, Pilani, for which the author is grateful to the Director, B.I.T.S. and the Dean, Faculty of Engineering and Technology.

The author is thankful to Dr. H.C. Miera, Professor in Civil Engineering Department, for many discussions regarding the numerical computations. The author wishes to thank Prof. M.M. Mukherjee, Head, Information Processing Centre, B.I.T.S., for extending the computer facilities. Assistance of the staff of I.P.C. is also sincerely acknowledged. Helpful discussions with Dr. P.K. Raman, Assistant Professor, Department of Mathematics and with Dr. W.S. Khokle, Scientist, C.E.E.R.I., Pilani, are also acknowledged. The author wishes to thank Mr. H.C. Mehta, the Librarian, and his staff for their assistance in procuring the required reference material in the shortest time.

The author is thankful to his colleague Mr. R.K. Gupta for his help at many stages, to Mr. P.L. Mehta for typing the manuscript and to Mr. K.N. Sharma for preparation of figures.

L.K. Maheshwari
(L.K. Maheshwari)

ABSTRACT

The improved performance of present-day semiconductor devices is achieved principally because such solid state-diffusion techniques as the planar process permit close control of junction depths, base width, and surface geometry. But the performance could be further improved if it were possible to optimise the impurity profile in the semiconductor material. It is a well known fact that the minority carrier base transit time is very much dependent on the base region impurity profile. Several investigations have been undertaken in the past to obtain optimum impurity profiles for minimum base transit time.

Base transit time is only one of the performance characteristics of the device. It is reasonable to expect that other criterion would lead to requirements for different base impurity profiles. A true index of the high frequency capability of a transistor is provided by the parameter - Figure of Merit. In recent years some attempts have been made to study the influence of base doping on figure of merit. Since the criterion for optimum figure of merit includes factors other than the base transit-time such as the total impurity content in the base and collector-base junction capacitance, it is logical to predict that the optimum impurity profiles which yield minimum base transit time may not be suitable from the view point of achieving optimum figure of merit. It is this expectation which motivated the present investigation that deals with the effect of base region doping distribution on the figure of merit of bipolar transistors.

The effect of base impurity distribution on minority carrier transit time - a constituent component in the figure of merit expression of the intrinsic device - is studied in detail. Optimum impurity distributions for minimum base transit time have been derived from two different approaches - the Field approach and the Stored charge approach. The electric field approach which has been suggested for the first time in this investigation is more appropriate if field-dependent mobility and device operation under moderate to high injection level have to be considered.

Since most devices have graded base with impurity-density varying two to three magnitudes over the base region, it is necessary to consider the spatial variation of the mobility and of the diffusion coefficient. Using the different available empirical relations of mobility dependence on doping, optimum impurity distributions have been derived by variational method. It is found that the optimum profile depends upon the particular mobility relation used. Electric field, minority carrier profiles and transit time have been evaluated for different impurity profiles.

By considering a special form of distribution, it is established that optimum impurity distributions do not necessarily offer a unique minimum in transit-time. It is concluded that the variational method is applicable only to a restricted class of smooth distributions. Impurity distributions and field configurations having a point of inflection, a corner or a discontinuity are not amenable to treatment by the variational method.

The above observed fact motivated an attempt to synthesise typical impurity distributions which may yield low transit-times. For the purpose of such a synthesis, a new technique called the segmentation technique has been adopted. Two segment distributions have been synthesised by combining segments of standard distributions. Some of these synthesised profiles are found to yield much lower base transit-time as compared with the optimum distributions based on variational method. A judicious combination of segments of impurity distributions which lead to faster and slower carrier transit, yields an overall transit time which is lower than that obtained for optimum profiles.

It has been observed that the synthesised profiles yielding low transit-times have typical electric field configurations in the base. This prompted an attempt to synthesise built-in field configurations which will yield minimum transit-time. Synthesis of two and three segment field configurations has been attempted and the corresponding impurity distributions have been derived. This study reveals the fact that considerable improvement in transit time can be achieved if there is a retarding field over a small portion of the base. Improvement in base transit-time upto the extent of 20 per cent can be achieved as compared with the optimum profiles.

A detailed study of the effect of base impurity distribution on figure of merit indicates that optimum doping distributions which yield minimum base transit-time do not necessarily give rise to improved figure of merit. On the contrary, some synthesised profiles which do not yield low transit-time are found to exhibit

a much higher figure of merit. The best improvement in figure of merit has been obtained in the case of doping distributions which give rise to retarding fields over a portion of the base region. This improvement is achieved without adversely affecting the emitter-base junction capacitance. Such distributions exhibit improvement both in transit-time and in figure of merit. This conclusion is interesting as it is contrary to the general impression that impurity profiles presenting a retarding field over a portion of the base cause deterioration both in transit time and figure of merit.

The theoretical conclusions of this investigation should find practical application in the design of devices without much difficulty. Recent attempts by some investigators have shown that it is possible to have tailor-made impurity profiles in semiconductor materials. By treating the problem of diffusion as an optimal control problem, it is possible to obtain a best-fit approximation to a given profile by controlling the gas stream impurity concentration. The current industrial practice restricts the profile only to two types - complementary error function and Gaussian - which is a serious limitation on the realisation of improved device performance characteristics. Once given the physical capability of obtaining any desired impurity profile and given the knowledge as to which profiles are necessary for optimising a particular performance characteristic, one can design optimum devices by using the proper profile in the fabrication of the device. It is hoped that the present investigation is a pointer in this new direction of device design.

+++++

TABLE OF CONTENTS

	<u>Page</u>
CERTIFICATE	ii
ACKNOWLEDGEMENTS	iii
ABSTRACT	iv
LIST OF SYMBOLS	xi
CHAPTER 1. INTRODUCTION	1-14
1.1 Historical synopsis	2
1.2 Outline of present investigation	8
References	11
CHAPTER 2. OPTIMUM IMPURITY DISTRIBUTIONS FOR MINIMUM BASE TRANSIT TIME THROUGH VARIATIONAL METHOD	15-38
2.1 Introduction	16
2.2 Optimum impurity distribution for minimum base transit time - Electric field approach	17
2.3 Optimum impurity distributions for minimum base transit time - Stored charge approach	23
2.4 Summary and discussion	35
References	37
CHAPTER 3. EFFECT OF IMPURITY DISTRIBUTION ON MINORITY CARRIER BASE TRANSIT TIME	39-104
3.1 Introduction	40
3.2 Basic impurity distribution in the base	41
3.3 Built-in electric field in the base	44
3.4 Excess minority carrier concentration in the base	46
3.5 Minority carrier base transit time when mobility is constant	62

3.6	Influence of doping dependent carrier mobility on base transit time	63
3.7	Special form of base impurity distribution	92
3.8	Summary and discussion	99
	References	103
CHAPTER 4. IMPURITY DISTRIBUTIONS FOR MINIMUM BASE TRANSIT TIME THROUGH SEGMENTATION TECHNIQUE		105-121
4.1	Introduction	106
4.2	Synthesis of typical base impurity distributions	107
4.3	Built-in electric field in the base	111
4.4	Excess minority carrier concentration in the base	113
4.5	Base transit time	115
4.6	Summary and discussion	121
CHAPTER 5. BUILT-IN ELECTRIC FIELD CONFIGURATIONS FOR MINIMUM BASE TRANSIT TIME THROUGH SEGMENTATION TECHNIQUE		122-146
5.1	Introduction	123
5.2	Synthesis of electric field configurations - two segments	123
5.3	Synthesis of electric field configurations - three segments	137
5.4	Summary and discussion	146
CHAPTER 6. EFFECT OF BASE IMPURITY DISTRIBUTION ON THE FIGURE OF MERIT OF TRANSISTORS		147-181
6.1	Introduction	148
6.2	General expression for figure of merit	149
6.3	Evaluation of figure of merit for basic impurity distributions	155

6.4	Evaluation of figure of merit for impurity distributions synthesised through segmentation technique	161
6.5	Evaluation of figure of merit for impurity distributions derived from synthesised base region electric field configurations	163
6.6	Remarks about the validity of f_T approximation	175
6.7	Summary and discussion	178
	References	180
CHAPTER 7.	SUMMARY, CONCLUDING REMARKS AND SCOPE FOR FURTHER WORK	182-190
7.1	Summary	183
7.2	Concluding remarks - feasibility of obtaining general impurity distributions	187
7.3	Scope for further work	188
	References	190
APPENDICES		191-210
Appendix-I.	Derivation of the first integral of Euler equation	192
Appendix-II.	Evaluation of nonlinear equation by Newton-Raphson method	193
Appendix-III.	Computer program for the evaluation of transit time - constant mobility case	195
Appendix-IV.	Computer program for the evaluation of transit time - doping dependent mobility case	200
Appendix-V.	Evaluation of C-B junction capacitance for arbitrary impurity distribution in the base	206

LIST OF SYMBOLS

a	--	Impurity gradient at the collector junction
a_{exp}	--	Linear grade constant for exponential doping distribution
a_N	--	Linear grade constant for arbitrary doping distribution
a_1	--	Width of C-B depletion layer in the base region
a_2	--	Width of the C-B depletion layer in the collector region
A	--	Cross-sectional area
C_c	--	Collector depletion-layer capacitance
C_e	--	Emitter depletion-layer capacitance
$C_c(exp)$	--	Collector depletion-layer capacitance for an exponential doping distribution in the base
$C_c(N)$	--	Collector depletion-layer capacitance for an arbitrary doping distribution in the base
D	--	Carrier diffusion coefficient
D_n	--	Electron diffusion coefficient
D_p	--	Hole diffusion coefficient
D_o	--	Reference value of D_p corresponding to the emitter end impurity ^p concentration N_o in the base
D_w	--	Reference value of D_p corresponding to the collector end impurity concentration N_w in the base
D_{avg}	--	Reference value of D_p corresponding to the average impurity concentration in the base
D_R	--	Reference value of D_p , when net impurity density is N_R .
$E, E(X)$	--	Electric field in the base region, caused by impurity density distribution
E_1	--	Electric field in the base side of C-B depletion layer

E_2	--	Electric field in the collector side of the C-B depletion layer
f	--	A function
f_T	--	Unity current gain frequency
f_{max}	--	Maximum frequency of oscillation
F	--	Figure of merit
F'	--	Modified figure of merit
FM	--	Figure of Merit of transistors
$FM(exp)$	--	Figure of Merit of a transistor having exponential doping in the base
$FM(N)$	--	Figure of Merit of a transistor having any arbitrary impurity distribution $N(x)$ in the base
h_{fe}	--	Common emitter forward current transfer ratio
I_e	--	d.c. emitter current
I_p	--	Hole current in the base
I_n	--	Electron current in the base
J_p	--	Hole current density
J_n	--	Electron current density
k	--	Relative dielectric constant of semiconductor
K	--	Boltzmann's constant
n	--	Electron concentration
$N, N(x), N(X)$	--	Impurity density distribution in the base region
$N_I, N_I(X)$	--	Impurity density distribution in region-I of the base for two and three segment distributions
$N_{II}, N_{II}(X)$	--	Impurity density distribution in region-II of the base for two and three segment distributions
$N_{III}, N_{III}(X)$	--	Impurity density distribution in region-III of the base for three segment distributions
N_0	--	Impurity density at emitter end of the base

- N_w -- Impurity density at collector end of the base
- N_s -- Impurity density at $X = s$ in the base
- N_1 -- Impurity density at $X = p_1$ in the base
- N_2 -- Impurity density at $X = p_2$ in the base
- N_{exp} -- Exponential doping distribution in the base
- $N_{exp}(X)$
- $N_N, N_N(X)$ -- Arbitrary doping distribution in the base
- N_R, N_{ref} -- Reference impurity density in the base
- N_o' -- Surface concentration of impurities for projected hyperbolic distribution in region-II of the base
- N_{o1} -- Surface concentration of impurities for projected Gaussian distribution in region-II of base
- N_B -- Background impurity concentration in the collector
- $p, p(x)$ -- Excess minority carrier hole concentration in the base
- p_1 -- X-coordinate of the first intersection point in the base for three segment impurity distributions
- p_2 -- X-coordinate of the second intersection point in the base for three segment impurity distributions
- q -- Charge of an electron
- Q_e -- Total stored charge in the base
- r_b' -- Base resistance
- $r_b'(exp)$ -- Base resistance when exponential doping is assumed in base
- $r_b'(N)$ -- Base resistance when any arbitrary doping is assumed in base
- r_{sc} -- Collector series resistance
- s -- X-coordinate of the intersection point in the base for two segment distributions
- t_B -- Minority carrier base transit time
- t_C -- Collector charging time

t_D	--	Collector depletion layer transit time
t_E	--	Emitter time constant
t_{ec}	--	Emitter to collector delay time
t_{BU}	--	Base transit time of a uniform base transistor
$t_{B0}, t_{BW}, t_{B_{avg}}$	--	Base transit times of a uniform base transistor having constant dopings corresponding to N_0, N_W and average impurity concentration in the base
$t_B(\text{exp})$	--	Base transit time when base is exponentially doped
$t_B(N)$	--	Base transit time when arbitrary doping is used in base
T	--	Temperature in degrees Kelvin
U	--	A function of X
$v, v(x)$	--	Velocity of minority carriers in base
v_{sc}	--	Scatter limited velocity of carriers
V	--	A function of X
V_1	--	Voltage drop at the L.H.S. of the C-B depletion layer
V_2	--	Voltage drop at the R.H.S. of the C-B depletion layer
V_B	--	Total voltage drop across the C-B depletion layer
W	--	Electrical base width
x	--	Position in the base region
x_j	--	Junction depth
x_m	--	C-B depletion layer thickness
λ	--	Normalised distance (x/W)
y	--	y -space coordinate
α	--	A dimensionless parameter
β	--	A parameter used in complementary error function distribution

γ	--	A parameter used in Marshak's optimum distribution
ϵ_0	--	Permittivity of free space
η	--	Base electric field parameter
η_1, η_2, η_3	--	Electric field parameters of region-I, II and III in the base for two and three segment impurity distributions
η'	--	Electric field parameter corresponding to hyperbolic distribution in region-II of the base
θ	--	Parameter in Sugano and Koshiga's functional definition of doping dependent mobility and diffusion coefficient
μ_n	--	Electron mobility
μ_p	--	Hole mobility
μ_{max}	--	Maximum value of mobility
μ_{min}	--	Minimum value of mobility
ρ	--	Net charge density

+++++

CHAPTER 1

I N T R O D U C T I O N

1.1 HISTORICAL SYNOPSIS

1.2 OUTLINE OF PRESENT INVESTIGATION

REFERENCES

CHAPTER 1

I N T R O D U C T I O N1.1 HISTORICAL SYNOPSIS

Since the invention of transistor by Bardeen and Brattain in 1948, attempts have been regularly made to increase its frequency capabilities. In the case of alloy transistors, the main frequency limitation comes into play due to the base-width. Hence the normal procedure used to increase the high frequency range of such transistors is to reduce the base-width. However, the decrease in the base-width also increases the base resistance and this increase in base resistance proves detrimental for high frequency operation. In order to bring the base resistance to its original value, the base resistivity is decreased. This in turn causes an increase in the collector transition capacitance and a decrease in the collector-base breakdown voltage. A more serious limitation occurs due to the phenomenon of 'Punch-through'. As the base width of the transistor is decreased, the collector depletion layer occupies whole of the base region, for a relatively low collector-base junction voltage causing a short between emitter to collector. This process of improving the high frequency behaviour by decreasing base width and base resistivity has been followed for the conventional low-frequency alloy transistors.

To avoid the limitations on base resistivity and base width, which affect the C-B breakdown voltage, it is necessary

to modify the physical structure of the transistor from the simple uniform-base model. One such attempt was made by Early¹ in the introduction of PNIP, or intrinsic-base transistor. The other major attempt was the graded base or drift transistor described by Krömer². The frequency characteristics of these structures were much improved. The PNIP structure proved cumbersome when actual fabrication was taken up. The introduction of I-layer was a problem. On the other hand, with the advent of solid-state diffusion techniques³, the non-uniform impurity distribution required in the graded base transistor was obtained as a byproduct. The non-uniform impurity distribution introduces a built-in electric field in the base region. This electric field effectively decreases the base transit time of the injected minority carriers and provides an increase in the cut-off frequency for a given base thickness.

In drift transistors, the impurity concentration in the base is maximum at the emitter end, and decreases towards the collector end. The lower concentration at the collector end reduces the collector capacitance and increases the C-B breakdown voltage, while the higher concentration at the emitter end results in a higher value of emitter transition capacitance. The increase in capacitance affects the high frequency performance in two principal ways: it lowers input impedance and it robs current from the injecting emitter. The higher concentration at the emitter end simultaneously leads to a smaller base resistance and the problem of punch-through is virtually eliminated.

As a result of the mutual effects of these various factors, there is an optimum frequency of operation for a particular transistor design. There are two high-frequency figures of merit which have received wide acceptance and usage for describing the high frequency performance capabilities of transistors.⁴ These are f_T , the frequency at which magnitude of $h_{fe} = 1$, and f_{max} , the maximum frequency of oscillation. Both these quantities characterizing the high frequency capabilities of transistors possess the following properties.

1. These quantities describe only the properties of the transistor and do not depend on the parameters of the circuit elements external to the transistor.
2. They have a sufficiently clear physical significance and can be measured with ease.

The characteristic frequency f_T is defined as the frequency at which the common emitter short-circuit, forward current transfer-ratio h_{fe} equals unity. It is related to the reciprocal of the emitter to collector delay time t_{ec} by the following expression⁵

$$f_T = \frac{1}{2\pi t_{ec}}$$

The maximum frequency of oscillation, f_{max} , is the highest frequency at which the transistor can be made to oscillate.

The maximum available power gain (MAG) is unity at this frequency. The mathematical relation describing f_{max} is⁶⁻⁸

$$f_{\max} = \sqrt{\frac{f_T}{8\pi r_b' C_c}}$$

where r_b' and C_c are the base resistance and collector capacitance, respectively.

The effect of base impurity distribution on the figure of merit has been studied in the past. Moll and Ross⁹, and Fedotov¹⁰ for the first time initiated such a study. Mathematical relations for base transit time, ohmic base resistance, etc., were derived for any arbitrary base impurity distribution. Tanenbaum and Thomas¹¹, and Lee¹² reported the formation and analysis of a high-frequency diffused base transistor. Fedotov¹³ studied the frequency characteristics of junction transistors. Armstrong¹⁴ presented the procedure of calculating current gain for transistors having an arbitrary impurity distribution in the base region. Kennedy and Murley^{15,16} published the calculations of injection and base transport characteristics of a diffused transistor. Beun and Tummers¹⁷ described the behaviour of alloy transistors with increasing frequency. The authors concluded that three principal factors limit the frequency range of a transistor: (1) the characteristic frequency $2D/W^2$, where D equals the minority carrier diffusion constant in the base and W equals the electrical base width, (2) the capacitance of the collector junction, (3) the internal base resistance.

In an excellent study, Vernerin¹⁸ defined the base transit time on the basis of stored charge method of transistor analysis. Through a qualitative high frequency transit analysis, it was

shown by him that shorter base transit time can result if retarding field impurity distributions are used in the base. The decrease in transit time is due to the possibility of reducing base thickness for such distributions. Kawamura¹⁹ calculated the current gain for a double diffused transistor having retarding field over a portion of the whole base width. It was shown that the current gain can fall by 15 to 20% of its original value due to the presence of the retarding field in the base. Shagurin²⁰ studied the effect of retarding field on the transport properties of double diffused transistors.

In order to achieve smaller base transit time in drift transistors, the emitter end impurity concentration should be kept high, but this high value of impurity concentration affects the minority carrier mobility. The influence of doping dependent mobility on the frequency properties of transistors was studied by Sugano and Koshiga²¹, Pritchard²² and Beale²³. The impurity distribution in the base was assumed to be exponential for this study. Das and Boothroyd²⁴, and Boothroyd and Trofimenkoff²⁵ determined the physical parameters of diffusion and drift transistors. For drift structures, single and double diffused structures were assumed. The variation of mobility with doping density was also considered in this study. Later on, Thomas and Boothroyd²⁶ continued this study. A new model for the base impurity distribution was investigated and the physical parameters of the device were determined by using the proposed model. Yansai, et al.²⁷ presented a new treatment in which the uniform-base transistor

was treated as the limiting case of the graded-base transistor. Based on this approach, they proved the validity of stored charge definition of base transit time. Asnar²⁸ provided a new definition for the base transit time based on the simultaneous effect of diffusion, drift and recombination in the base. Tada and Yanai²⁹ attempted to investigate the charge control analysis of transistor cut-off frequency with a general approach and verified that the conventional method of calculating f_T from base transit time was valid. Both Varnerin's and Ashar's transit time definitions were considered by him. The effect of emitter barrier capacitance on f_T of drift transistor was studied by Maeda, Imai and Furumoto³⁰. The same authors in another paper³¹ obtained the high frequency figure of merit $F = f_T/r_b' C_c$ from the expression of available power gain. This figure of merit indicates that the performance of transistors is independent of the circuit conditions. In another paper by Maeda, Imai and Furumoto³², the design considerations of base impurity distribution for high-frequency figure of merit of transistors were discussed. A new form of figure of merit $F' = f_T/r_b'$ was investigated. The base impurity distributions were conceived in such a way that collector capacitance did not affect the figure of merit. It was found that under certain conditions the retarding field gives a maximum value for the figure of merit F' .

Bogachev³³ and Marshak³⁴ derived optimum impurity distributions for minimum base transit time by making use of the

method of calculus of variations. The minority carrier mobility was assumed to vary with doping density. Bogachev obtained a hyperbolic distribution while Marshak derived another distribution function. When carrier mobility was constant, exponential distribution was observed to be optimum for minimum base transit time^{33,35}.

1.2 OUTLINE OF PRESENT INVESTIGATION

Previous investigations outlined above indicate that the minority carrier base transit time is very much dependent on the base region impurity distribution. The distribution can be optimised to yield minimum transit time. Base transit time is but one of the performance characteristics of the transistor. It is reasonable to expect that optimisation of other performance characteristics like the figure of merit would lead to different impurity distributions. It is this expectation which has motivated the present investigation reported here.

The major objective of the present investigation is to study the effect of different impurity distributions on the minority carrier transit time^{and} the figure of merit of transistors, and thereby arrive at an optimum doping distribution which significantly improves the above parameters. The analysis is confined to a one dimensional p-n-p junction transistor operating at low injection levels, but the results are equally valid for an n-p-n transistor operating under same conditions. The computed results of transit time and figure of merit are presented in a normalised manner.

In Chapter 2, the method of deducing optimum doping distributions for minimum base transit time through variational method is discussed. Two approaches - the Electric field approach and the Stored charge approach - are used for this purpose. For different empirical relations of doping dependent mobility, optimum impurity distributions are derived. It is found that under the assumption of constant mobility, both the approaches yield identical distribution functions for minimum base transit time.

Chapter 3 is devoted to the evaluation of built-in electric field, minority carrier profiles and base transit time for different impurity distributions. Both constant and doping dependent mobility and diffusion coefficient are considered. Different empirical relations of mobility are discussed. The doping dependent mobility affects the dependence of base transit time on the field factor in an interesting manner. This has also been studied in detail. A special form of base doping distribution is also synthesised. The evaluated results of transit time in this case lead to the conclusion that the optimum impurity distributions do not necessarily yield a unique minimum in base transit time. It is pointed out that the variational method of deducing optimum impurity distributions for minimum transit time is restricted to a class of smooth curves.

A new technique called the segmentation technique is used to synthesise impurity distributions having a corner or a point of inflection. This is done in Chapter 4. Computations of

built-in electric field, excess carrier concentration and base transit time are carried out for the synthesised profiles. It is shown that a judicious combination of faster and slower segments of impurity distributions can yield lower values of transit times as compared with those obtained in the case of optimum distributions.

In Chapter 5, an attempt has been made to synthesise two segment and three segment built-in electric field configurations through segmentation technique. The corresponding impurity distributions are also derived and calculations of minority carrier concentration and base transit time are made. It is observed that low values of transit time are obtained for impurity distributions which present a retarding field over a small portion of the base. The influence of mobility variation on transit time is also studied.

The normalised figure of merit is defined in Chapter 6. The effect of different base impurity distributions on this figure of merit is studied in detail and it is found that a significant improvement in figure of merit is possible if the impurity distributions providing retarding field over a small portion of the whole base are used. It is also observed that an optimum distribution which leads to a minimum in transit time does not necessarily give rise to an improvement in the figure of merit.

Chapter 7 contains the summary, concluding remarks about the practical feasibility of obtaining general impurity distributions and scope for further work.

REFERENCES

1. J.M. Early, 'P-N-I-P and N-P-I-N Junction Transistor Triodes', Bell. Sys. Tech. J., Vol. 33, pp. 517-533, 1954.
2. H. Kromer, 'The Drift Transistor', in Transistors I, RCA Labs., Princeton, New Jersey, pp. 202-220, 1956.
3. F.M. Smits, 'Formation of Junction Structures by Solid-State Diffusion', Proc. IRE, Vol. 46, No.6, p. 1049, 1958.
4. L.P. Hunter, 'Hand Book of Semiconductor-Electronics', McGraw-Hill Book Co., New York, 3rd edition, 1970, Sec.12
5. J.L. Moll, 'Physics of Semiconductors', McGraw-Hill Book Co., New York, 1964, Ch. 8.
6. J. Lindmayer and C. Wrigley, 'Fundamentals of Semiconductor Devices', D. Van Nostrand Co., Inc., New York, 1965, Ch. 5.
7. R.L. Pritchard, 'High-Frequency Power Gain of Junction Transistors', Proc. IRE, Vol. 43, pp. 1075-1085, 1955.
8. A.B. Phillips, 'Transistor Engineering', McGraw-Hill Book Co., New York, 1962.
9. J.L. Moll, and I.M. Ross, 'The dependence of transistor parameters, on the distribution of Base Layer Resistivity', Proc. IRE, Vol. 44, pp. 72-78, 1956.
10. Ya. A. Fedotov, 'The effect of the distribution of impurities in the base of drift transistors on their frequency characteristics,' Radio tekhn. i Elektr., Vol. 2, pp. 1261-1270, 1957, English Translation - Radio Engg. Electron. Phys.
11. M. Tanenbaum and D.E. Thomas, 'Diffused Emitter and Base Silicon Transistors', Bell Sys. Tech. J., Vol. 35, pp. 1-22, 1956.

12. C.A. Lee, 'A High-frequency Diffused-Base Germanium Transistors,' Bell Sys. Tech. J., Vol. 35, p. 23, 1956.
13. Ya. A. Fedotov, 'Frequency Characteristics of Junction Transistors', Radio Tekh. i Elektr., Vol. 2, pp. 1189-1199, 1957.
14. H.L. Armstrong, 'On calculating the current gain of Junction Transistors with arbitrary doping', Trans. IRE, Vol. ED-6, pp. 1-5, 1959.
15. D.P. Kennedy and P.C. Murley, 'Minority Carrier Injection Characteristics of the Diffused Emitter Junction', Trans. IRE, Vol. ED-9, pp. 136-142, 1962.
16. D.P. Kennedy and P.C. Murley, 'Base Region Transport Characteristics of a Diffused Transistor', JAP, Vol. 33, pp. 120-125, 1962.
17. Beun, M. and Tummers, L.J., 'The Behaviour of Transistors with increasing Frequency', Phillips Technical Review, 25, pp. 156-76, 1963/1964.
18. L.J. Varnerin, 'Stored Charge Method of Transistor Base Transit Analysis', Proc. IRE, Vol. 47, pp. 523-527, 1959.
19. N. Kawamura, 'Investigation of current gain of drift Transistor having retarding field', NEC Research Development Reports, Japan, No.6, pp. 44-52, 1963.
20. I. Shagurin, 'Effect of the Retarding Field in the Base of a Drift Transistor on the Transfer Coefficient of Minority Carriers', IZV. V.U.Z., Radio Elektronika, Vol. 11, pp. 603-607, 1968.
21. T. Sugeno and F. Koshiga, 'The Calculation of cut-off Frequency of Minority-Carrier Transport Factors in Drift Transistors when the Mobilities are not constant', Proc. IRE, Vol. 49, p. 1218, 1961.

22. R.L. Pritchard, 'Cut-off Frequency of a Junction Transistor when Mobilities are not constant', Proc. IRE, Vol. 50, pp. 91-92, 1962.
23. J.R.A. Beale, 'The Calculation of Transit Times in Junction Transistors when the Mobilities are not constant', Proc. IRE, Vol. 48, p. 1341, 1960.
24. M.B. Das and A.R. Boothroyd, 'Determination of Physical Parameters of Diffusion and Drift Transistors', Trans. IRE, Vol. ED-8, pp. 15-30, 1961.
25. A.R. Boothroyd and F.N. Trofimenkoff, 'Determination of the Physical Parameters of Transistors of Single- and Double Diffused Structure', Trans. IEEE, Vol. ED-10, pp. 149-163, 1963.
26. R.E. Thomas and A.R. Boothroyd, 'Determination of a Physical Model for Double Diffused Transistors', Solid State Electronics, Vol. 11, pp. 365-375, 1968.
27. H. Yanai, et al., 'Basic Considerations concerning the Small Signal Operation of Transistors', Electronics and Comm. in Japan, Vol. 47, pp. 265-275, 1964.
28. K.G. Ashar, 'The Transit Time in Transistors', Proc. IEEE Vol. 51, p. 617, 1963.
29. K. Tada and H. Yanai, 'Basic Considerations in Charge Control Analysis of the Transistor cut-off Frequency', Electronics and Comm. in Japan, Vol. 48, pp. 48-56, 1965.
30. M. Maeda, et al., 'Effect of Emitter Barrier Capacitance on f_{α} and f_T of Drift Transistors', Electronics and Comm. in Japan, Vol. 48, pp. 68-75, 1965.
31. M. Maeda, et al., 'Figure of Merit of High Frequency Transistors', Electronics and Comm. in Japan, Vol. 48, pp. 60-67, 1965.

32. M. Maeda, et al., 'Design Consideration of Base Impurity Distribution for Figure of Merit of High-Frequency Transistors', Electronics and Comm. in Japan, Vol. 49, pp. 59-66, 1966.
33. V.M. Bogachev, 'A Calculation of the Cut-off Frequency of a Drift Transistor by the Stored Charge Method', Radio Tekh. i Elektronika, Vol. 10, pp. 124-131, 1965.
34. A.H. Marshak, 'Optimum Doping Distribution for Minimum Base Transit Time', IEEE Trans., Vol. ED-14, pp. 190-194, 1967.
35. A.E. Mostafa and W.A. Wassef, 'Transit Time in the Base Region of Drift Transistors considering Diffusion, Recombination, and Variable built-in Electric Field', IEEE Trans., Vol. ED-17, pp. 55-63, 1970.

+++++

CHAPTER 2OPTIMUM IMPURITY DISTRIBUTIONS FOR MINIMUM
BASE TRANSIT TIME THROUGH VARIATIONAL METHOD

- 2.1 INTRODUCTION
 - 2.2 OPTIMUM IMPURITY DISTRIBUTION FOR MINIMUM BASE TRANSIT TIME - ELECTRIC FIELD APPROACH
 - 2.2.1 INTRODUCTION
 - 2.2.2 BASIC RELATIONS
 - 2.2.3 CONDITION FOR MINIMUM TRANSIT TIME
 - 2.2.4 OPTIMUM ELECTRIC FIELD FOR MINIMUM TRANSIT TIME
 - 2.2.5 ELECTRIC FIELD AS A FUNCTION OF IMPURITY CONCENTRATION IN BASE
 - 2.2.6 DERIVATION OF OPTIMUM IMPURITY DISTRIBUTION AT LOW INJECTION
 - 2.3 OPTIMUM IMPURITY DISTRIBUTIONS FOR MINIMUM BASE TRANSIT TIME - STORED CHARGE APPROACH
 - 2.3.1 INTRODUCTION
 - 2.3.2 BASIC RELATIONS
 - 2.3.3 OPTIMUM IMPURITY DISTRIBUTION FOR MINIMUM TRANSIT TIME - CONSTANT MOBILITY CASE
 - 2.3.4 OPTIMUM IMPURITY DISTRIBUTION FOR MINIMUM TRANSIT TIME - DOPING DEPENDENT MOBILITY CASE
 - 2.4 SUMMARY AND DISCUSSION
- REFERENCES

+++++

CHAPTER 2

OPTIMUM IMPURITY DISTRIBUTIONS FOR MINIMUM BASE TRANSIT TIME THROUGH VARIATIONAL METHOD

2.1 INTRODUCTION

The transit time of the current carriers traversing the base region is an important factor in limiting the frequency behaviour of junction transistors. In this chapter, the method of deducing optimum doping distributions for minimum base transit time through calculus of variations is discussed. Two approaches are suggested for this purpose. One focusses attention on the optimum electric field configuration while the other concentrates on optimum impurity distribution based on stored charge approach. Applying the electric field approach, optimum doping distribution function is obtained for the case of constant mobility. From the stored charge approach, optimum impurity distributions are derived for both constant and doping dependent mobility. At low injection levels of device operation, optimum impurity distribution functions obtained from both the approaches are found to be identical. It is suggested that the electric field approach of finding optimum distribution for minimum base transit time will be more pertinent when field dependent carrier mobility in the base and device operation under moderate injection levels are to be considered.

2.2 OPTIMUM IMPURITY DISTRIBUTION FOR MINIMUM BASE TRANSIT TIME - ELECTRIC FIELD APPROACH

2.2.1 Introduction

The motivation for adopting the electric field approach to establish optimum impurity distributions is derived from the base transit time definition of Moll and Ross¹. According to this, the base transit time t_B is

$$t_B = \int_0^W \frac{dx}{v(x)} \quad \dots (2.1)$$

where $v(x)$ is the velocity of the carriers in the base and W is the base width. But $v(x)$ is related to the minority carrier concentration p in the n-type base of a p-n-p transistor through the following relation.

$$J_p = q p v(x) \quad \dots (2.2)$$

Substituting eqn. 2.2 in eqn. 2.1, we obtain for base transit time

$$t_B = \frac{q}{J_p} \int_0^W p \, dx \quad \dots (2.3)$$

2.2.2 Basic Relations

In order to obtain the minority carrier concentration and base transit time as a function of electric field, the following current transport equation is used.

$$J_p = -q D_p \frac{dp}{dx} + q \mu_p p E \quad \dots (2.4)$$

Since the base width is small in practical transistors, recombination in the base region can be neglected. Under this assumption the current transport eqn. 2.4 is transformed to the following differential equation in p

$$\frac{dp}{dx} - \frac{qW}{KT} E \cdot p + \frac{J_p W}{q D_p} = 0 \quad \dots (2.5)$$

In the above equation normalised distance $X = x/w$ is used.

Substituting p as a product of two functions U and V , i.e.,

$$p = UV \quad \dots (2.6)$$

eqn. 2.5 can be written as

$$V \left[\frac{dU}{dX} - \frac{qW}{KT} E U \right] + U \frac{dV}{dX} + \frac{J_p W}{q D_p} = 0 \quad \dots (2.7)$$

The function U should be determined in such a way that the coefficient of V in eqn. 2.7 is zero, i.e.,

$$\frac{dU}{dX} - \frac{qW}{KT} E U = 0 \quad \dots (2.8)$$

This equation has a general solution of the form

$$U = C_1 e^{\frac{qW}{KT} \int E(X) dX} \quad \dots (2.9)$$

where C_1 is a constant.

On substituting U from eqn. 2.9 into eqn. 2.7 and solving for V , the following relation is obtained

$$V = - \frac{J_p W}{q D_p C_1} \int_0^1 e^{-qW/KT} \int_0^x E(x) dx \cdot dx + C_2 \quad \dots (2.10)$$

where C_2 is the constant of integration.

Substituting eqns. 2.9 and 2.10 in eqn. 2.6 and using the boundary condition that the hole density is zero at $x = 1$, the minority carrier concentration as a function of electric field is obtained as follows.

$$p = \frac{J_p W}{q D_p} \frac{\int_0^1 e^{-qW/KT} \int_0^x E(x) dx \cdot dx}{e^{-qW/KT} \int_0^1 E(x) dx} \quad \dots (2.11)$$

The base transit time is obtained by substituting eqn. 2.11 for p in eqn. 2.3. In the case of constant mobility, the expression is given by

$$t_B = \frac{W^2}{D_p} \int_0^1 \frac{\int_0^x e^{-qW/KT} \int_0^x E(x) dx \cdot dx}{e^{-qW/KT} \int_0^1 E(x) dx} \cdot dx \quad \dots (2.12)$$

2.2.3 Condition for Minimum Transit Time

If the double integral in the above relation is transformed to the functional

$$\int_0^1 f(x, y, y) dx, \quad \dots (2.13)$$

the electric field distribution $E(x)$ which will minimise this

integral can be determined from the Euler-Lagrange equation

$$\frac{\partial f}{\partial y} - \frac{d}{dx} \frac{\partial f}{\partial \dot{y}} = 0, \quad \dots (2.14)$$

where $\dot{y} = \dot{y}(x)$ denotes the derivative (dy/dx) .

Let us define

$$y = - \int_0^x e^{-qW/KT} \int_0^x E(x) dx \cdot dx \quad \dots (2.15)$$

Then

$$\dot{y} = e^{-qW/KT} \int_0^x E(x) dx \quad \dots (2.16)$$

Therefore,

$$\frac{t_B}{W^2/D_p} = - \int_0^1 y(\dot{y})^{-1} dx = \int_0^1 f(y, \dot{y}) dx \quad \dots (2.17)$$

To obtain the extremising function $E(x)$, Euler-Lagrange equation can be used. In the present case, the integrand function f is explicitly independent of the variable x . Hence, a particularly simple first order Euler-Lagrange equation results^{2,3} (Appendix - I). The equation is

$$f - \dot{y} \frac{\partial f}{\partial \dot{y}} = C \quad \dots (2.18)$$

where C is an arbitrary constant.

This form of the Euler-Lagrange equation is invariably used to derive optimum distribution function $N(x)$ from both the electric field and the stored charge approaches.

2.2.4 Optimum Electric Field for Minimum Transit Time

Applying the first order Euler-Lagrange relation obtained in eqn. 2.18 to the functional of eqn. 2.17, the optimum electric field configuration $E(X)$ can be determined. Solving eqn. 2.18, we obtain

$$y = - \frac{qW}{KTC} e^{-qW/KT \int_0^X E(X) dx} \quad \dots (2.19)$$

Differentiation of y w.r.t. X yields

$$\dot{y} = - \frac{qW}{KTC} e^{-qW/KT \int_0^X E(X) dx} \left(- \frac{qW}{KT} E \right) \quad \dots (2.20)$$

Equating this to eqn. 2.16, the following expression for electric field is obtained

$$E(X) = \frac{KT}{qW} \cdot \frac{2}{C} \quad \dots (2.21)$$

The constant $2/C$ can be obtained with the help of the boundary conditions. This is deferred till section 2.2.6.

2.2.5 Electric Field as a Function of Impurity Concentration in Base

The current transport equation for the base region majority carriers in a one dimensional p-n-p transistor is

$$J_n = q D_n \frac{dn}{dx} + q \mu_n n E \quad \dots (2.22)$$

If the injection efficiency is assumed to be near unity, the majority carrier current will be zero. Hence,

$$E = - \frac{KT}{q} \frac{1}{n} \frac{dn}{dx} \quad \dots (2.23)$$

But the assumption of space charge neutrality requires that

$$n = N + p \quad \dots (2.24)$$

where N represents the donor concentration in the base.

Substitution of eqn. 2.24 in eqn. 2.23 yields

$$E = - \frac{KT}{q} \frac{1}{N} \frac{dn}{dx} - \frac{KT}{q} \frac{1}{1 + \frac{p}{N}} \frac{d(1 + \frac{p}{N})}{dx} \quad \dots (2.25)$$

p/N represents the injection factor.

At low injection levels, p/N becomes negligible as compared with 1 and the above equation for electric field truncates to yield the following:

$$E = - \frac{KT}{qW} \cdot \frac{1}{N} \frac{dN}{d\lambda} \quad \dots (2.26)$$

where $\lambda = x/W$

Thus it is clear that at low injection, the electric field is a consequence of doping distribution in the base. Hence it is termed as the built-in electric field.

2.2.6 Derivation of Optimum Impurity Distribution at Low Injection

The optimum impurity distribution function $N(X)$ can be derived by combining the base region electric field expressions obtained in sections 2.2.4 and 2.2.5. Equating the two expressions for field given by eqns. 2.21 and 2.26 and integrating we get

$$\ln N = - \frac{2}{C} X + C_1 \quad \dots (2.27)$$

where C_1 is a constant of integration.

Applying the following boundary conditions

$$N = N_0 \quad \text{at } x = 0 \quad \dots (2.28)$$

$$N = N_W \quad \text{at } x = 1$$

We obtain

$$N(x) = N_0 e^{-\eta x} \quad \dots (2.29)$$

and

$$E(x) = \frac{KT}{qW} \eta \quad \dots (2.30)$$

where $\eta (= \ln \frac{N_0}{N_W})$ is the electric field parameter and is a measure of the strength of the built-in electric field in the base.

Eqn. 2.29 shows that it is the exponential doping distribution which offers minimum base transit time in the case of constant mobility. The resulting electric field is constant throughout the base region for this impurity distribution (eqn. 2.30).

2.3 OPTIMUM IMPURITY DISTRIBUTIONS FOR MINIMUM BASE TRANSIT TIME - STORED CHARGE APPROACH

2.3.1 Introduction

In the previous section, Moll and Ross's classical definition of base transit time was discussed. An altogether new approach - electric field approach - was introduced and used to obtain optimum impurity distribution for minimum base transit time for the case of constant mobility. In this section, Varnerin's⁴ stored charge definition of base transit time is elucidated and with the help of this stored charge

approach, optimum impurity distributions for minimum base transit time are derived for both constant and doping dependent carrier mobility.

According to Varnerin, the base transit time is the ratio of total minority carrier stored charge Q_s in the base to the emitter current I_e , i.e.,

$$t_B = \frac{Q_s}{I_e} \quad \dots (2.31)$$

The total stored charge in the base is given by

$$Q_s = q A \int_0^W p \, dx \quad \dots (2.32)$$

Assuming unity injection efficiency, $I_e = I_p$.

Hence, the base transit time can be expressed as

$$t_B = \frac{qA}{I_p} \int_0^W p \, dx \quad \dots (2.33)$$

2.3.2 Basic Relations

The general expressions relating minority carrier concentration p and the base transit time t_B to an arbitrary impurity distribution N can be obtained as follows.

The hole current transport eqn. 2.4 assumes the following form if the electric field E is substituted from eqn. 2.26.

$$J_p = -q D_p \left(\frac{dp}{dx} + \frac{dN/dx}{N} p \right) \quad \dots (2.34)$$

This relation transforms to the following first-order linear differential equation in p if base recombination is neglected.

$$\frac{dp}{dx} + \frac{dN/dx}{N} p + \frac{J_p}{q D_p} = 0 \quad \dots (2.35)$$

This equation can be solved, subject to the boundary condition that the hole concentration is zero at W , to yield

$$p = \frac{J_p W}{q D_p} \frac{\int_0^1 N(x) dx}{N} \quad \dots (2.36)$$

The base transit time t_B is obtained by substituting eqn. 2.36 into eqn. 2.33 as

$$t_B = \frac{W^2}{D_p} \int_0^1 \frac{\int_0^1 N(x) dx}{N(x)} dx \quad \dots (2.37)$$

When mobility cannot be assumed to be independent of doping, the above expression modifies to the following form

$$t_B = W^2 \int_0^1 \frac{\int_0^1 \frac{N(x)}{D_p(x)} dx}{N(x)} dx \quad \dots (2.38)$$

In all the above relations, $N(x)$ is an arbitrary impurity distribution in the base.

2.3.3 Optimum Impurity Distribution for Minimum Transit Time - Constant Mobility Case

The double integral in the transit time relation 2.37 can be reduced to the functional form discussed in section 2.2.3. Let us introduce

$$y = - \int_0^1 N(x) dx \quad \dots (2.39)$$

Then

$$\dot{y} = N(X) \quad \dots (2.40)$$

Therefore eqn. 2.37 can be reduced to the functional

$$\frac{c_B}{W^2/D_P} = - \int_0^1 y(\dot{y})^{-1} dx = \int_0^1 f(y, \dot{y}) dx \quad \dots (2.41)$$

Since f is not an explicit function of x , the following first integral of the Euler-Lagrange equation is used for obtaining $N(X)$.

$$f - \dot{y} \frac{\partial f}{\partial \dot{y}} = C \quad \dots (2.42)$$

(This condition has been discussed in Section 2.2.3 and is given in Appendix I).

Equation 2.42 can be solved to yield the extremising function $N(X)$. Applying the boundary conditions,

$$\begin{aligned} N &= N_0 \quad \text{at } X = 0 \\ N &= N_W \quad \text{at } X = 1 \end{aligned} \quad \dots (2.43)$$

the following result is derived for $N(X)$.

$$N(X) = N_0 e^{-\eta X} \quad \dots (2.44)$$

where $\eta = \ln N_0/N_W$

N_0 = Impurity concentration at the emitter end of the base

N_W = Impurity concentration at the collector end of the base.

Thus it is established that in the case of constant mobility both the approaches of deriving optimum impurity distribution yield an identical impurity distribution function $N(X)$ in the

base and this distribution function is exponential in nature. This is due to the fact that at low injection, both the approaches are equivalent to each other.

2.3.4 Optimum Impurity Distribution for Minimum Transit-Time - Doping dependent Mobility Case

When the carrier mobility cannot be assumed to be independent of doping density in the base region, the transit time relation 2.38 is applicable. It is imperative to note that the spatial variation of diffusion coefficient or mobility is a consequence of their dependence on impurity concentration. Since the impurity concentration varies in the base region, the diffusion coefficient should also vary. In this case also, it is possible to reduce the transit time to the functional form discussed earlier. Hence the condition 2.42 can be used to derive the extremizing function $N(x)$ in these cases.

In the following sections, different empirical relations for doping dependent mobility are used and corresponding optimum impurity distributions are derived.

Sugano and Koshiga's Mobility Relation⁵

This relation of mobility is based on measurements conducted by Prince⁶ on actual samples of semiconductor materials such as silicon and germanium. Sugano and Koshiga derived this expression to study the effect of doping dependent mobility on the cut-off frequency of transistors. Later on, Boothroyd and Trofimenkoff⁷ have also used it. The expression

for diffusion coefficient is given by

$$D = D_R \left(\frac{N}{N_R} \right)^{-\theta}$$

where D_R is the diffusion coefficient for the reference material of impurity concentration N_R and θ is a positive fractional index.

To obtain optimum impurity concentration for minimum base transit time, the following expression for diffusion coefficient is used.

$$D = D_0 \left(\frac{N}{N_0} \right)^{-0.25}$$

where D_0 is the diffusion coefficient corresponding to N_0 , the emitter end impurity concentration in the base. θ for silicon is assumed to be 0.25.

Substituting this relation into the transit time expression 2.38, we obtain

$$t_B = \frac{W^2}{D_0} \int_0^1 \frac{\left(\frac{N(x)}{N_0} \right)^{1.25}}{N(x)/N_0} dx \quad \dots (2.45)$$

Introducing $y = - \int_x^1 \left(\frac{N(x)}{N_0} \right)^{1.25} dx$, the above integral can

be transformed to the functional.

$$\frac{t_B}{W^2/D_0} = - \int_0^1 y (\dot{y})^{-1/1.25} dx = \int_0^1 f(y, \dot{y}) dx \quad \dots (2.46)$$

The solution of the differential equation 2.42 subject to the boundary conditions expressed in eqn. 2.43, yields the following hyperbolic distribution⁸ for minimum base transit time.

$$N(X) = N_0 (1 + (e^{\eta/4} - 1) X)^{-4} \quad \dots (2.47)$$

Marshak's⁹ Mobility Relation

Referring to a plot of mobility versus impurity concentration in silicon¹⁰, Marshak has derived this mobility relation. At a fixed temperature, the diffusion coefficient is approximated by

$$D = a - b \ln N(X) \quad \dots (2.48)$$

where the values of a and b are given in Table 2.1.

The optimum doping distribution for minimum base transit time has also been obtained by Marshak. In a slightly altered form, the impurity distribution function is

$$N(X) = N_0 e^{(\sqrt{B} - \sqrt{B + \gamma X})} \quad \dots (2.49)$$

where

$$B = (\ln A/N_0)^2$$

$$\gamma = (\ln A/N_w)^2 - B$$

$$A = \exp\left(\frac{a}{b} + \frac{1}{2}\right)$$

Ho and Cho's Mobility Relation¹¹

This relation has been obtained by combining the available resistivity vs. concentration data of Irvin¹² and the mobility vs. resistivity data of Runyan¹³. A close empirical relation for mobility is obtained as

$$\mu = \frac{a}{1 + b N^c} \quad \dots (2.50)$$

where a , b , and c are constants given in Table 2.1.

A similar relation for mobility has independently been derived by Caughey and Thomas¹⁴. The relation is

$$\mu = \frac{\mu_{\max} - \mu_{\min}}{1 + (N/N_{\text{ref}})^\alpha} + \mu_{\min} \quad \dots (2.51)$$

The parameter values are given in Table 2.1.

On a closer look at eqns. 2.50 and 2.51, it is evident that the two mobility relations have equivalent analytical form, provided μ_{\min} in eqn. 2.51 is neglected. μ_{\max} and $(N_{\text{ref}})^{-\alpha}$ in Caughey and Thomas's relation resemble a and b respectively in Ho and Cho's expression. One more common point in the two mobility relations is that both of them exhibit a strong resemblance to the Fermi-Dirac distribution function at high temperatures. The optimum impurity distribution function $N(x)$ is derived here for Ho and Cho's mobility relation but the procedure will be exactly similar for Caughey and Thomas's mobility expression.

Substitution of eqn. 2.50 in transit time relation 2.38 yields

$$\frac{t_B}{W^2 / \frac{KT}{q} a} = \int_0^1 \frac{\int_0^1 N(1 + bN^c) dx}{N} dx \quad \dots (2.52)$$

Let us define

$$y = - \int_0^1 N(1 + bN^c) dx \quad \dots (2.53)$$

Then eqn. 2.52 is transformed to the functional

$$\int_0^1 f(y, \dot{y}) dx = - \int_0^1 \frac{y}{N} dx \quad \dots (2.54)$$

The optimum impurity distribution $N(x)$ can be obtained by making use of the condition 2.42.

Now

$$\frac{\partial f}{\partial y} = \frac{\partial f}{\partial N} \cdot \frac{dN}{dy} = \frac{y}{N^2} \frac{1}{1 + \frac{1+c}{c} bN^c}$$

Then eqn. 2.42 yields

$$- \frac{y}{N} \left(1 + \frac{1 + bN^c}{1 + \frac{1+c}{c} bN^c} \right) = K' \quad \dots (2.55)$$

where K' is an arbitrary constant (since C has been used in Ho and Cho's mobility relation, constant K' is used in the condition 2.42).

Introduction of a dimensionless parameter $\alpha = bN^c$ transforms eqn. 2.55 to the following form.

$$y = - KN' \frac{1 + \sqrt{1+c} \alpha}{2 + 2 + c \alpha} \quad \dots (2.56)$$

Hence,

$$\dot{y} = -K' \alpha N(1 + \alpha) \frac{2 + \alpha(2 + 3c + c^2)}{c\alpha(2 + 2 + c\alpha)^2} \quad \dots (2.57)$$

Differentiation of eqn. 2.53 yields

$$\dot{y} = N(1 + \alpha)$$

Equating the above two values of \dot{y} , we obtain

$$\int \frac{g(\alpha)}{\alpha} d\alpha = -\frac{c}{K'} X + c_1 \quad \dots (2.58)$$

where c_1 is the constant of integration, and

$$g(\alpha) = \frac{2 + \alpha(2 + 3c + c^2)}{(2 + 2 + c\alpha)^2} \quad \dots (2.59)$$

Solving eqn. 2.58, we get

$$\ln \frac{2}{\alpha} \left(1 + \frac{c+2}{2} \alpha\right) + \frac{c}{1 + \frac{c+2}{2} \alpha} = \frac{2c}{K'} X - 2c_1 \quad \dots (2.60)$$

The above equation cannot be explicitly solved for α and hence for $N(X)$ due to its non-linear nature. For defined values of X , eqn. 2.60 can be solved by Newton-Raphson's iterative method to yield $N(X)$ as a tabulated function of X . (The method of solution is outlined in Appendix II.)

For a ratio of $N_0/N_w = 10^3$, a third degree polynomial computer fit to the numerically obtained results of the above non-linear equation has been deduced as

$$N(X) = N_0 \exp(-8.71435 X + 3.6408 X^2 - 1.8072 X^3) \quad \dots (2.61)$$

Fig. 2.1 shows a plot of all the optimum impurity distributions obtained above. For comparison, the other conventional impurity distributions such as Gaussian and complementary error function

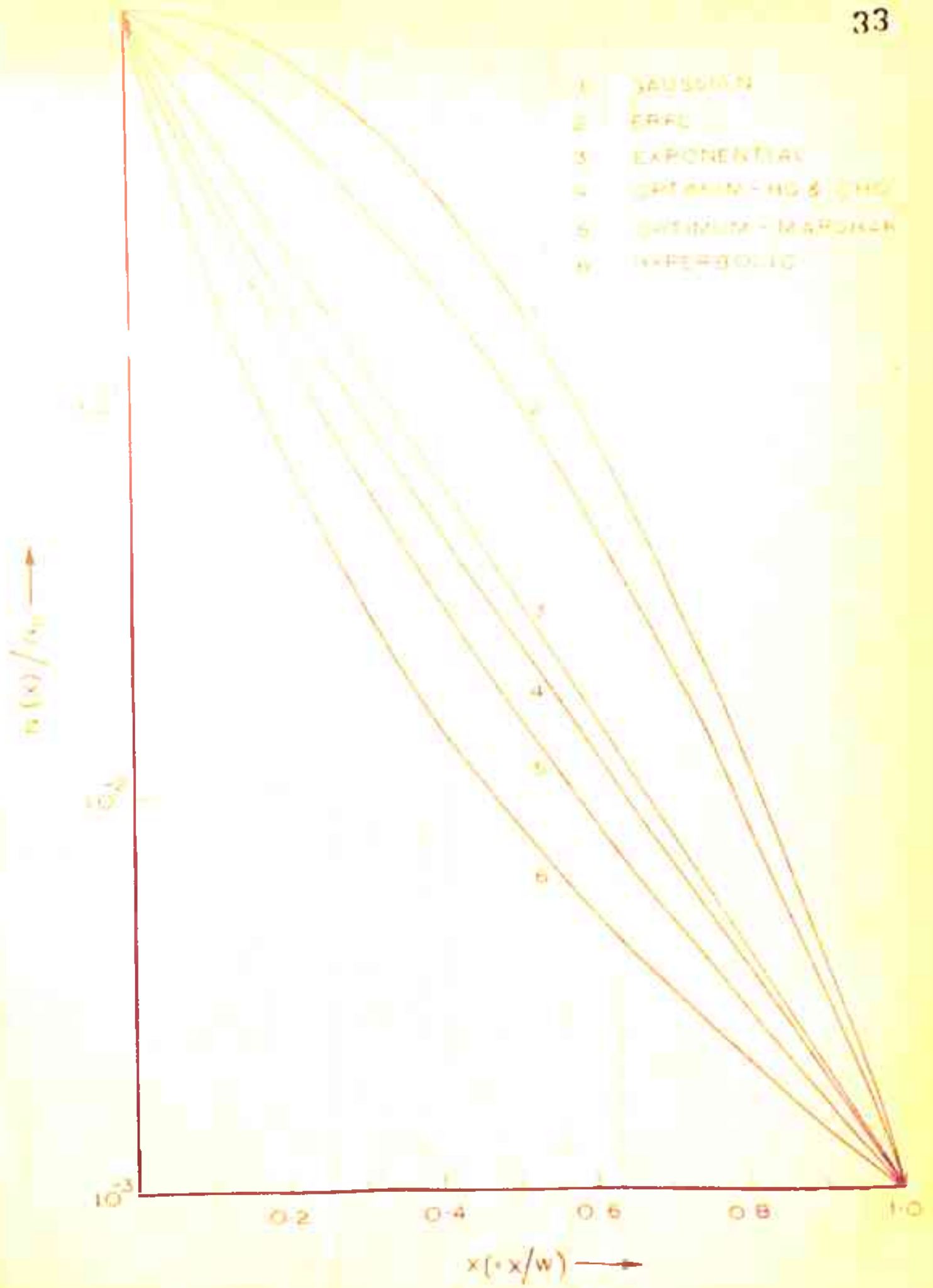


FIG. 21 BASIC IMPURITY DISTRIBUTIONS IN THE BASE

TABLE 2.1

Constants for Different Empirical Relations of Carrier Mobility
(or Diffusion Coefficient)

	Marshak's Relation		Ho and Cho's Mobility Relation		Caughy and Thomas's Mobility Relation		Gaughey and Thomas's Mobility Relation		
	a	b	a	b	c	μ_{max}	μ_{min}	N_{ref}	
	(cm^2/s)	(cm^2/s)	($cm^2/V.s$)	(cm^3c)		($cm^2/V.s$)	($cm^2/V.s$)	(cm^{-3})	
Holes	56	1.22	475	1.4×10^{-14}	0.77	495	47.7	6.3×10^{16}	0.76
Electrons	152	3.46	1370	8.78×10^{-11}	0.59	1330	65.0	8.5×10^{16}	0.72

(erfc.) are also plotted. The distributions are normalised so that their boundary values coincide for $N_o/N_w = 10^3$.

2.4 SUMMARY AND DISCUSSION

Two different approaches for obtaining optimum impurity distributions for minimum base transit time have been discussed. The stored charge approach has been used to derive optimum impurity distributions for different empirical relations of doping dependent mobility. It has been shown that for a given empirical relation of mobility the optimum distribution function is unique. If the exponential distribution is taken as reference, all optimum distributions obtained in the case of doping dependent mobility are found to be concave up on $\ln N$ vs. X plot, while the conventional distributions, such as, Gaussian and erfc., are concave down on such a plot (Fig. 2.1).

The typical nature of the optimum impurity distributions on a $\ln N$ vs. X plot can be attributed to the doping dependent mobility. Since the carrier mobility near the emitter end of the base decreases due to the larger doping, the electric field should simultaneously increase to yield minimum transit time. The required increase in electric field necessitates a steeper gradient $(\frac{d}{dx} \ln N)$ at the emitter end of the base. Hence, the optimum doping distributions derived through calculus of variations are concave up.

If the spatial dependence of diffusion coefficient in the base arises from the field dependent mobility rather than the doping dependent mobility, the electric field approach will

be more apt for the derivation of optimum doping distribution function. This approach is also useful to deal with the case of device operation under intermediate injection levels.

In the next chapter, the calculated results of built-in electric field, excess minority carrier concentration, and base transit time (all at low injection) are presented. The influence of doping dependent carrier mobility on excess carrier concentration and base transit time is also studied.

+++++

REFERENCES

1. J.L. Moll and I.M. Ross, 'The dependence of transistor parameters on the distribution of base layer resistivity', Proc. IRE, Vol. 44, pp 74-78, Jan. 1956.
2. L.E. Elsgolc, 'Calculus of Variations', Pergamon Press, London, 1961, Ch. 1.
3. R. Wienstock, 'Calculus of Variations', McGraw-Hill Book Co., New York, 1952, Ch. 3.
4. L.J. Varnerin, 'Stored charge method of transistor base transit analysis', Proc. IRE, Vol. 47, pp 523-527, April 1959.
5. T. Sugano and F. Koshiga, 'The calculation of cut-off frequencies of minority-carrier transport factors in drift transistors when the mobilities are not constant', Proc. IRE, Vol. 49, p 1218, July 1961.
6. M.B. Prince, 'Drift mobilities in semiconductors, Part II - Silicon', Phys. Rev., Vol. 93, pp 1204-1206, 1954.
7. A.R. Boothroyd and F.N. Trofimenkoff, 'Determination of the physical parameters of transistors of single- and double-diffused structure', IEEE Trans. Electron Devices, Vol. ED-10, pp 149-163, May 1963.
8. V.M. Bogachev, 'A calculation of the cut-off frequency of a drift transistor by the stored charge method', Radio Engg. and Electron. Phy., pp 124-131, Jan. 1965.
9. A.H. Marshak, 'Optimum doping distribution for minimum base transit time,' IEEE Trans. Electron Devices, Vol. ED-14, pp 190-194, April 1967.
10. A.K. Jonscher, 'Principles of semiconductor device operation', G. Bell, London, 1960, p. 25.

11. B.L. Ho and C.C. Cho, 'Effect of mobility gradient in inhomogenously doped semiconductors', JAP, Vol. 39, No.7, June 1968, pp. 3333-3336.
12. J.C. Irvin, 'Resistivity of bulk silicon and diffused layers in silicon', Bell Sys. Tech. J., pp 387-410, March 1962.
13. W.R. Runyan, 'Silicon semiconductor technology', McGraw-Hill Book Co., New York, 1965, p 179.
14. D.M. Caughey and R.E. Thomas, 'Carrier mobilities in Silicon empirically related to doping and field', Proc. IEEE, Vol. 55, pp 2192-2193, Dec. 1967.

+++++

CHAPTER 3

EFFECT OF IMPURITY DISTRIBUTION ON MINORITY CARRIER BASE TRANSIT TIME

- 3.1 INTRODUCTION
 - 3.2 BASIC IMPURITY DISTRIBUTIONS IN THE BASE
 - 3.3 BUILT-IN ELECTRIC FIELD IN THE BASE
 - 3.4 EXCESS MINORITY CARRIER CONCENTRATION IN THE BASE
 - 3.4.1 CONSTANT MOBILITY CASE
 - 3.4.2 DOPING DEPENDENT MOBILITY CASE
 - 3.5 MINORITY CARRIER BASE TRANSIT TIME WHEN MOBILITY IS CONSTANT
 - 3.6 INFLUENCE OF DOPING DEPENDENT CARRIER MOBILITY ON BASE TRANSIT TIME
 - 3.6.1 SUGANO AND KOSHIGA'S MOBILITY RELATION
 - 3.6.2 MARSHAK'S MOBILITY RELATION
 - 3.6.3 HO AND CHO'S MOBILITY RELATION
 - 3.6.4 DISCUSSION
 - 3.7 SPECIAL FORM OF BASE IMPURITY DISTRIBUTION
 - 3.8 SUMMARY AND DISCUSSION
- REFERENCES

CHAPTER 3

EFFECT OF IMPURITY DISTRIBUTION ON MINORITY CARRIER BASE TRANSIT TIME

3.1 INTRODUCTION

The fact that the minority carrier base transit time depends upon the actual distribution of impurities in the base region of junction transistors has been well established in the past^{1,2}. The purpose of the present chapter is to evaluate the effect of base doping distribution on the minority carrier base transit time in transistors. Several doping distributions including the optimum ones derived in the previous chapter and the conventional ones such as Gaussian and erfc. are considered. Since the minority carrier mobility in the base depends on the impurity concentration, the carrier transit behaviour is studied for different empirical relations of doping dependent mobility. Excess minority carrier concentration and base transit time are calculated by numerical computational methods while the base region built-in electric field is evaluated through analytical expressions.

A special form of base doping distribution is also studied. This distribution is concave down over part of the base and changes over to concave up over rest of the base region. Built-in electric field, excess carrier concentration and base transit time are evaluated and the results are compared with those obtained for optimum distributions. This

study reveals the fact that the optimum impurity distributions obtained through variational method do not necessarily offer a unique minimum in base transit time. It is concluded that the variational method applies only to a restricted class of smooth distributions.

3.2 BASIC IMPURITY DISTRIBUTIONS IN THE BASE

In order to study the effect of base doping distribution on the built-in electric field, excess carrier concentration and base transit time, the following impurity distributions are treated. Some common symbols used in the description of these distributions are given below.

N_0 = impurity concentration at the emitter end of the base region

N_w = impurity concentration at the collector end of the base region

x = x/W , normalised distance

η = $\ln N_0/N_w$

W = electrical base width

Gaussian Distribution

This distribution is obtained when a two step diffusion process³, predeposition followed by a drive-in, is used. The following mathematical relation describes the distribution:

$$N(x) = N_0 \exp(-\eta x^2) \quad \dots (3.1)$$

Complementary Error Function (erfc.) Distribution

This impurity distribution is achieved when a single-step diffusion process³ is used for device fabrication. The distribution is

$$N(x) = N_0 \operatorname{erfc}(\beta x) \quad \dots (3.2)$$

where $\operatorname{erfc}(\beta) = N_w/N_0$

Exponential Distribution

In order to reduce the complications in the analysis of graded base transistors, the above two distributions are approximated by an exponential distribution. Quite interestingly, exponential distribution is also the optimum distribution for minimum base transit time in the case of constant mobility. It is described as

$$N(x) = N_0 \exp(-\eta x) \quad \dots (3.3)$$

Optimum distribution - Ho and Cho's

With Ho and Cho's mobility relation, this optimum distribution has been derived in the previous chapter through variational method. An explicit mathematical relation is not possible in this case. Hence the following approximate computer fit to the numerically obtained results of the non-linear equation 2.60 (Chapter 2), describes the distribution for $N_0/N_w = 10^3$.

$$N(x) = N_0 \exp(-8.71435 x + 3.6408 x^2 - 1.8072 x^3) \quad \dots (3.4)$$

For the computation of base transit time, the numerical results are used as such.

Optimum Distribution - Marshak's

The following equation describes this distribution.

$$N(x) = N_0 \exp(\sqrt{B} - \sqrt{B + \gamma x}) \quad \dots (3.5)$$

where

$$B = (\ln A/N_0)^2$$

$$\gamma = (\ln A/N_w)^2 - B$$

$$A = \exp\left(\frac{a}{b} + \frac{1}{2}\right)$$

a and b are constants given in Table 2.1 (Chapter 2).

This distribution is also the result of optimising the doping distribution function for minimum base transit time⁴.

Hyperbolic Distribution - Sugano and Koshiga's Mobility Relation

When Sugano and Koshiga's relation of mobility is used, the variation^{al} method of finding optimum distribution yields the following hyperbolic distribution⁵.

$$N(x) = N_0 (1 + (e^{\eta/4} - 1) x)^{-4} \quad \dots (3.6)$$

Parabolic-I Distribution

This distribution has been synthesised by assuming a parabolic relation between $\ln N$ and x . The analytical relation is

$$N(x) = N_0 \exp(\eta x - 2\eta \sqrt{x}) \quad \dots (3.7)$$

Parabolic-II Distribution

For $N_0/N_w = 10^3$, this distribution is expressed as

$$N(X) = N_0 \exp(-0.86 X - 6.05 X^2) \quad \dots (3.8)$$

Arbitrary Distribution

This distribution is given by the relation

$$N(X) = N_0 (1 - C e^{-7.75 X} + C e^{-2.7 X}) \quad \dots (3.9)$$

where
$$C = \frac{e^{-7.75} - e^{-\eta}}{e^{-7.75} - e^{-2.7}}$$

The last two distributions - Parabolic-II and the Arbitrary - are included to study the nature of the built-in electric field in the base. The base transit times for these distributions are computed for few ratios of N_0/N_w only.

Fig. 3.1 shows a plot of all the basic impurity distributions in the base region for $N_0/N_w = 10^3$. The impurity concentration $N(X)$ is normalised with respect to the emitter end concentration in the base.

3.3 BUILT-IN ELECTRIC FIELD IN THE BASE

The inhomogeneous impurity distribution in the base region results in an internal built-in electric field. Under low-level operation of graded-base transistor, the transport of injected carriers is controlled by both diffusion and drift. At high injection, the benefits due to the built-in electric field are lost and the current flow becomes effectively

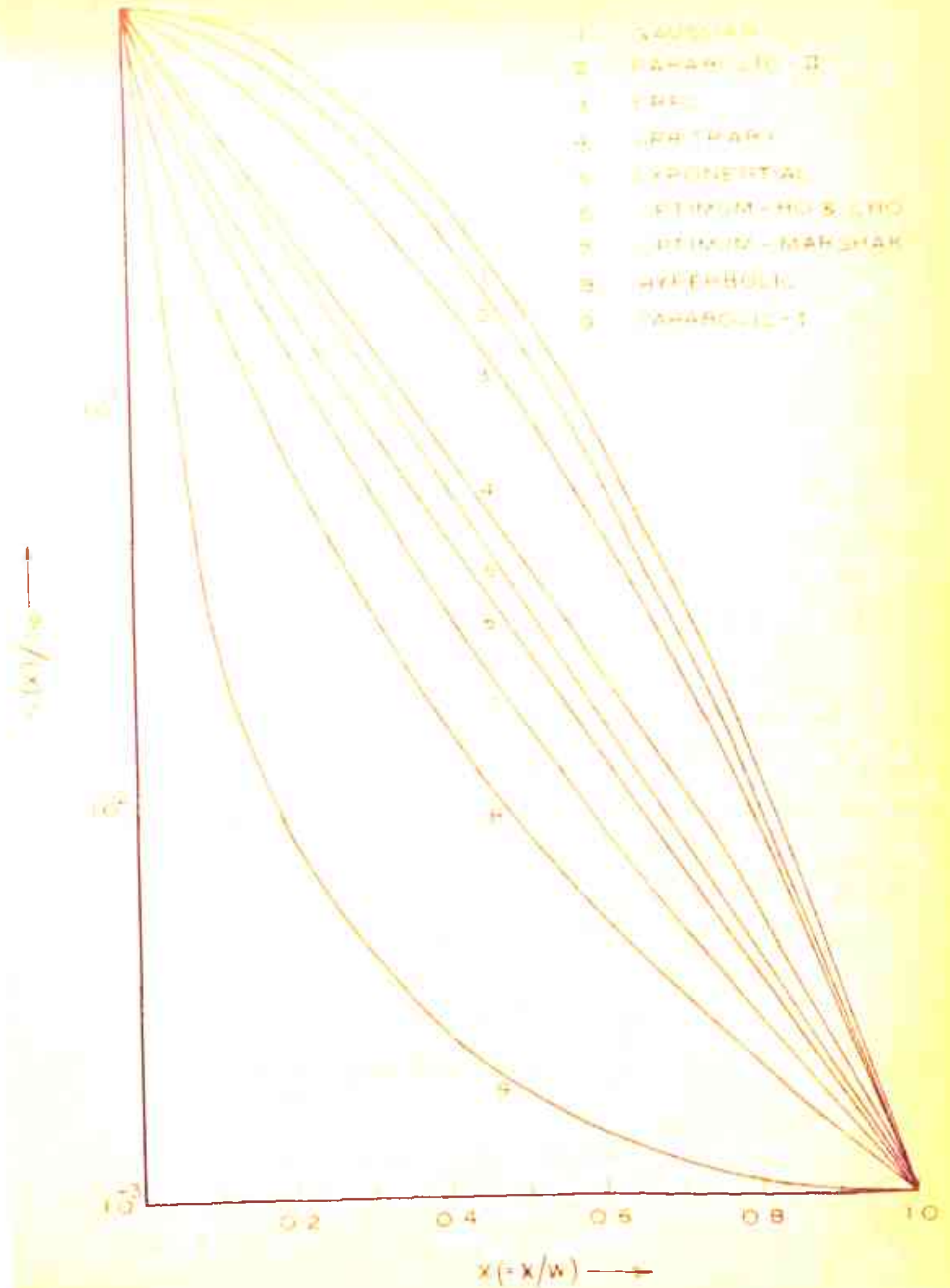


FIG 31 BASIC IMPURITY DISTRIBUTIONS IN THE BASE

diffusive. The expression for built-in electric field has been derived in the previous chapter (Sec. 2.2.5) and is reproduced below.

$$E = - \frac{KT}{qW} \frac{1}{N} \frac{dN}{dx} \quad \dots (3.10)$$

where KT/qW is the thermal electric field and N is the donor concentration in the n-type base region of a p-n-p transistor.

In this section, the built-in electric field is calculated for all the impurity distributions treated in Sec. 3.2. The analytical expressions obtained from eqn. 3.10, are given in Table 3.1. For $N_0/N_w = 10^3$, the variation of the built-in electric field in the base is shown in Figs. 3.2 and 3.3.

3.4 EXCESS MINORITY CARRIER CONCENTRATION IN THE BASE

For transistors operating under low-current conditions, the excess minority carrier concentration in the base has been derived in the previous chapter (Sec. 2.3.2). Lindmeyer and Wrigley³ have also obtained this relation. In the case of constant mobility, the expression is

$$\left(\frac{q D_D}{J_p} \right) p = \frac{\int_0^x N(x) dx}{N(x)} \quad \dots (3.11)$$

When carrier mobility in the base region depends upon doping density, the above expression assumes the altered form⁵

TABLE 3.1

Analytical Expressions of Base
Region Built-in Electric Field

Impurity Distribution	Normalised built-in electric field (q W / KT) E
Gaussian	$2 \eta x$
Erfc.	$2 \beta e^{-\beta^2 x^2} / \sqrt{\pi} \operatorname{erfc}(\beta x)$
Exponential	η
Optimum - Ho and Cho's	$8.71435 - 7.2816 x + 5.4216 x^2$ (Valid for $N_o/N_w = 10^3$ only)
Optimum - Marshak's	$\gamma / 2 \sqrt{\beta + \gamma x}$
Hyperbolic	$4 (e^{\eta/4} - 1) / (1 + (e^{\eta/4} - 1) x)$
Parabolic-I	$\eta (1 - \sqrt{x}) / \sqrt{x}$
Parabolic-II	$12.1 x + 0.86$ (Valid for $N_o/N_w = 10^3$)
Arbitrary	$\frac{7.75 (1 - C) e^{-7.75 x} + 2.7 C e^{-2.7 x}}{(1 - C) e^{-7.75 x} + C e^{-2.7 x}}$

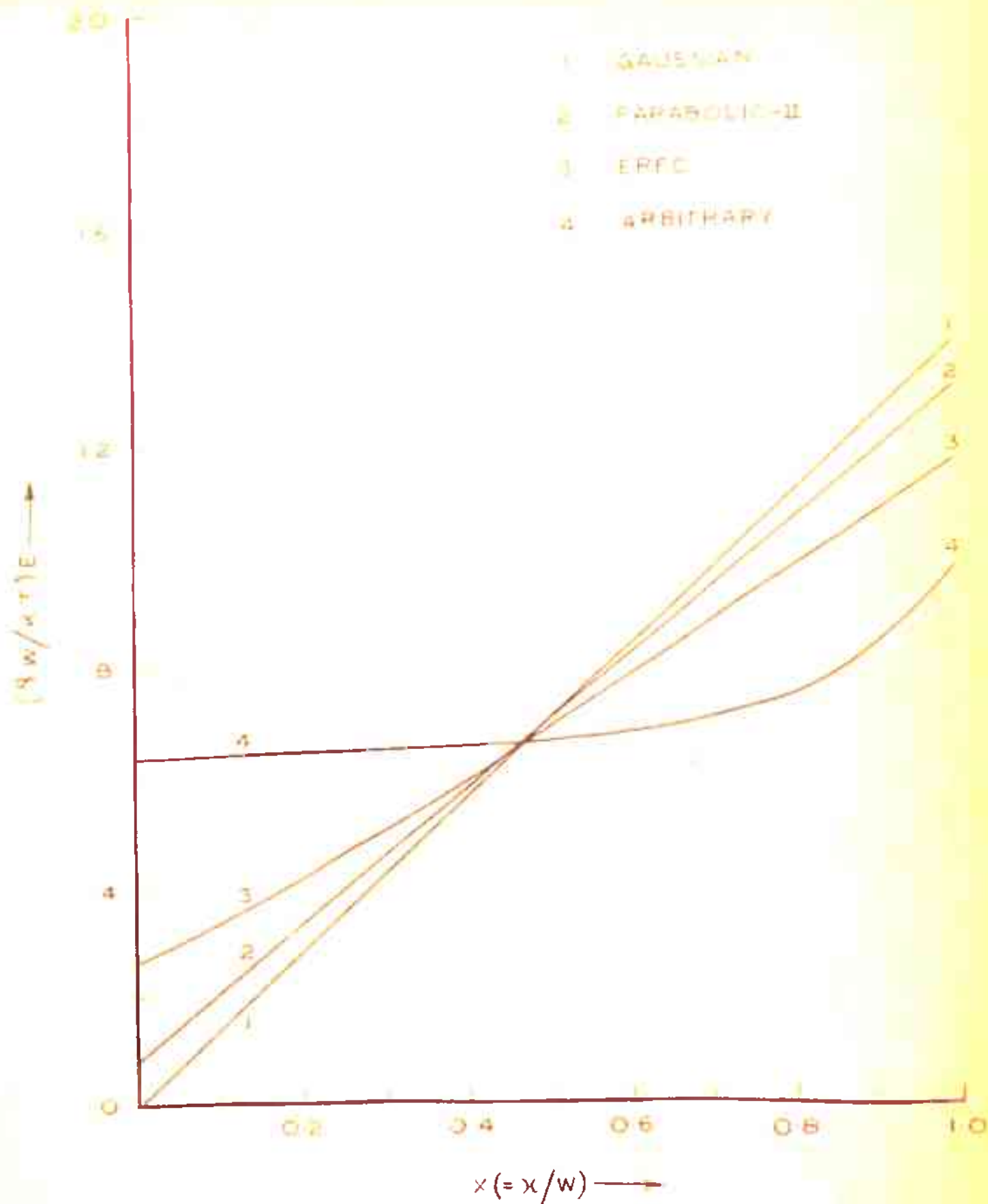


FIG.32 NORMALISED BUILT-IN ELECTRIC FIELD IN THE BASE FOR CONCAVE DOWN IMPURITY DISTRIBUTIONS OF FIG. 31

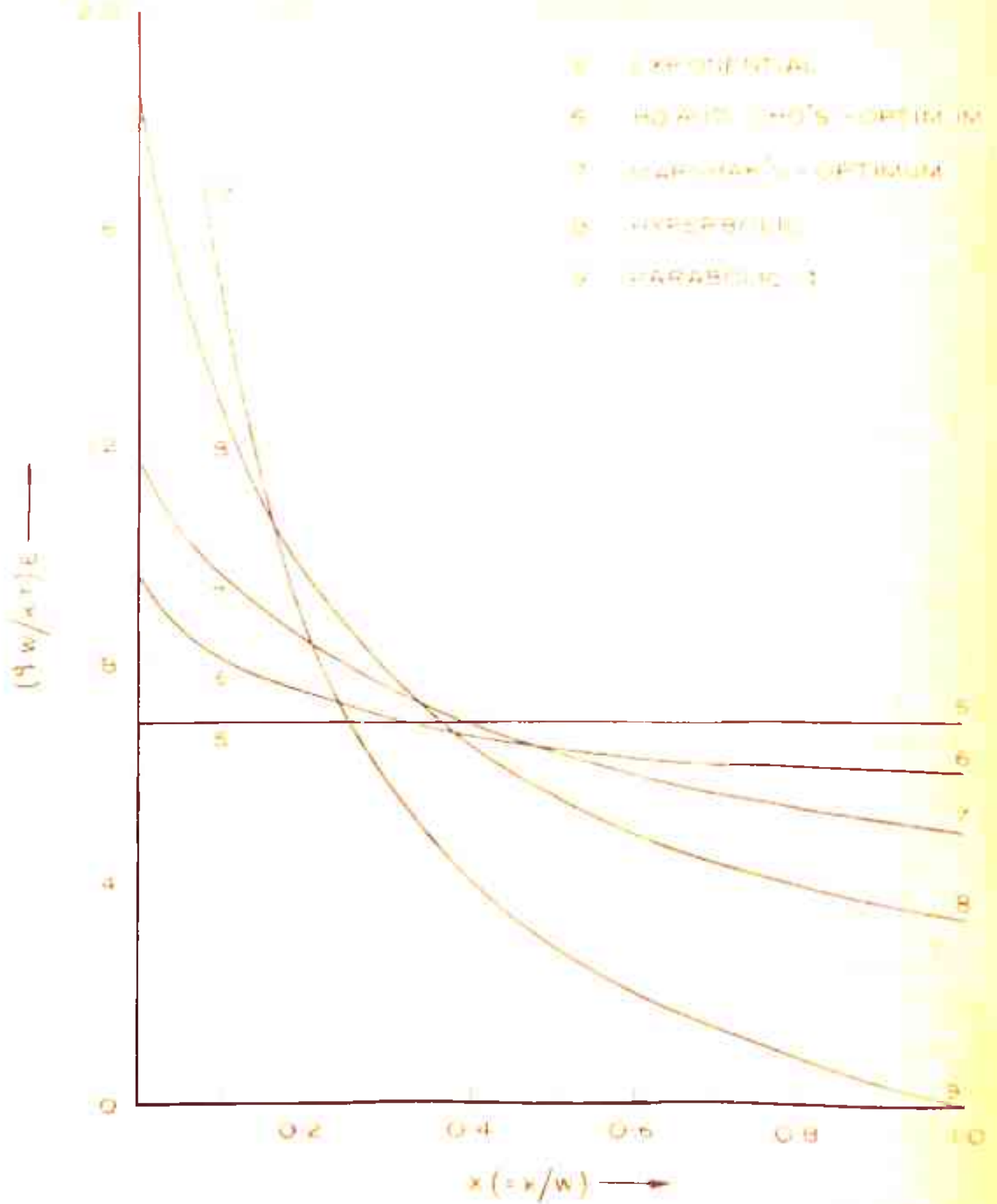


FIG. 3.3 NORMALISED BUILT-IN ELECTRIC FIELD IN THE BASE FOR CONCAVE UP IMPURITY DISTRIBUTIONS OF FIG. 3.1.

$$\left(\frac{q}{J_p W}\right) P = \frac{\int_x^1 \frac{N(x)}{D_p(x)} dx}{N(x)} \quad \dots (3.12)$$

where $D_p(x)$ is the doping dependent diffusion coefficient for minority carriers (holes) in the base region.

In this section the results of excess minority carrier concentration, calculated for several base doping distributions, are presented. The cases of both constant and doping dependent mobility are treated. Sugeno and Koshiga's power law relation of doping dependent mobility is used. Three reference values D_0 , D_w , and D_{avg} of the diffusion coefficient, corresponding to the emitter end concentration N_0 , collector end concentration N_w , and the average impurity concentration in the base, are chosen.

3.4.1 Constant Mobility Case

In this case, the computer evaluation is based on the relation 3.11. For defined values of x , the integral is evaluated with the help of Simpson's integration formula⁶. The minority carrier concentrations (in normalised form) are plotted in Figs. 3.4 to 3.10 with N_0/N_w as a parameter for different base distributions.

The minority carrier concentration plot for exponentially doped base (Fig. 3.6) indicates that the current flow in the base is mainly by drift mechanism, except near the collector end where it becomes purely diffusive. This

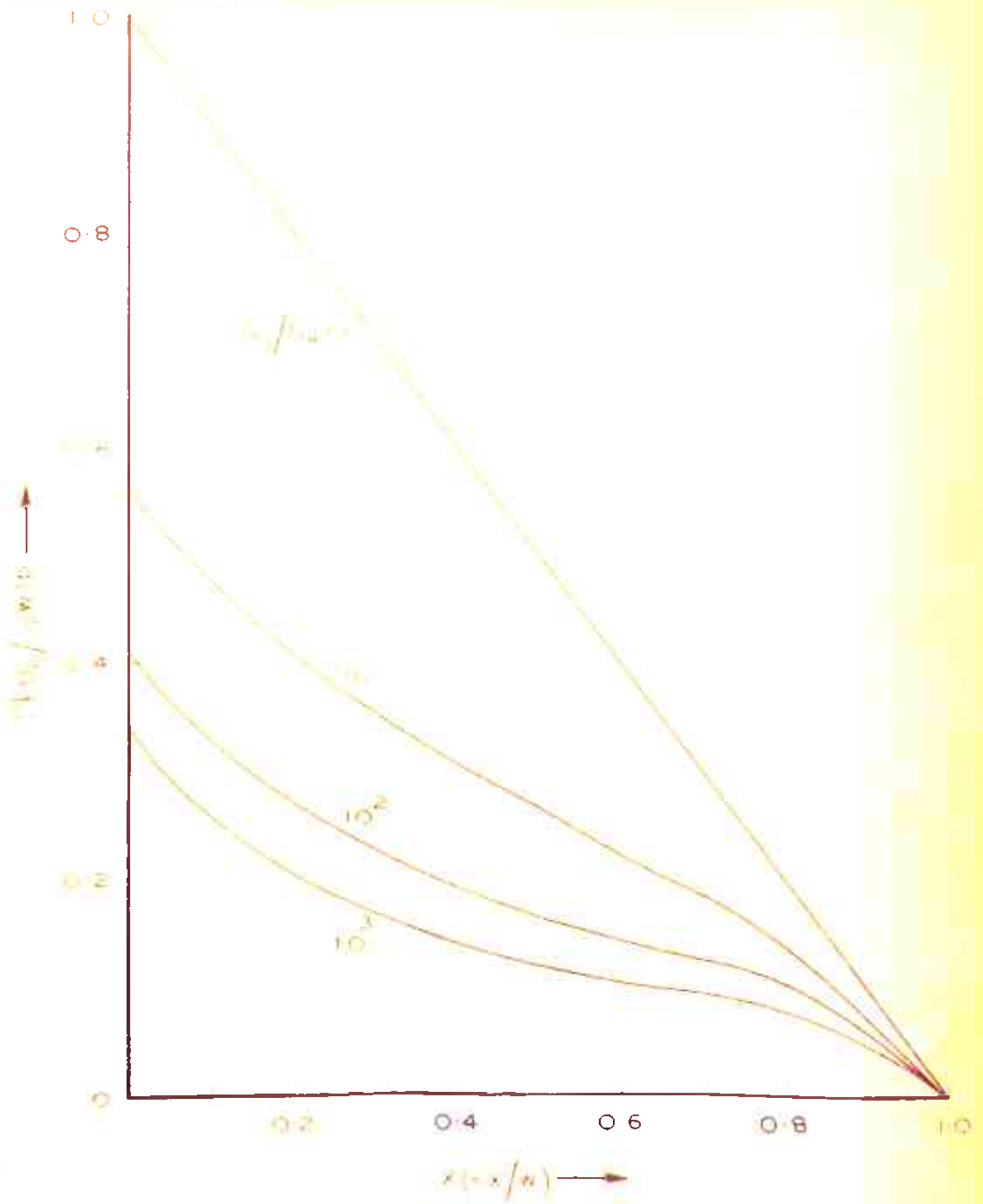


FIG 3.4 MINORITY CARRIER CONCENTRATION IN THE BASE REGION FOR GAUSSIAN DISTRIBUTION.

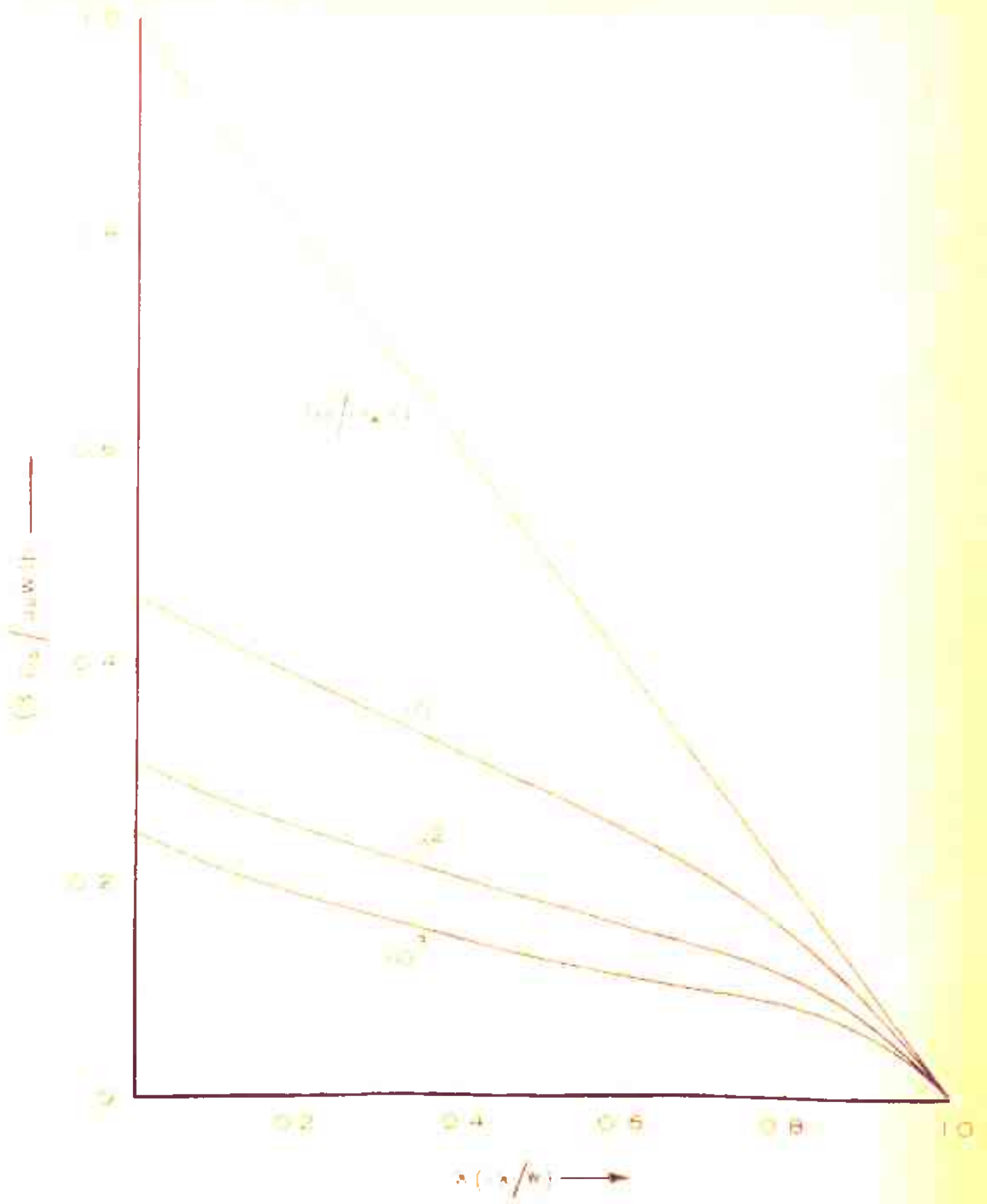


FIG. 35. MINORITY CARRIER CONCENTRATION IN THE BASE FOR EREC DISTRIBUTION.

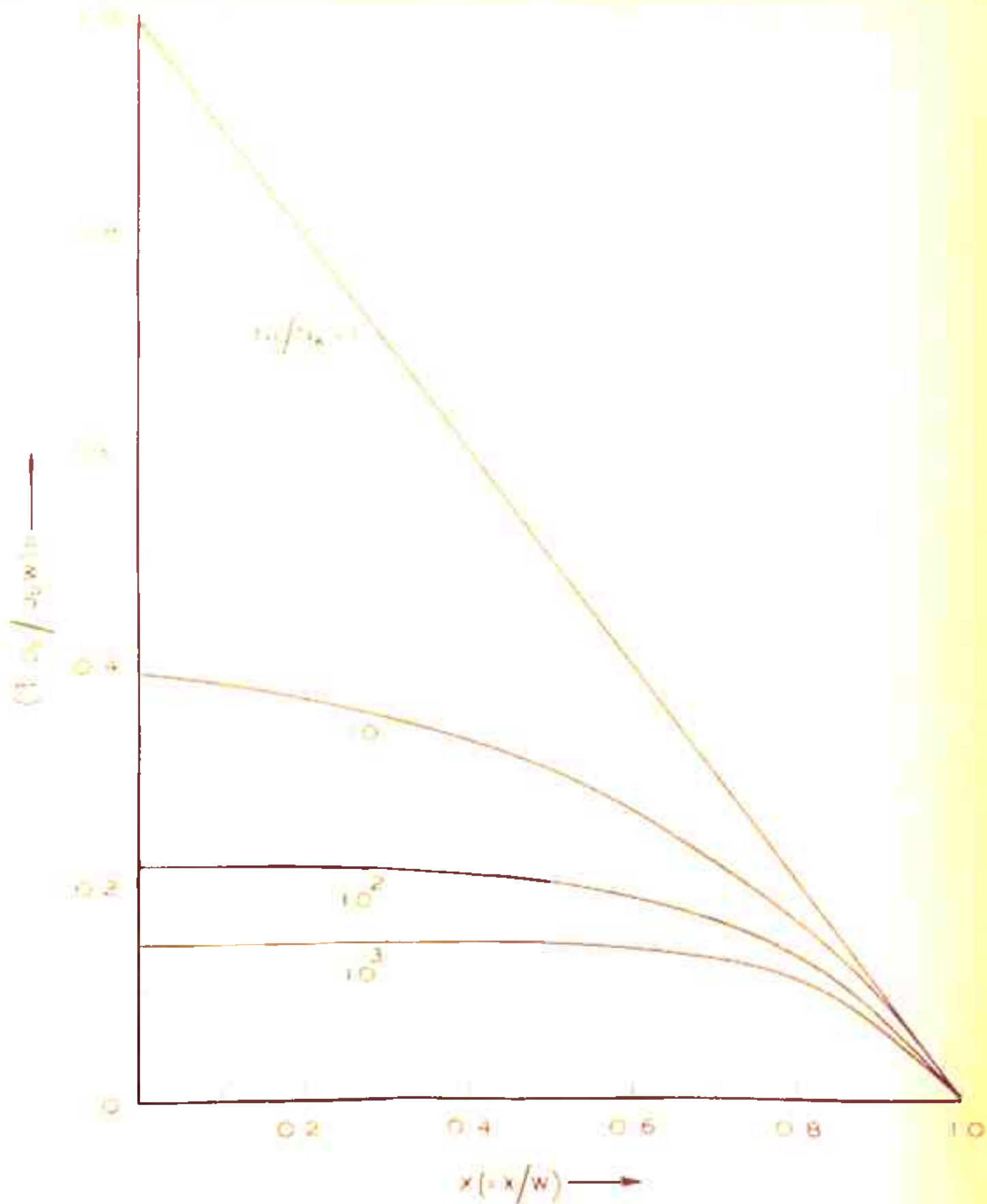


FIG. 3.6 MINORITY CARRIER CONCENTRATION IN THE BASE FOR EXPONENTIAL DISTRIBUTION.

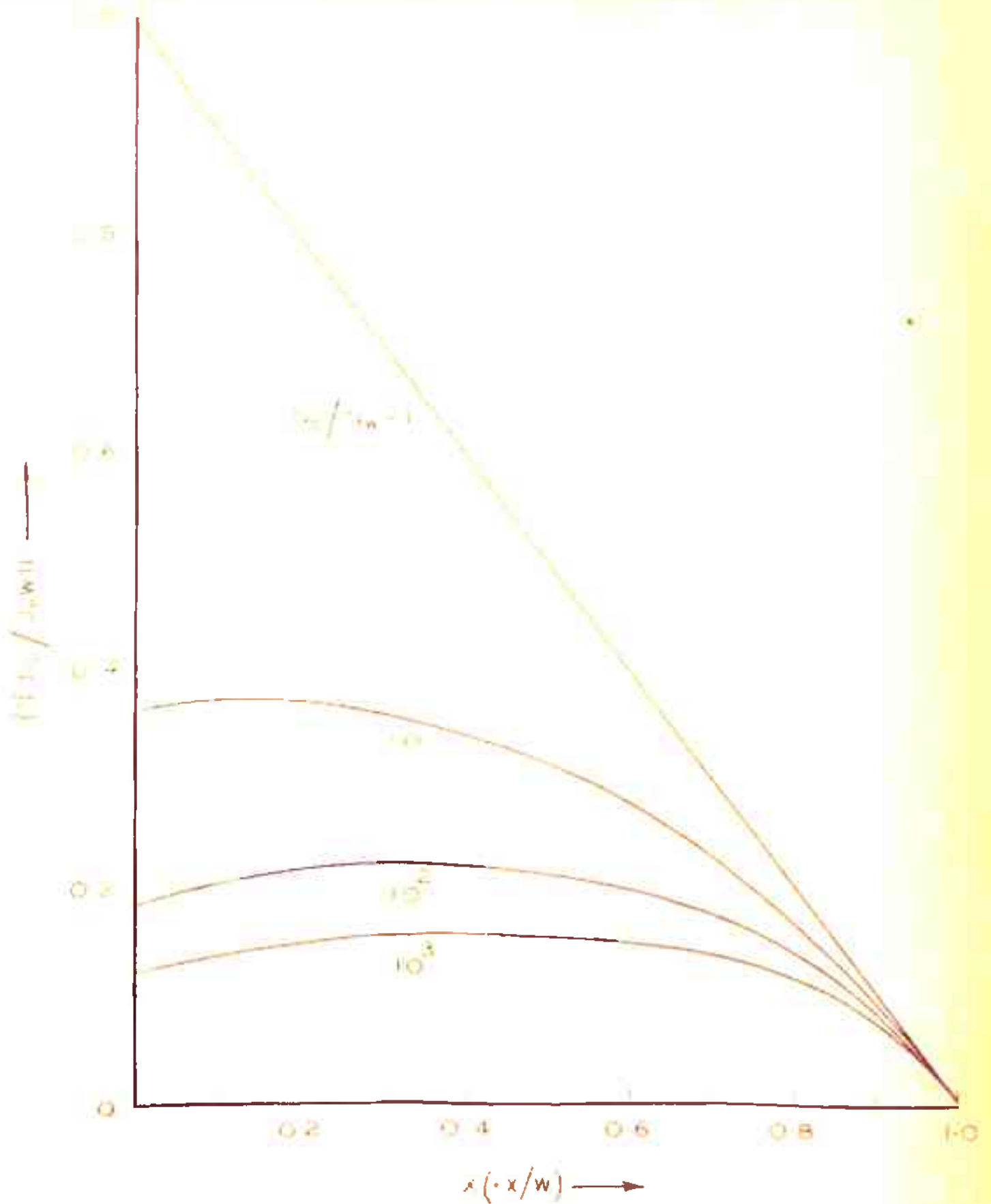


FIG. 37 MINORITY CARRIER CONCENTRATION IN THE BASE FOR HCB & GHB'S OPTIMUM DISTRIBUTION

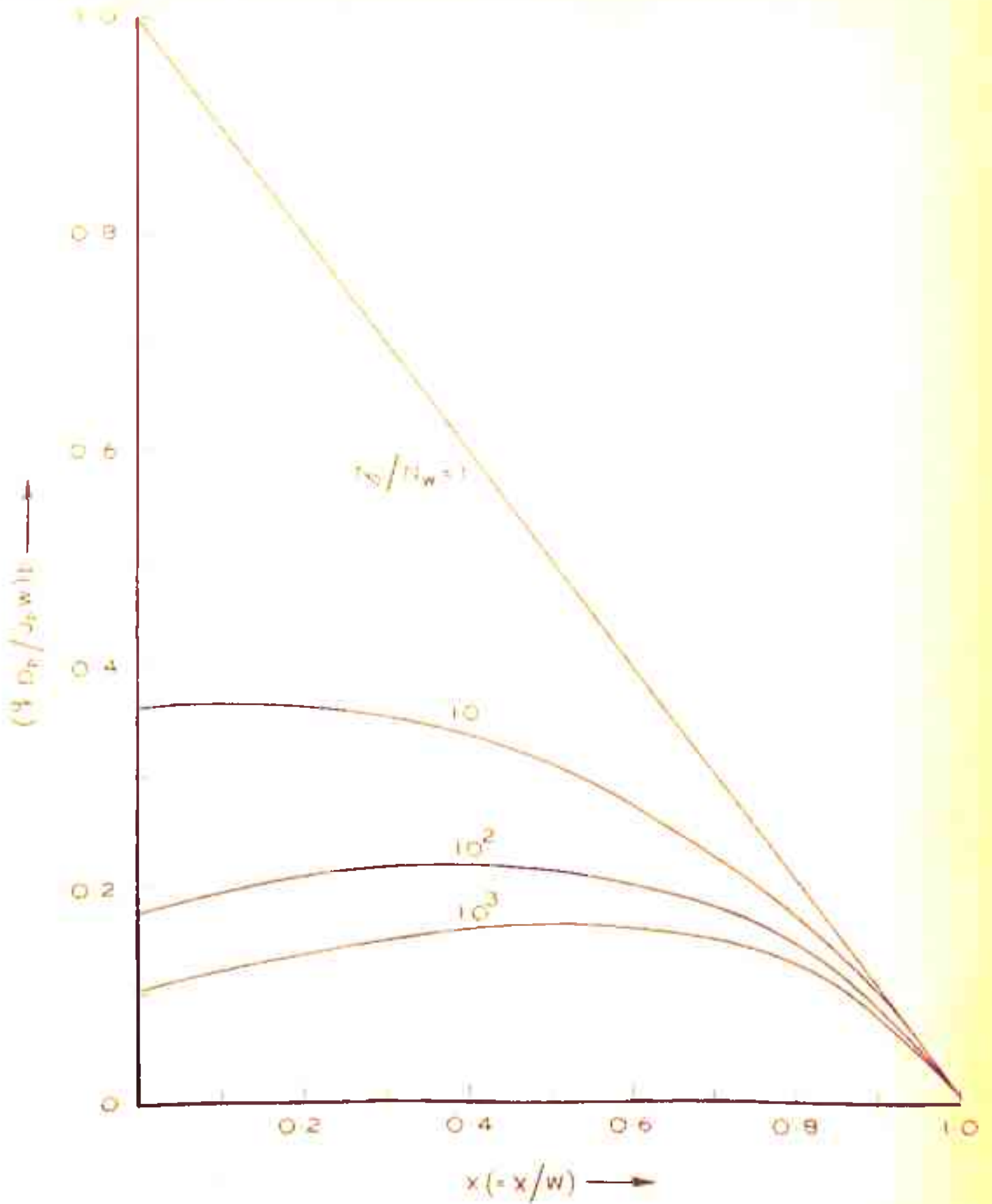


FIG. 3.8 MINORITY CARRIER CONCENTRATION IN THE BASE FOR MARSHAK'S OPTIMUM DISTRIBUTION

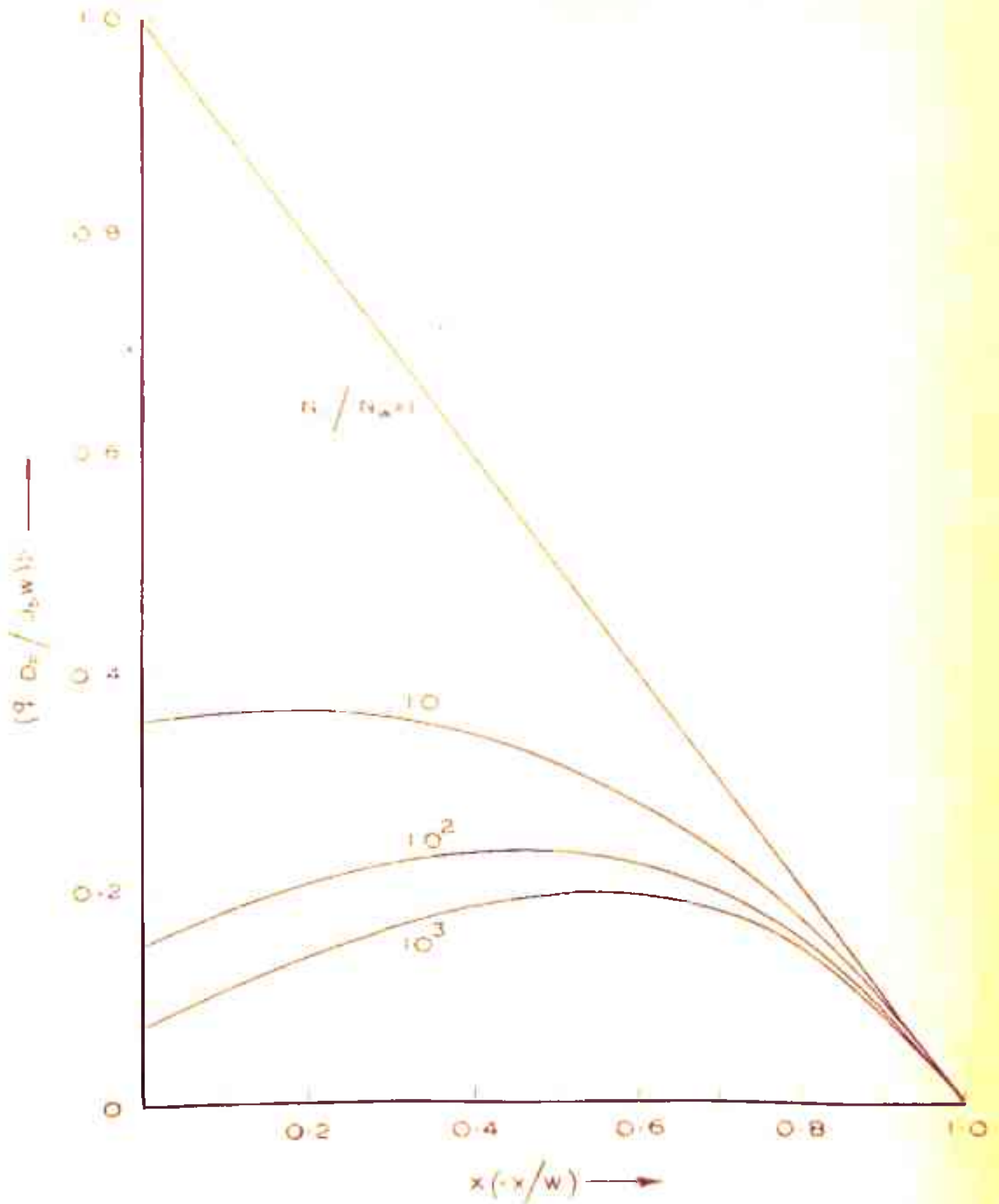


FIG. 3.9 MINORITY CARRIER CONCENTRATION IN THE BASE FOR HYPERBOLIC DISTRIBUTION.

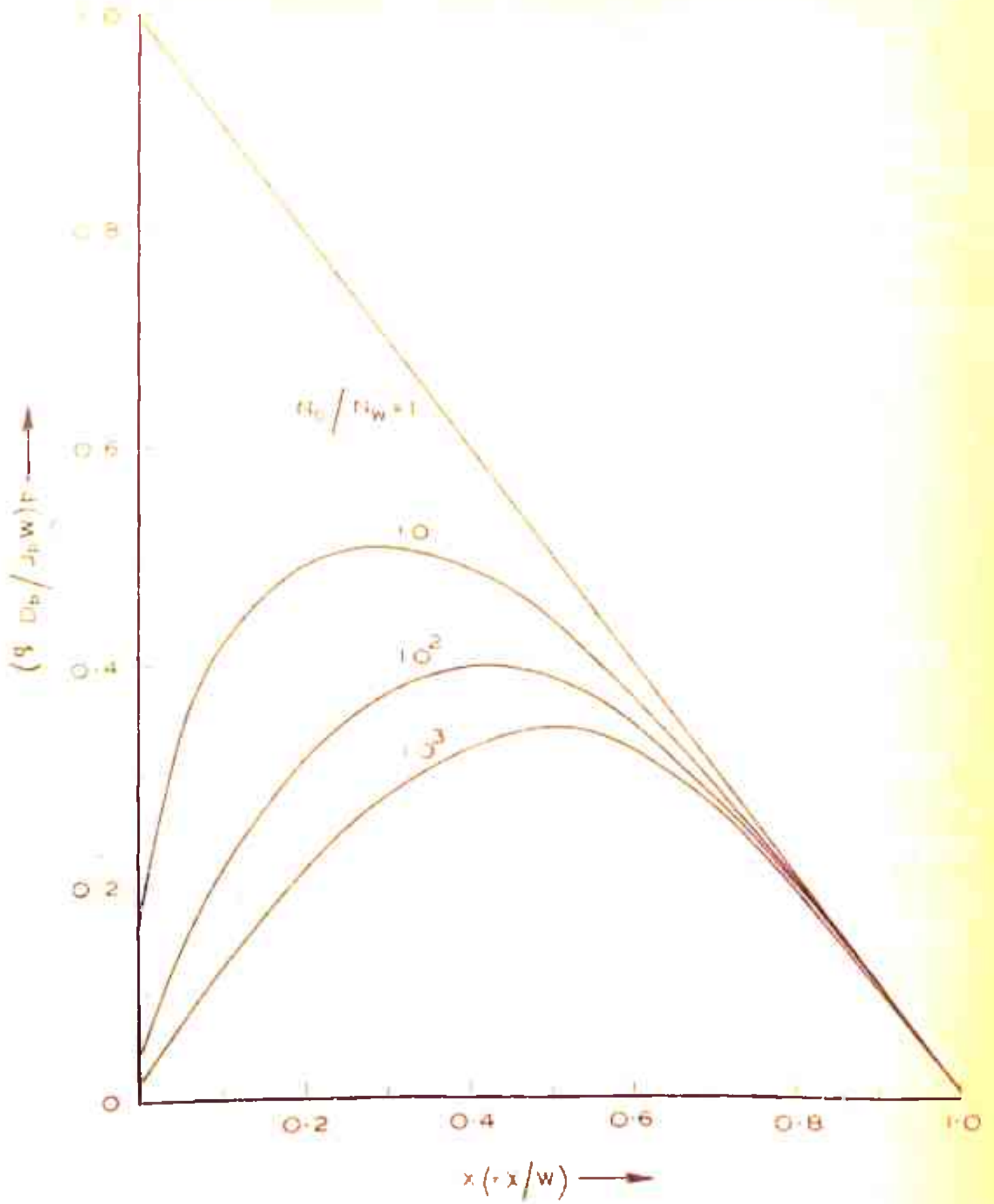


FIG 310 MINORITY CARRIER CONCENTRATION IN THE BASE FOR PARABOLIC-I DISTRIBUTION.

behaviour is in agreement with a similar study by Das and Boothroyd⁷, and Lindmeyer and Wrigley⁸. For impurity distributions which are concave down on a $\ln N$ Vs. X plot (Gaussian and Erfc.), the concentration plots show that the current flow in the base is due to a combination of diffusion and drift mechanisms. For all impurity distributions which are concave up on a $\ln N$ Vs. X plot, the minority carrier concentration is maximum somewhere in the base region resulting in a small diffusive flow of carriers towards emitters, while the major diffusive flow is towards the collector.

3.4.2 Doping Dependent Mobility Case

According to Sugano and Koshiga's mobility relation, the diffusion coefficient can be expressed as

$$D_p = D_o \left(\frac{N}{N_o}\right)^{-\theta} \quad \dots (3.13)$$

$$D_p = e^{-\eta/4} \cdot D_w \left(\frac{N}{N_o}\right)^{-\theta} \quad \dots (3.14)$$

$$D_p = \frac{2}{1 + e^{-\eta/4}} D_{avg} \left(\frac{N}{N_o}\right)^{-\theta} \quad \dots (3.15)$$

where D_o = diffusion coefficient corresponding to the emitter end impurity concentration N_o ,

D_w = diffusion coefficient corresponding to the collector end impurity concentration N_w ,

and $D_{avg} = \frac{D_o + D_w}{2}$

When the above relations for diffusion coefficients with $\theta = 0.25$ are substituted in eqn. 3.12, the following expressions for minority carrier concentration are obtained.

$$\left(\frac{q D_0}{J_p W}\right) p = \frac{\int_0^x (N(x)/N_0)^{1.25} dx}{N(x)/N_0} \quad \dots (3.16)$$

$$\left(\frac{q D_w}{J_p W}\right) p = e^{\eta/4} \frac{\int_0^x (N(x)/N_0)^{1.25} dx}{N(x)/N_0} \quad \dots (3.17)$$

$$\left(\frac{q D_{avg}}{J_p W}\right) p = \frac{1 + e^{\eta/4}}{2} \frac{\int_0^x (N(x)/N_0)^{1.25} dx}{N(x)/N_0} \quad \dots (3.18)$$

In the above relations, it is interesting to note that the minority carrier concentration corresponding to the diffusion coefficient D_0 (eqn. 3.16) is common to all. Calculations based on eqn. 3.16 are made for several base doping distributions discussed earlier. The results are given in Figs. 3.11 and 3.12 for $N_0/N_w = 10^2$ and 10^3 , respectively.

A study of these figures shows that in comparison with constant mobility case, the diffusive tendency of the carriers towards collector increases for distributions which are concave down on $\ln N$ Vs. X plot, whereas the diffusive tendency towards emitter is reduced for distributions which are concave up on such a plot.

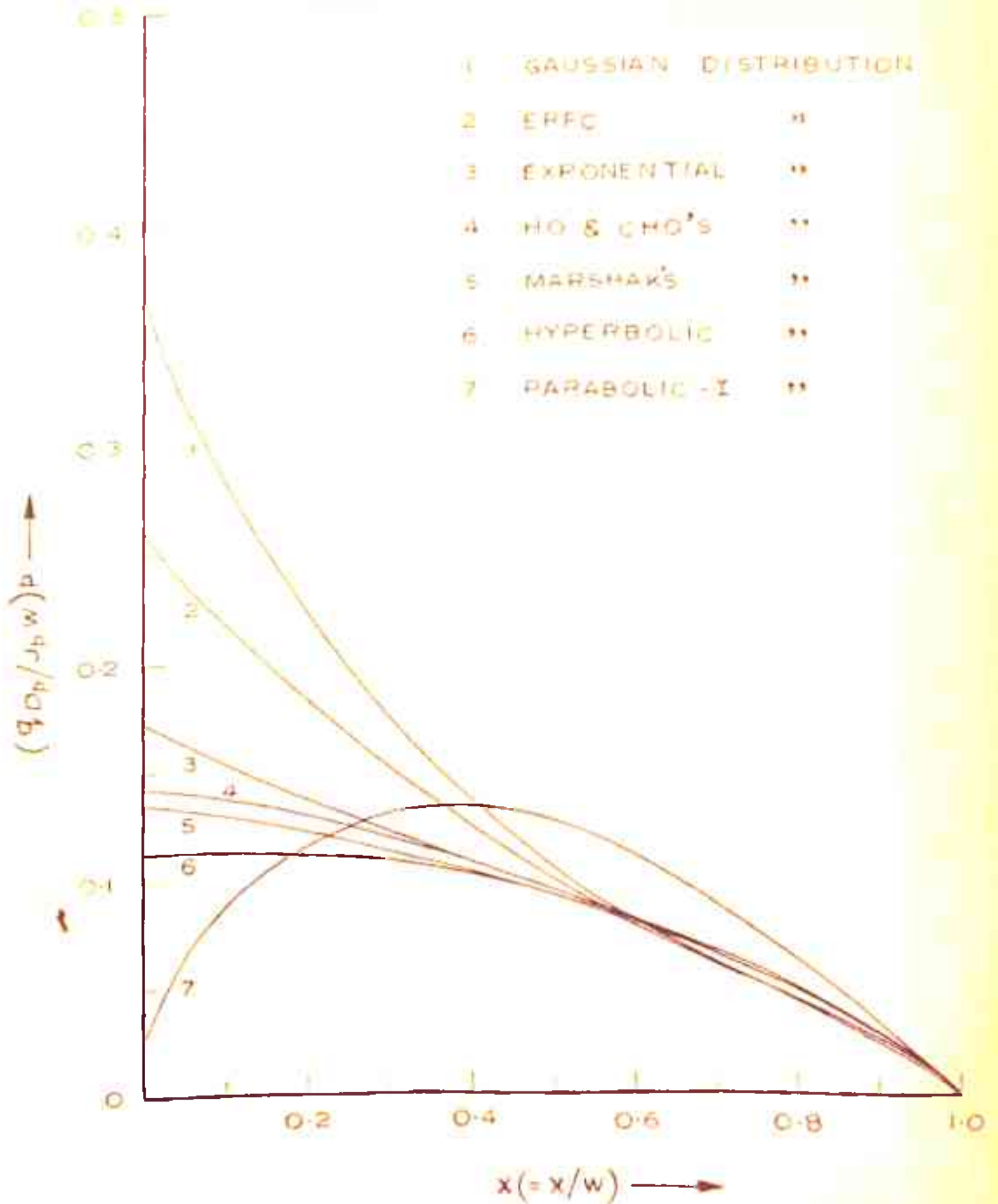


FIG 3.11 MINORITY CARRIER CONCENTRATION IN THE BASE WHEN THE MOBILITY IS NOT CONSTANT ($N_0/N_w = 10^2$).

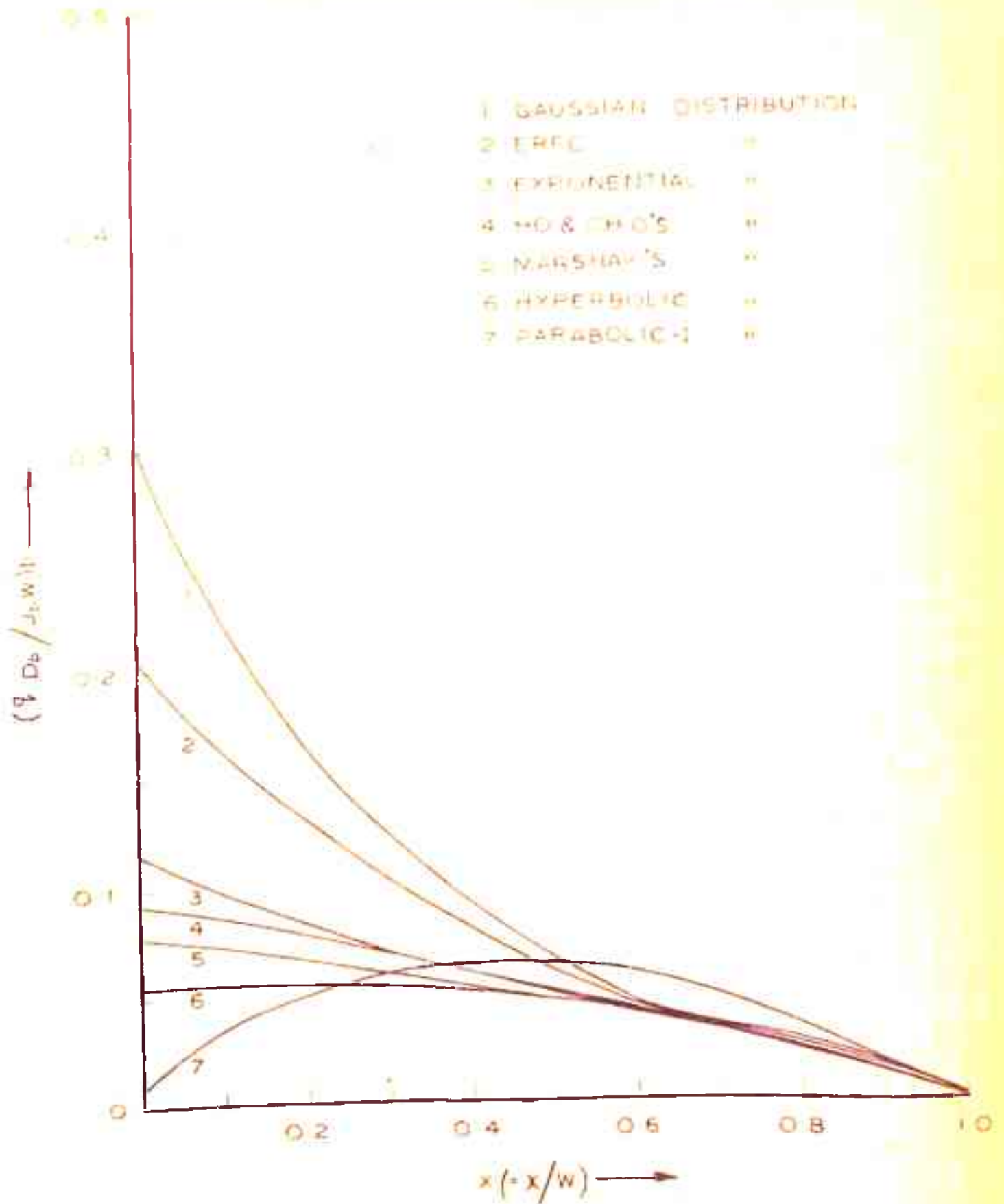


FIG 3.12 MINORITY CARRIER CONCENTRATION IN THE BASE WHEN MOBILITY IS NOT CONSTANT ($N_0/N_W = 10^3$).

3.5 MINORITY CARRIER BASE TRANSIT TIME WHEN MOBILITY IS CONSTANT

When the carrier mobility in the base is assumed to be independent of doping density, the base transit time relation 2.37 (Chapter 2) can be written in the following form.

$$\frac{t_B}{t_{BU}} = 2 \int_0^1 \frac{\int_0^1 N(x)/N_0 dx}{N(x)/N_0} \cdot dx \quad \dots (3.19)$$

where $t_{BU} (= w^2/2 D_p)$ denotes the base transit time of a uniform base transistor.

All impurity distributions considered in Section 3.2 are treated and the base transit time is obtained by numerical computational methods. The need for numerical method arises from the fact that an explicit solution of eqn. 3.19 is not always possible. The integrals are evaluated with the help of Simpson's integration formula. The computer program for such an evaluation is described in Appendix-III. As an illustrative example, Gaussian impurity distribution is considered, but the procedure will be same for all other impurity distributions except Ho and Cho's optimum distribution where the impurity distribution is not expressible explicitly. The impurity distribution in this case is evaluated using Newton-Raphson's method as described in Appendix-II.

The results of normalised base transit time, as obtained by the computer solution of eqn. 3.19, are presented

in Table 3.2. It is obvious that the transit time is minimum when exponential doping distribution is used in the base region.

3.6 INFLUENCE OF DOPING DEPENDENT CARRIER MOBILITY ON BASE TRANSIT TIME

In present-day discrete and integrated circuit transistors, formed by solid-state diffusion techniques, the impurity concentration in the base is quite high near the emitter end. Hence the minority carrier mobility cannot be assumed to be independent of doping. In this section, the influence of doping dependent mobility on base transit time is investigated.

The general expression relating base transit time to an arbitrary base impurity distribution can be written as (Sec. 2.3.2, Chapter 2)

$$t_B = w^2 \int_0^1 \frac{\int_0^1 \frac{N(x)}{D_p(x)} dx}{N(x)} dx \quad \dots (3.20)$$

The calculations of transit time for several impurity distributions of Sec. 3.2 are carried out with the aid of eqn. 3.20. Different empirical relations of carrier mobility discussed in the previous chapter are treated.

3.6.1 Sugano and Koshige's Mobility Relation

This power law relation of doping dependent mobility has been discussed in Chapter 2. In this relation, the problem

TABLE 3.2

Calculation of Normalised Base Transit Time
(t_B/t_{B0}) for Constant Mobility Case

$\frac{N_0}{N_w}$	Impurity Distributions								
	Gaussian	Parebo-lic-II	Erfc.	Arbit-rary	Expo-nential	Ho and Cho's optimum	Marshak's optimum	Hyper-bolic	Parabo-lic-I
1	1.00	-	1.0	-	1.0	1.0	1.0	1.0	1.0
10	0.54110	-	0.53270	0.53140	0.52908	0.53444	0.53140	0.53297	0.68594
10 ²	0.36398	-	0.35020	0.34254	0.34093	0.34820	0.34760	0.35737	0.54827
10 ³	0.27595	0.26887	0.26099	0.25226	0.24765	0.25355	0.25745	0.28031	0.43467

is to choose a suitable value of reference mobility μ_R . In the original equation⁹, Sugeno and Koshiga have used a reference mobility value corresponding to the collector end impurity concentration in the base. For a study of carrier transport through the base, Pritchard¹⁰ has stressed that the reference mobility value corresponding to the average impurity concentration in the base should be used. As there is no convergent opinion in this matter, both the above values of reference mobility are considered. In addition, the reference mobility value corresponding to the emitter end concentration is also used.

Since mobility and diffusion coefficient are related to each other through Einstein's relation, the above arguments apply to the carrier diffusion coefficient as well. Using the diffusion coefficient relations expressed through eqns. 3.13, 3.14, and 3.15, the base transit times corresponding to the reference diffusion coefficients D_0 , D_w , and D_{avg} , can be expressed as follows.

$$\frac{t_B}{t_{B0}} = 2 \int_0^1 \frac{(N(x)/N_0)^{1.25} dx}{N(x)/N_0} \quad \dots (3.21)$$

$$\frac{t_B}{t_{BW}} = \frac{\eta}{4} \cdot \frac{t_B}{t_{B0}} \quad \dots (3.22)$$

$$\frac{t_B}{t_{B_{avg}}} = \frac{1 + \frac{\eta}{4}}{2} \cdot \frac{t_B}{t_{B0}} \quad \dots (3.23)$$

where $t_{B0} (= w^2/2 D_0)$, $t_{BW} (= w^2/2 D_w)$ and $t_{B_{avg}} (= w^2/2 D_{avg})$

denote base transit times of a uniform base transistor having base impurity concentration corresponding to N_o , N_w , and average impurity concentration.

The average value of the diffusion coefficient is given as

$$D_{avg} = \frac{D_o + D_w}{2} \quad \dots (3.24)$$

The above equations are evaluated numerically for base impurity distributions treated earlier. The results of the normalised transit time t_B/t_{B0} are summarised in Table 3.3. This value is common to all the transit time relations (eqns. 3.21 to 3.23). The computer program for calculating base transit time in the case of doping dependent mobility is given in Appendix-IV. Ho and Cho's optimum distribution has been used for this illustration.

The normalised values of transit time versus $\ln(N_o/N_w)$ are plotted in Figs. 3.13 to 3.18 for several impurity distributions. The reference values of diffusion coefficients D_o , D_w , and D_{avg} serve as parameters. For comparison, the values of transit time obtained in the case of constant mobility are also plotted. The solid curves in the figures correspond to the doping dependent mobility case while the dotted curves are for the case of constant mobility.

TABLE 3.3

Calculation of Normalised Base Transit Time (t_B/t_{30})

Yoshiz Sugano and Kosmiga's Mobility Relation

$\frac{N_0}{N_w}$	Impurity Distributions					
	Gaussian	Erfc.	Exponential	Marehak's optimum	Hyperbolic	Parabolic-I
10	0.43663	0.40042	0.37557	0.36861	0.36537	0.40114
10^2	0.25976	0.22192	0.18272	0.17039	0.16381	0.18099
10^3	0.18136	0.14746	0.10431	0.08990	0.08184	0.08742
10^4	0.13834	0.10858	0.06601	0.05149	0.04320	0.04411

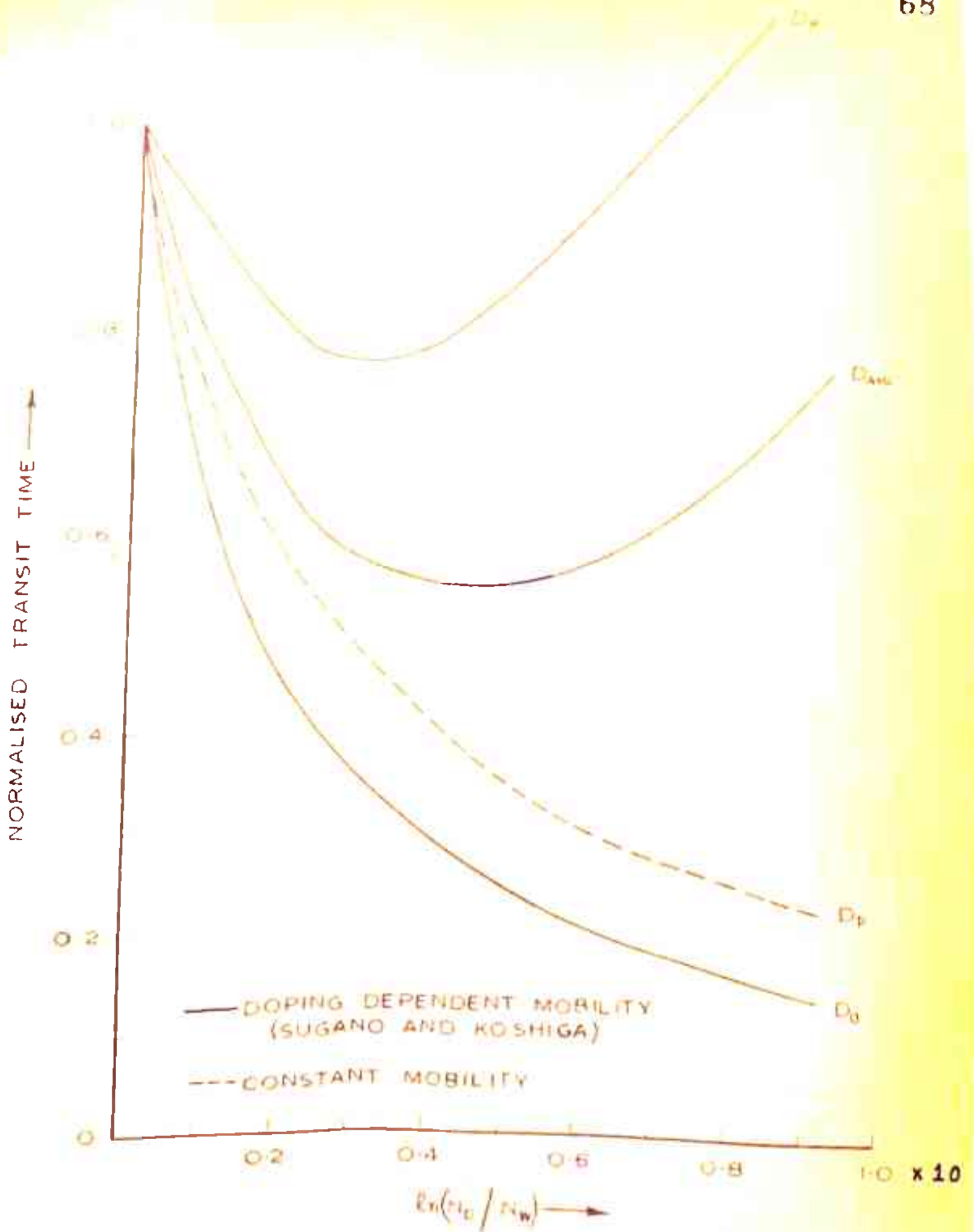


FIG.313 DEPENDENCE OF TRANSIT TIME ON THE BUILT-IN ELECTRIC FIELD IN THE BASE-GAUSSIAN DISTRIBUTION.

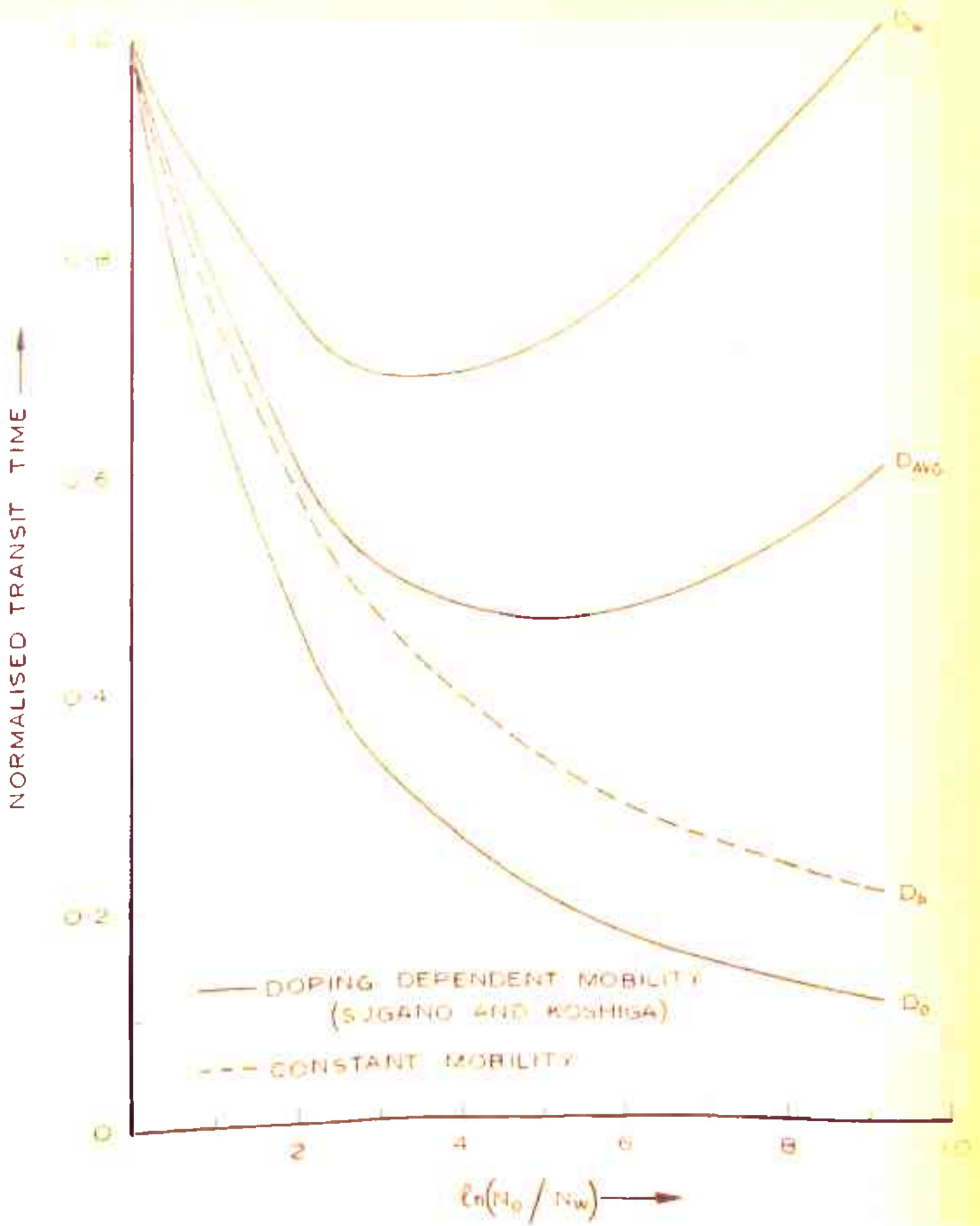


FIG. 3.14 DEPENDENCE OF BASE TRANSIT TIME ON THE BUILT-IN ELECTRIC FIELD IN THE BASE—BREC DISTRIBUTION

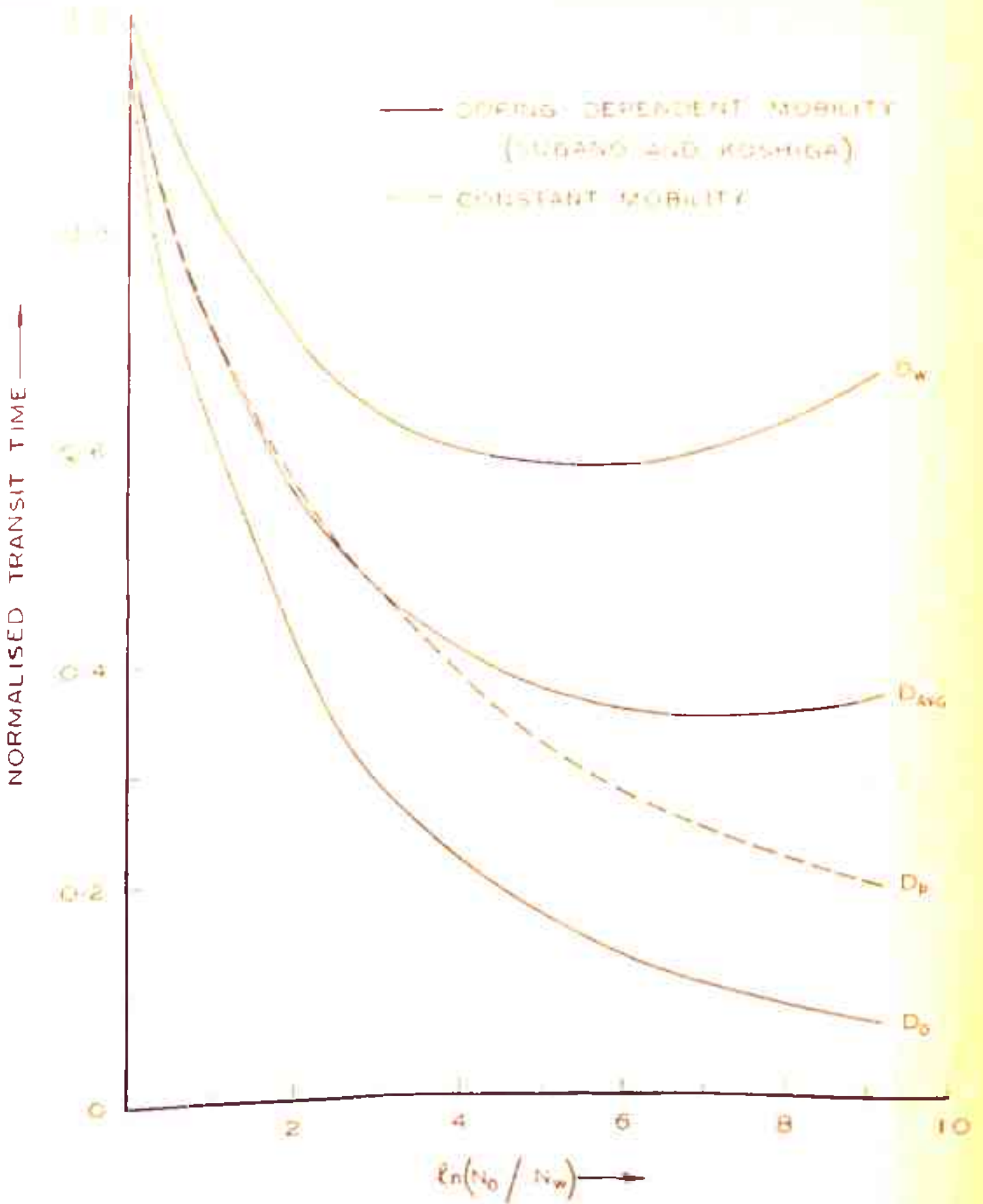


FIG. 315 DEPENDENCE OF BASE TRANSIT TIME ON THE BUILT-IN ELECTRIC FIELD IN THE BASE-EXPONENTIAL DISTRIBUTION.

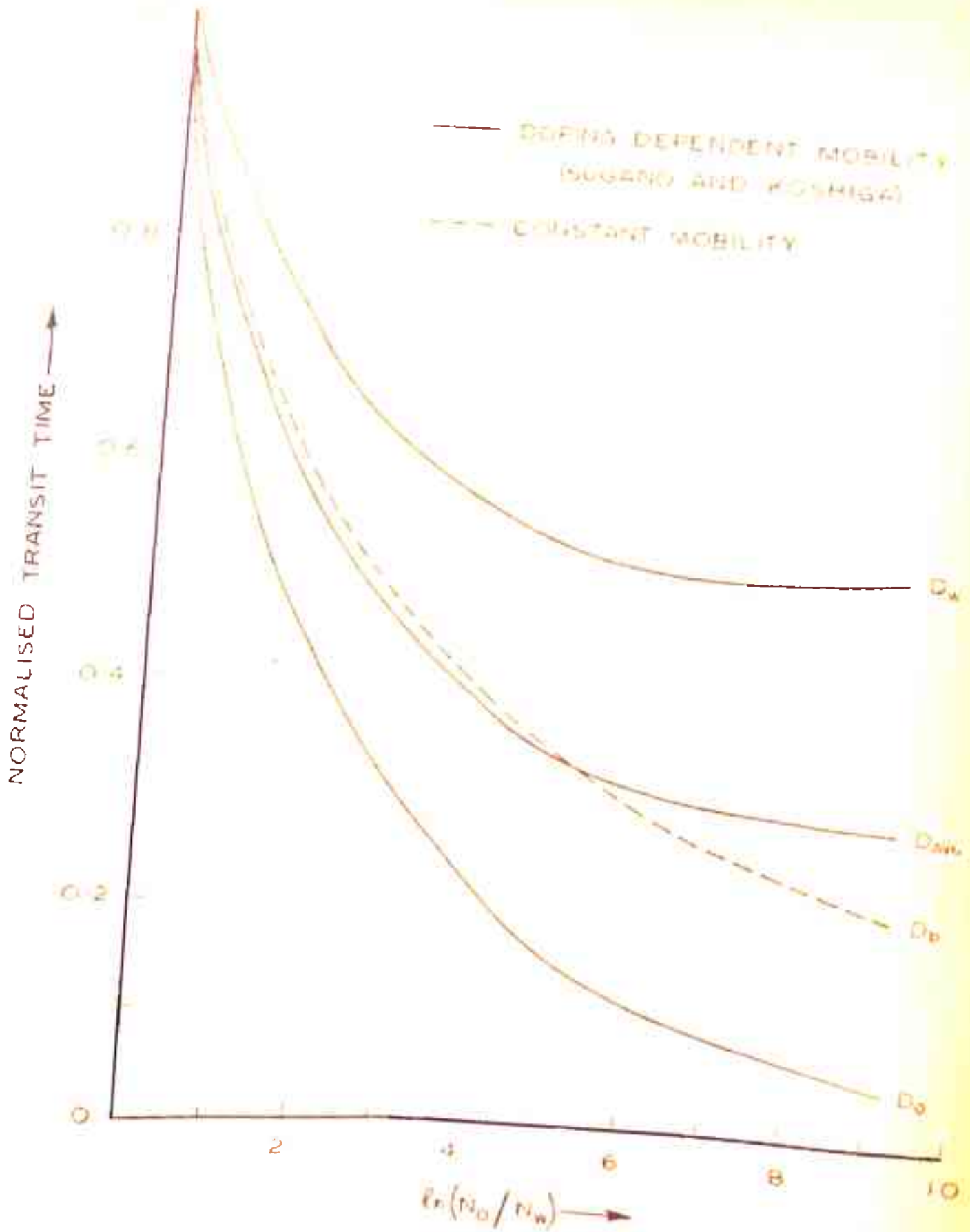


FIG. 3.16 DEPENDENCE OF BASE TRANSIT TIME ON THE BUILT-IN ELECTRIC FIELD IN THE BASE-MARSHAK'S OPTIMUM DISTRIBUTION.

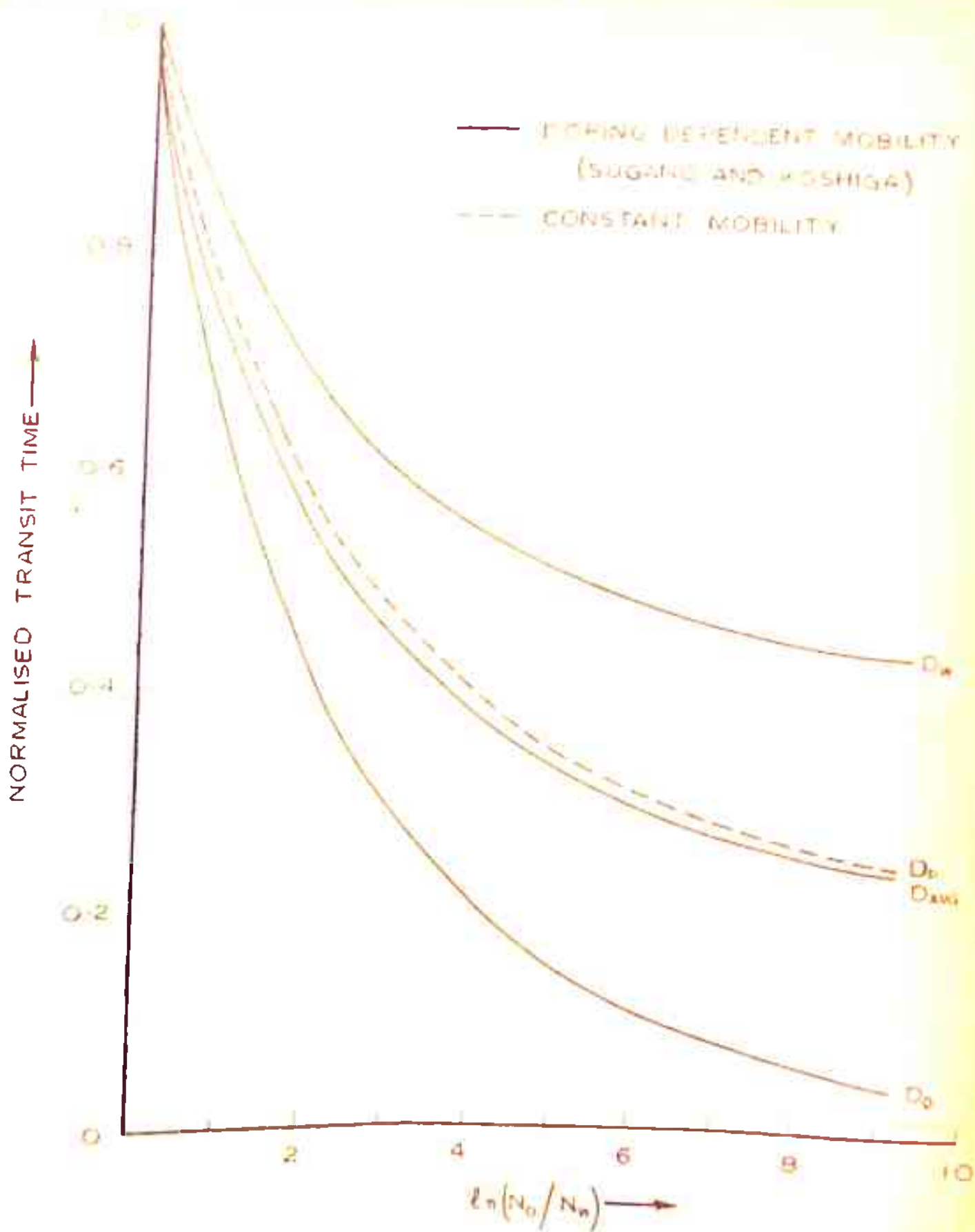


FIG.317 DEPENDENCE OF BASE TRANSIT TIME ON THE BUILT-IN ELECTRIC FIELD IN THE BASE—HYPERBOLIC DISTRIBUTION.

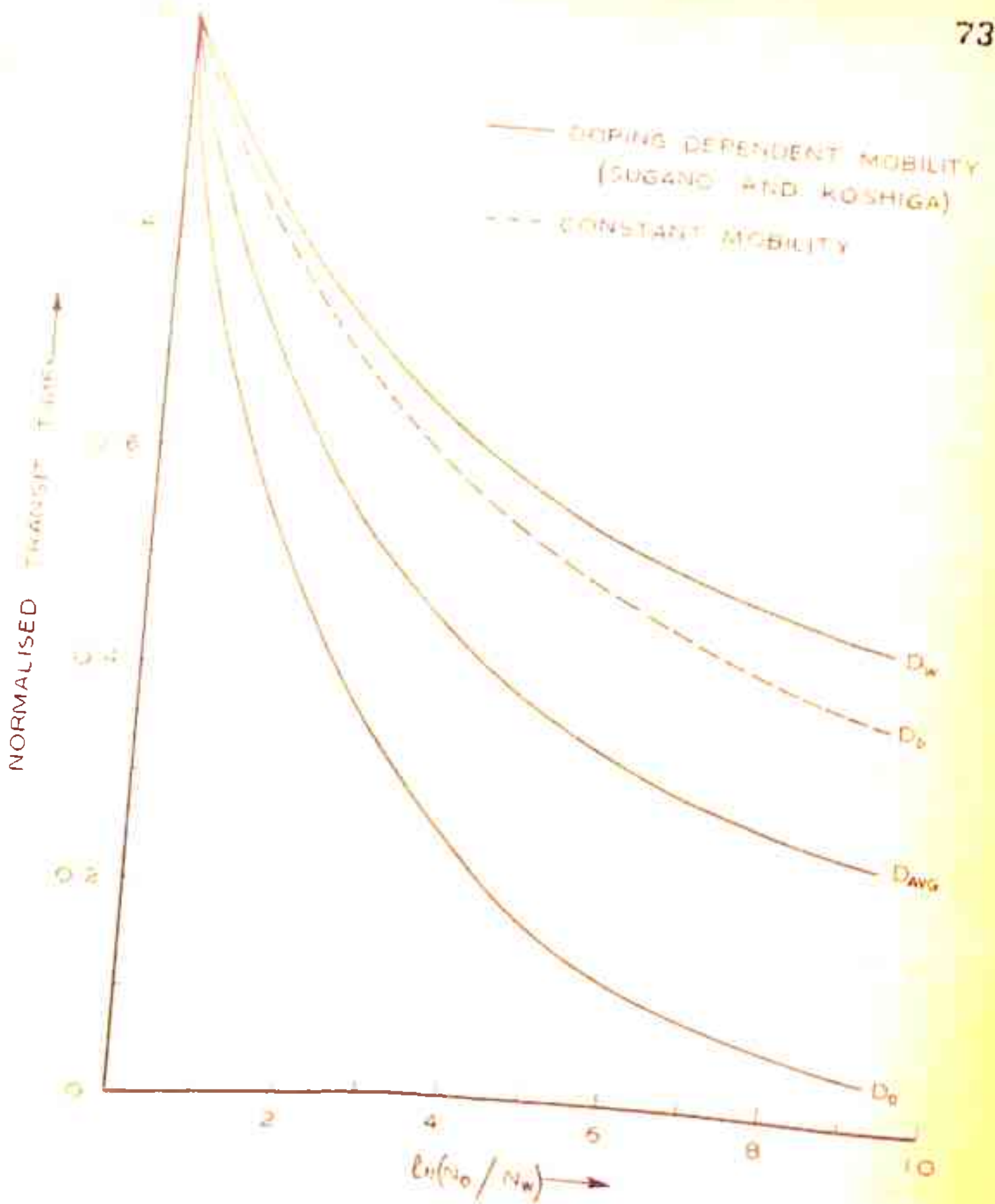


FIG 3 18 DEPENDENCE OF BASE TRANSIT TIME ON THE BUILT-IN ELECTRIC FIELD IN THE BASE-PARABOLIC-I DISTRIBUTION.

3.6.2 Marshak's Mobility Relation

In this case also, the evaluation of transit time expression 3.20 is attempted with reference values of diffusion coefficient D_0 , D_w and D_{avg} . The diffusion constant can be written as

$$D_p = D_0 \left(1 - \frac{b}{D_0} \ln N/N_0 \right) \quad \dots (3.25)$$

$$D_p = \frac{D_w}{\left(1 + \frac{b}{D_0} \eta \right)} \left(1 - \frac{b}{D_0} \ln N/N_0 \right) \quad \dots (3.26)$$

$$D_p = \frac{D_{avg}}{\left(1 + \frac{b}{D_0} \frac{\eta}{2} \right)} \left(1 - \frac{b}{D_0} \ln N/N_0 \right) \quad \dots (3.27)$$

where $D_0 = a - b \ln N_0$, and a, b are constants given in Table 2.1 (Chapter 2).

Substituting the above relations in eqn. 3.20, the transit time is given by

$$\frac{t_B}{t_{B0}} = 2 \int_0^1 \frac{\left\{ \frac{N(x)/N_0}{1 - \frac{b}{D_0} \ln N(x)/N_0} \right\} dx}{N(x)/N_0} \quad \dots (3.28)$$

$$\frac{t_B}{t_{Bw}} = \left(1 + \frac{b}{D_0} \eta \right) \frac{t_B}{t_{B0}} \quad \dots (3.29)$$

$$\frac{t_B}{t_{Bavg}} = \left(1 + \frac{b}{D_0} \frac{\eta}{2} \right) \frac{t_B}{t_{B0}} \quad \dots (3.30)$$

For different impurity distributions, the transit time calculations are made on digital computer. The results of normalised transit time t_B/t_{B0} are given in Table 3.4. Figs. 3.19 to 3.24

TABLE 3.4

**Calculation of Normalised Base Transit Time (t_b/t_{30})
using Marahak's Mobility Relation**

$\frac{N_0}{N_w}$	Impurity Distributions				
	Gaussian	Erfc.	Exponential	Marahak's optimum	Hyperbolic - I
10	0.45574	0.42551	0.40576	0.40107	0.39902
10^2	0.28189	0.25017	0.21956	0.21262	0.21066
10^3	0.20265	0.17385	0.13969	0.13223	0.13280
10^4	0.15805	0.13243	0.09795	0.09060	0.09437
					0.17782
					0.26923
					0.46305

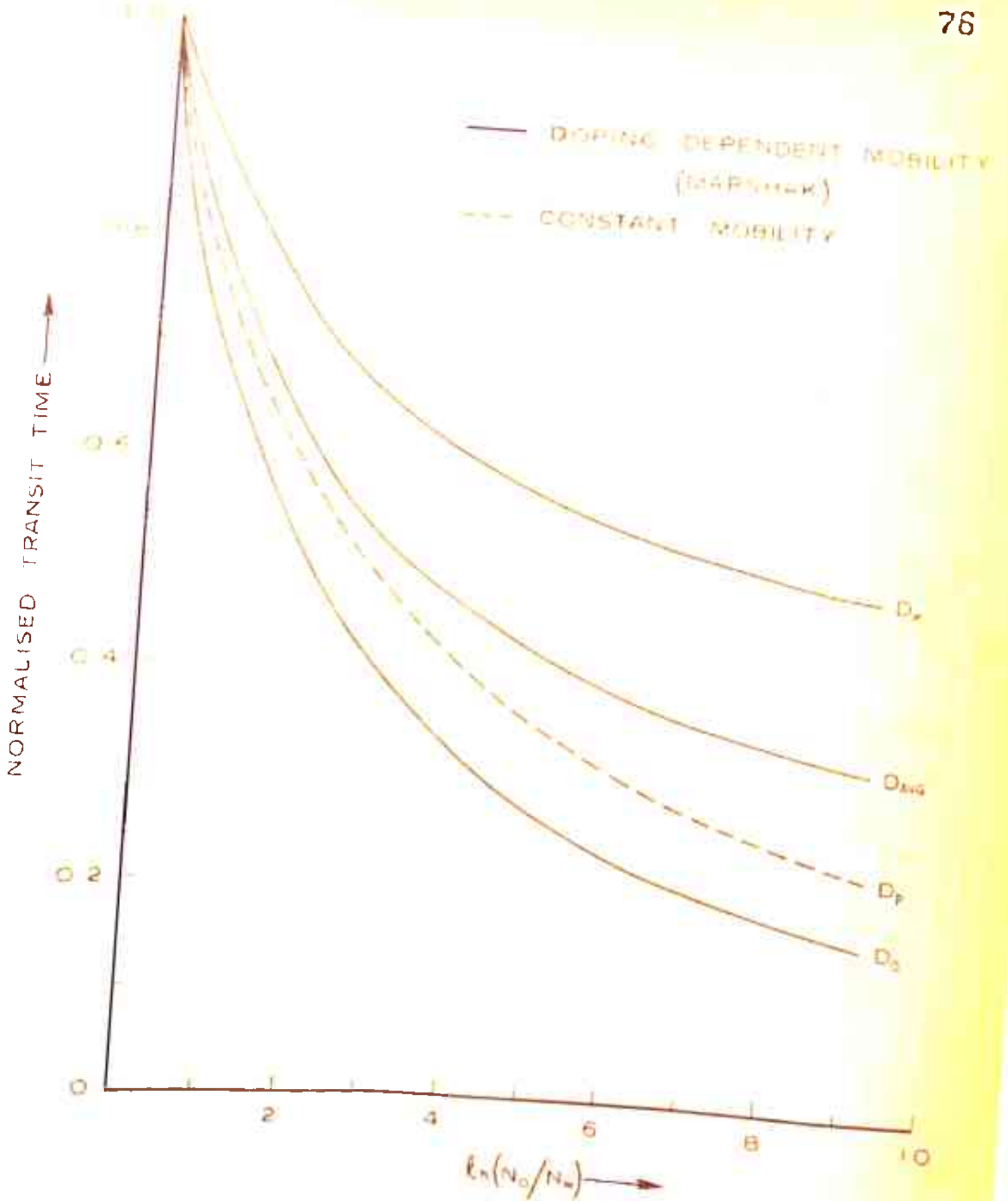


FIG. 3:19 DEPENDENCE OF BASE TRANSIT TIME ON THE BUILT-IN ELECTRIC FIELD IN THE BASE — GAUSSIAN DISTRIBUTION.

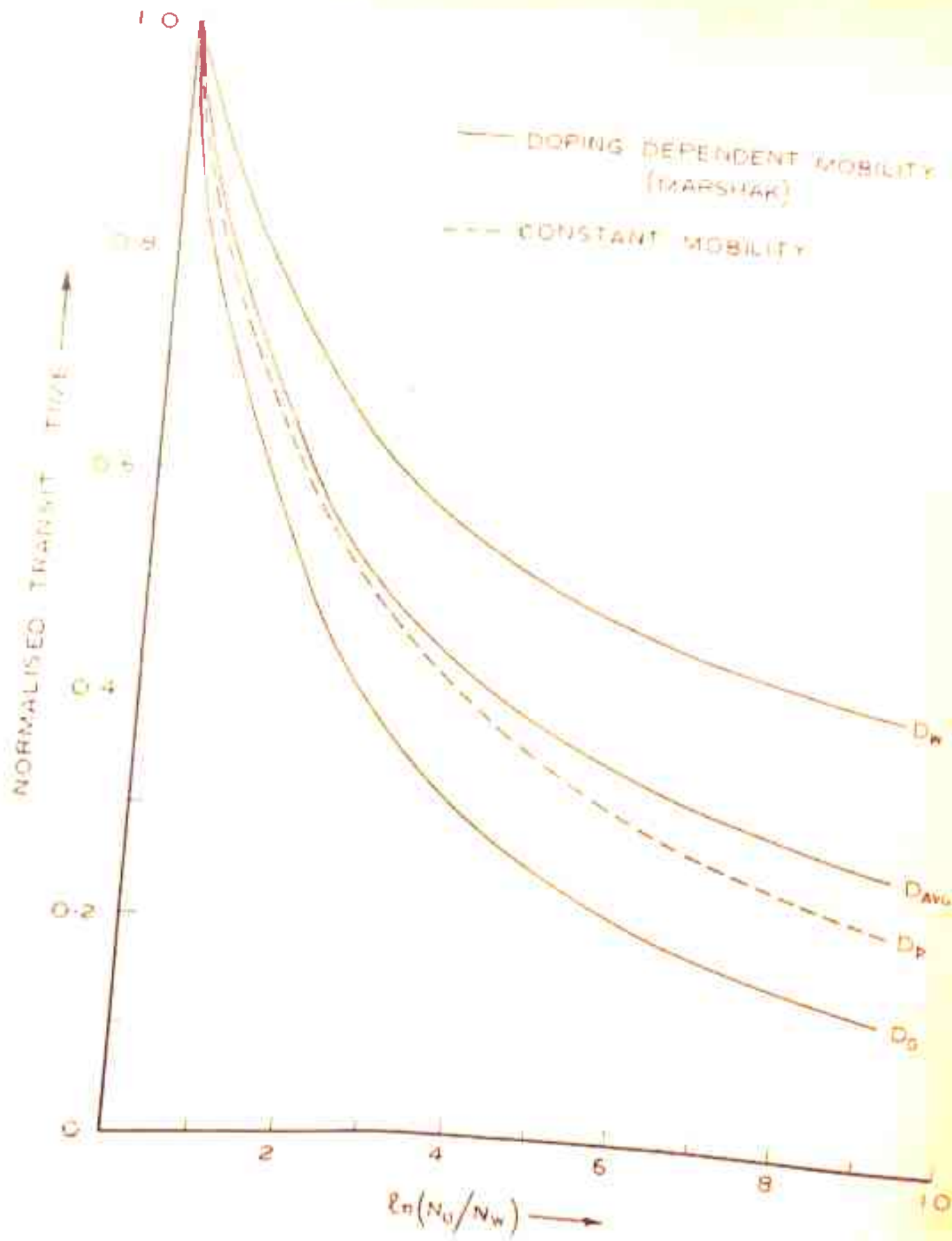


FIG 3.20 DEPENDENCE OF BASE TRANSIT TIME ON THE BUILT-IN ELECTRIC FIELD IN THE BASE — ERFC. DISTRIBUTION.

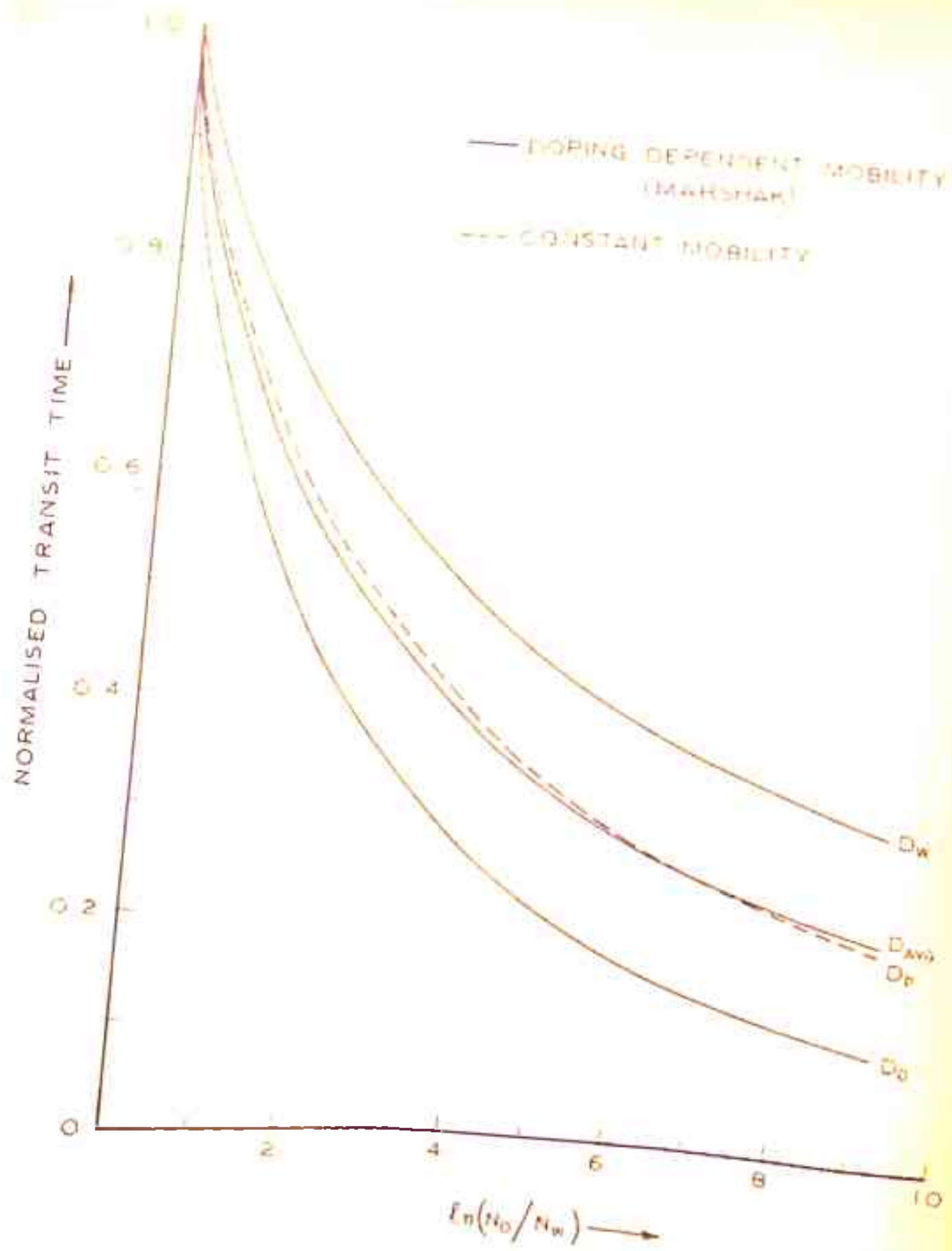


FIG 3.21 DEPENDENCE OF BASE TRANSIT TIME ON THE BUILT-IN ELECTRIC FIELD IN THE BASE—EXPONENTIAL DISTRIBUTION

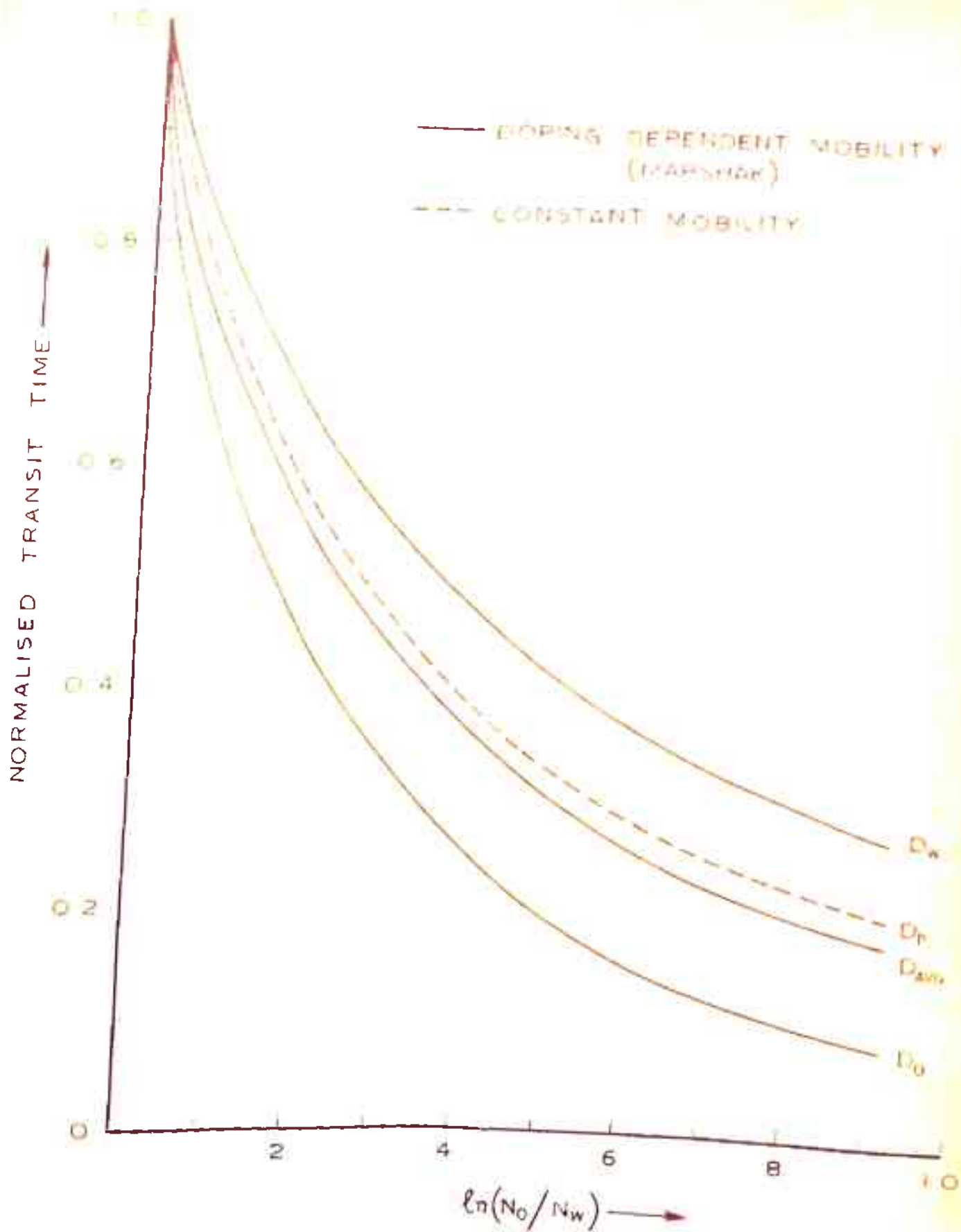


FIG 3.22 DEPENDENCE OF BASE TRANSIT TIME ON THE BUILT-IN ELECTRIC FIELD IN THE BASE-MARSHAK'S OPTIMUM DISTRIBUTION

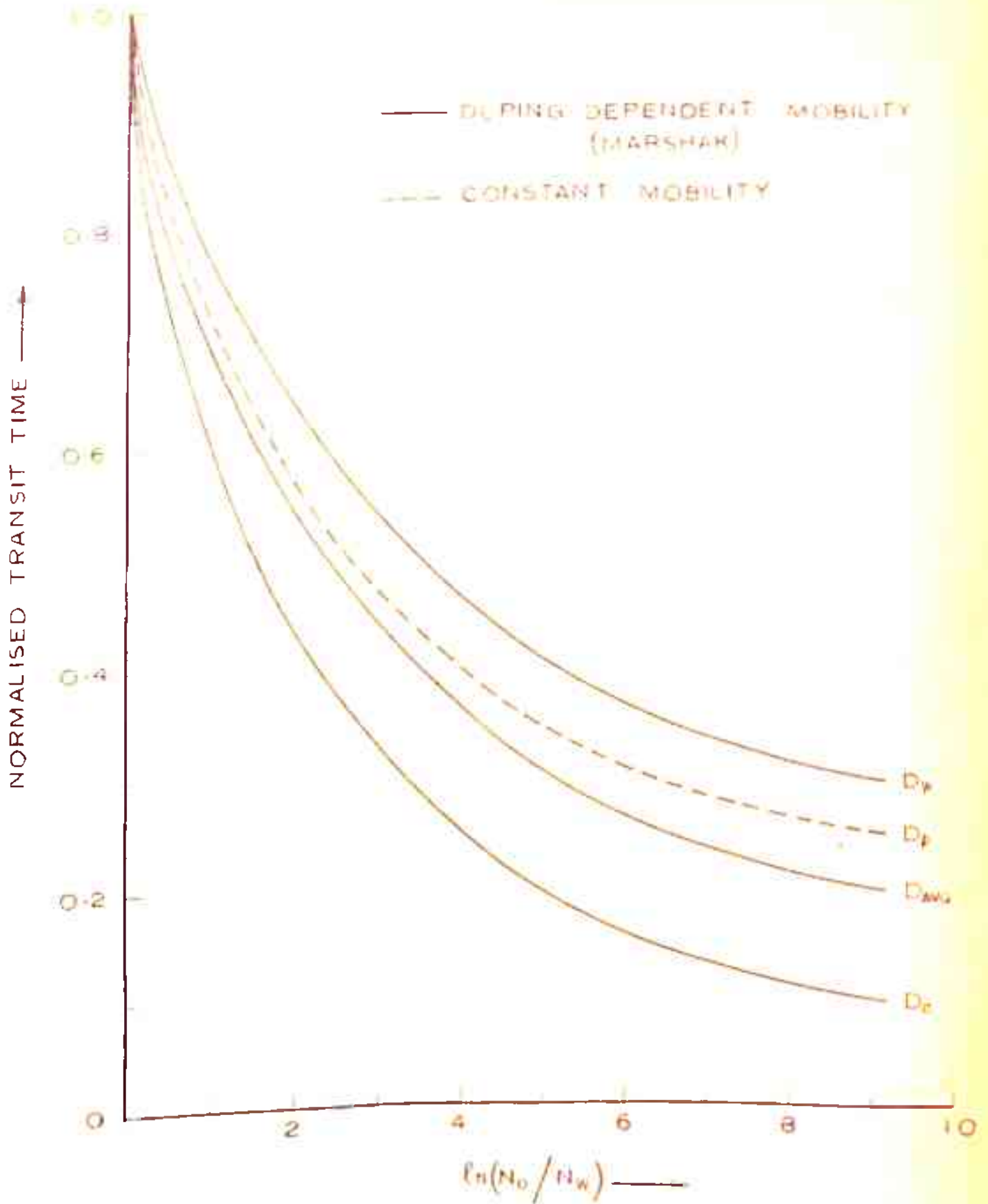


FIG. 3-23 DEPENDENCE OF TRANSIT TIME ON THE BUILT-IN ELECTRIC FIELD IN THE BASE—HYPERBOLIC DISTRIBUTION.

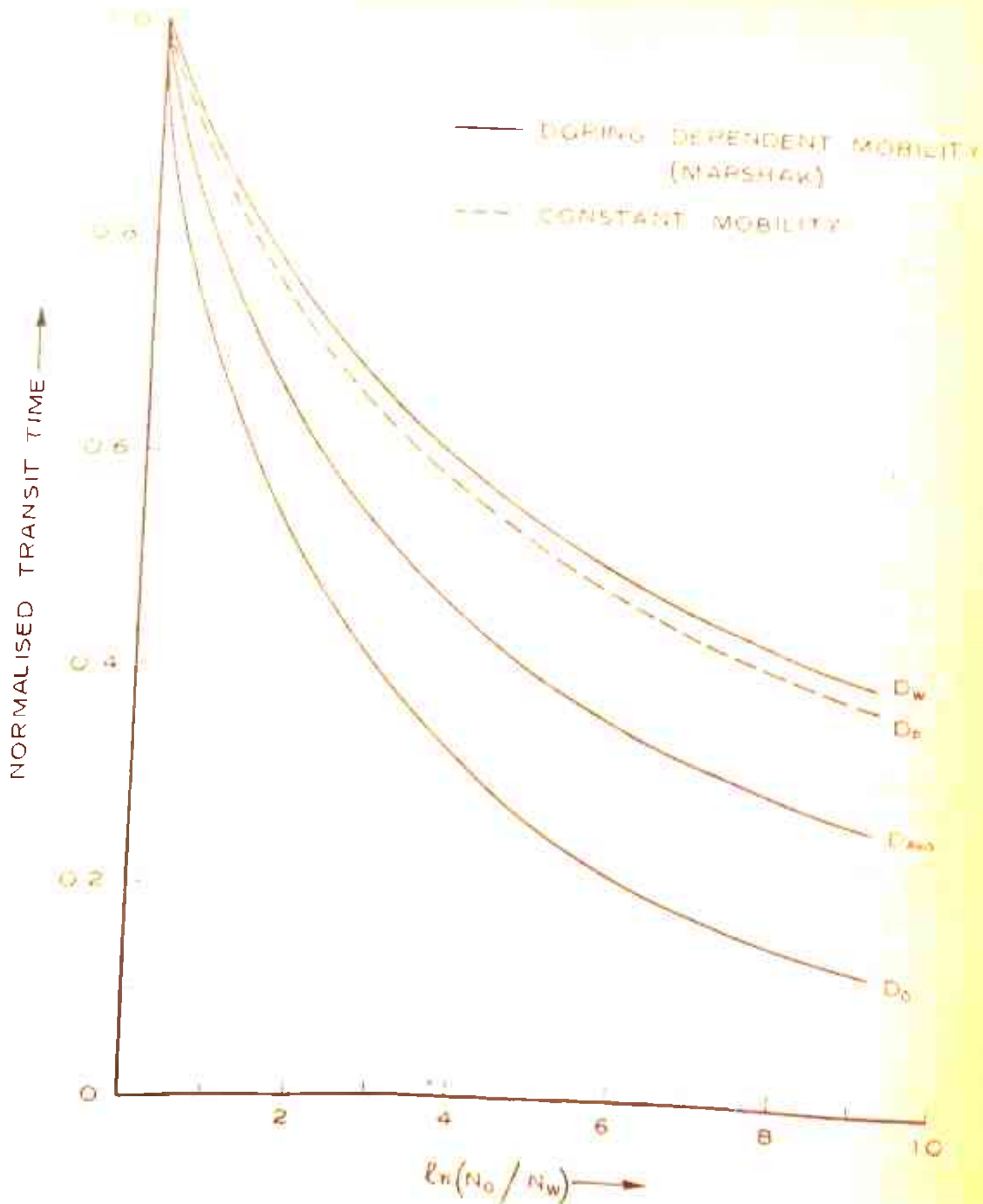


FIG. 3-24 DEPENDENCE OF BASE TRANSIT TIME ON THE BUILT-IN ELECTRIC FIELD IN THE BASE—PARABOLIC DISTRIBUTION.

illustrate the normalised transit time variation with $\ln N_0/N_w$ corresponding to the reference values of diffusion constant D_0 , D_w , and D_{avg} (solid curves). The transit time variation with $\ln(N_0/N_w)$ obtained in the case of constant mobility is also given for comparison (dotted curves). The value of $N_0 = 10^{16}$ is used wherever necessary in the above computations.

3.6.3 Ho and Cho's Mobility Relation

Based on the above mobility relation, the diffusion coefficient variation with doping can be expressed as

$$D_p = D_0 \frac{1+k}{1+bN^c} \quad \dots (3.31)$$

$$D_p = D_w \frac{1+k e^{-\eta c}}{1+bN^c} \quad \dots (3.32)$$

$$D_p = D_{avg} \frac{(1+k)(1+k e^{-\eta c})}{(1+bN^c)(1+\frac{k}{2}(1+e^{-\eta c}))} \quad \dots (3.33)$$

where $D_0 = \frac{KT}{q} \cdot \frac{a}{1+k}$, and $k = bN_0^c$, a , b , and c are constants given in Table 2.1 (Chapter 2). The base transit time obtained by substituting above relations in eqn. 3.20 can be expressed as

$$\frac{t_B}{t_{B0}} = \frac{2}{1+k} \int_0^1 \frac{\left(\frac{N(x)}{N_0} (1+k(N(x)/N_0)^c \right) dx}{N(x)/N_0} \quad \dots (3.34)$$

$$\frac{t_B}{t_{Bw}} = \frac{1+k}{1+k e^{-\eta c}} \cdot \frac{t_B}{t_{B0}} \quad \dots (3.35)$$

$$\frac{t_B}{t_{B\text{avg}}} = \frac{1 + \frac{k}{2} (1 + e^{-\eta c})}{1 + k e^{-\eta c}} \cdot \frac{t_B}{t_{B0}} \quad \dots (3.36)$$

The normalised transit times are computed by numerical techniques. Table 3.5 gives a summary of the results of t_B/t_{B0} . The base transit time as a function of $\ln(N_0/N_w)$ is plotted in Figs. 3.25 to 3.30 for several impurity distributions considered in Sec. 3.2. D_0 , D_w , D_{avg} are used as reference values of diffusion constants. For comparison, the results obtained in the case of constant mobility are also plotted on the same graph. The solid curves in these figures correspond to the doping dependent mobility case while the dotted curves are for the case of constant mobility.

3.6.4 Discussion

The actual calculations of transit time indicate that only those distributions which are derived earlier as the optimum distributions by variational method yield minimum transit time (except for a slight discrepancy in some cases, Tables 3.4 and 3.5). For Sugeno and Koshiga's mobility relation, the hyperbolic distribution yields minimum transit time. Marshak's and Ho and Cho's distributions provide lowest transit time when corresponding mobility relations are assumed (Ref. Tables 3.3 to 3.5).

The transit time variation with $\ln N_0/N_w$ shows a minimum only for Sugeno and Koshiga's mobility relation and

TABLE 3.5

Calculation of Normalised Base Transit Time (t_B/t_{BC})

using Ho and Cho's Mobility Relation

$\frac{N_D}{N_A}$	Impurity Distributions				
	Gaussian	Exponential	Ho and Cho's optimum	Marshak's optimum	Hyperbolic Parabolic-I
10	0.42004	0.36199	0.35805	0.35650	0.35410
10^2	0.26058	0.20234	0.20092	0.19825	0.19875
10^3	0.18620	0.13831	0.13810	0.13723	0.14500

0.40761

0.27270

0.20800

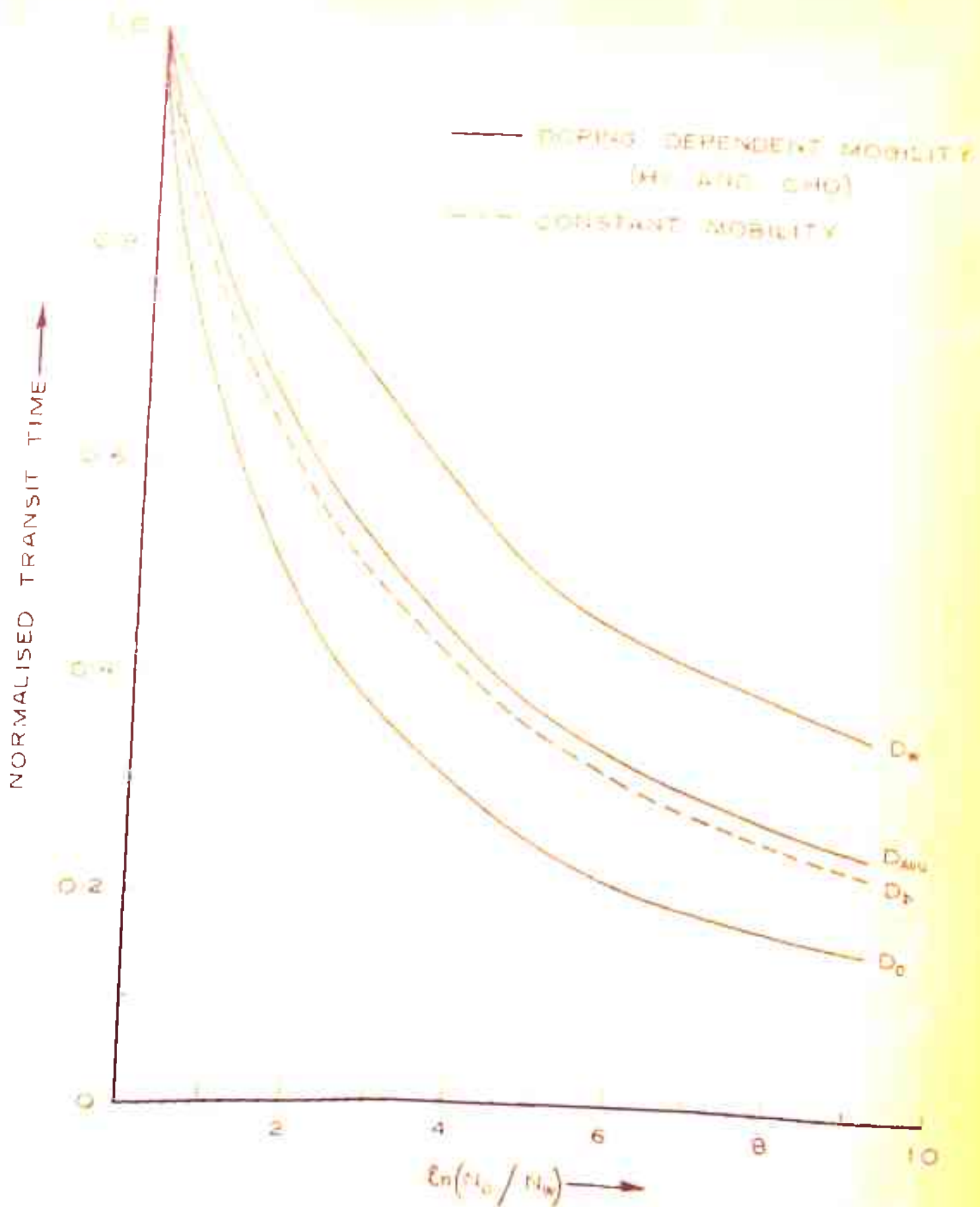


FIG. 3-25 DEPENDENCE OF BASE TRANSIT TIME ON THE BUILT-IN ELECTRIC FIELD IN THE BASE—GAUSSIAN DISTRIBUTION.

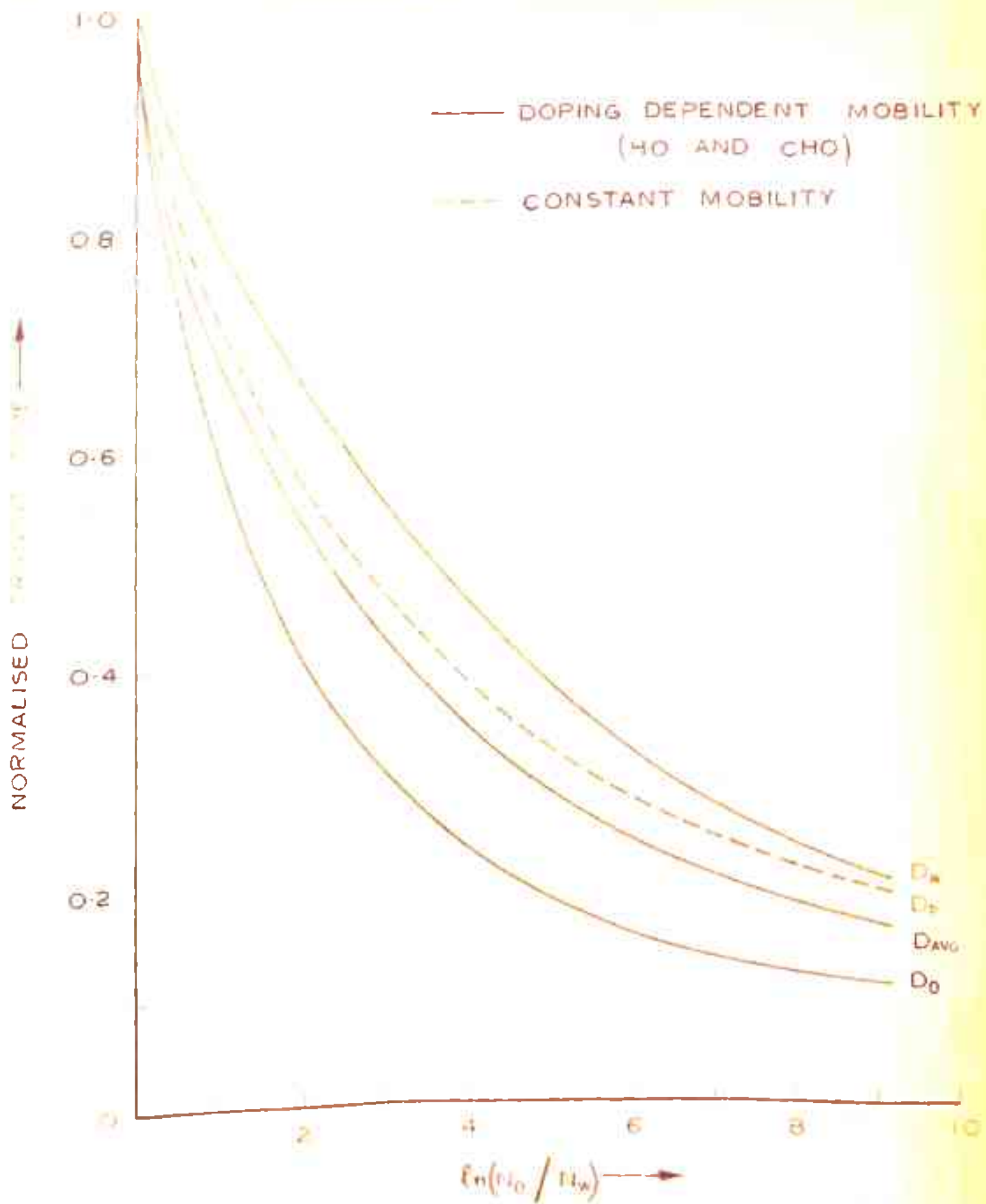


FIG 3.26 DEPENDENCE OF BASE TRANSIT TIME ON THE BUILT-IN ELECTRIC FIELD IN THE BASE—EXPONENTIAL DISTRIBUTION.

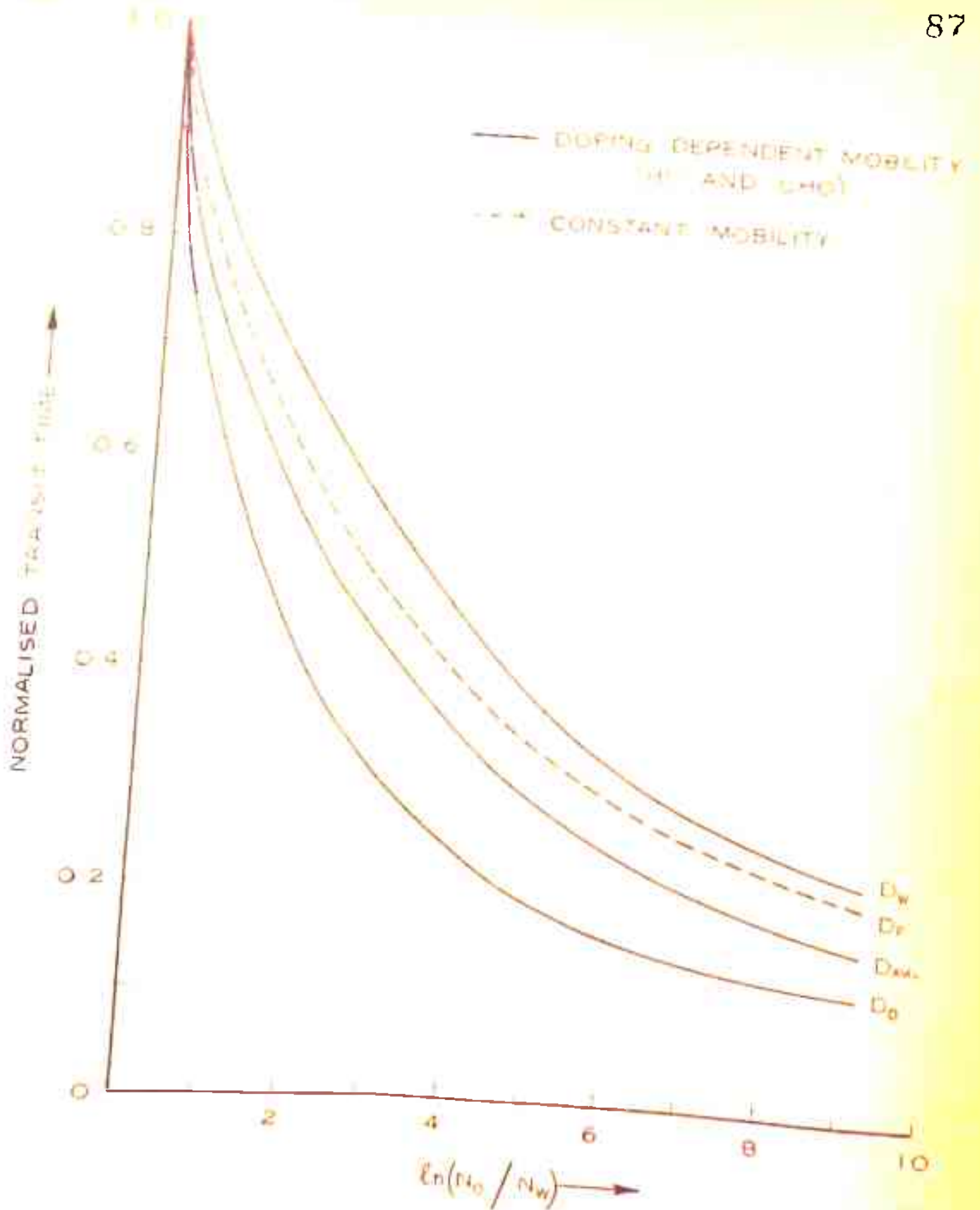


FIG. 3.27 DEPENDENCE OF BASE TRANSIT TIME ON THE BUILT-IN ELECTRIC FIELD IN THE BASE—HO AND CHO'S OPTIMUM DISTRIBUTION.

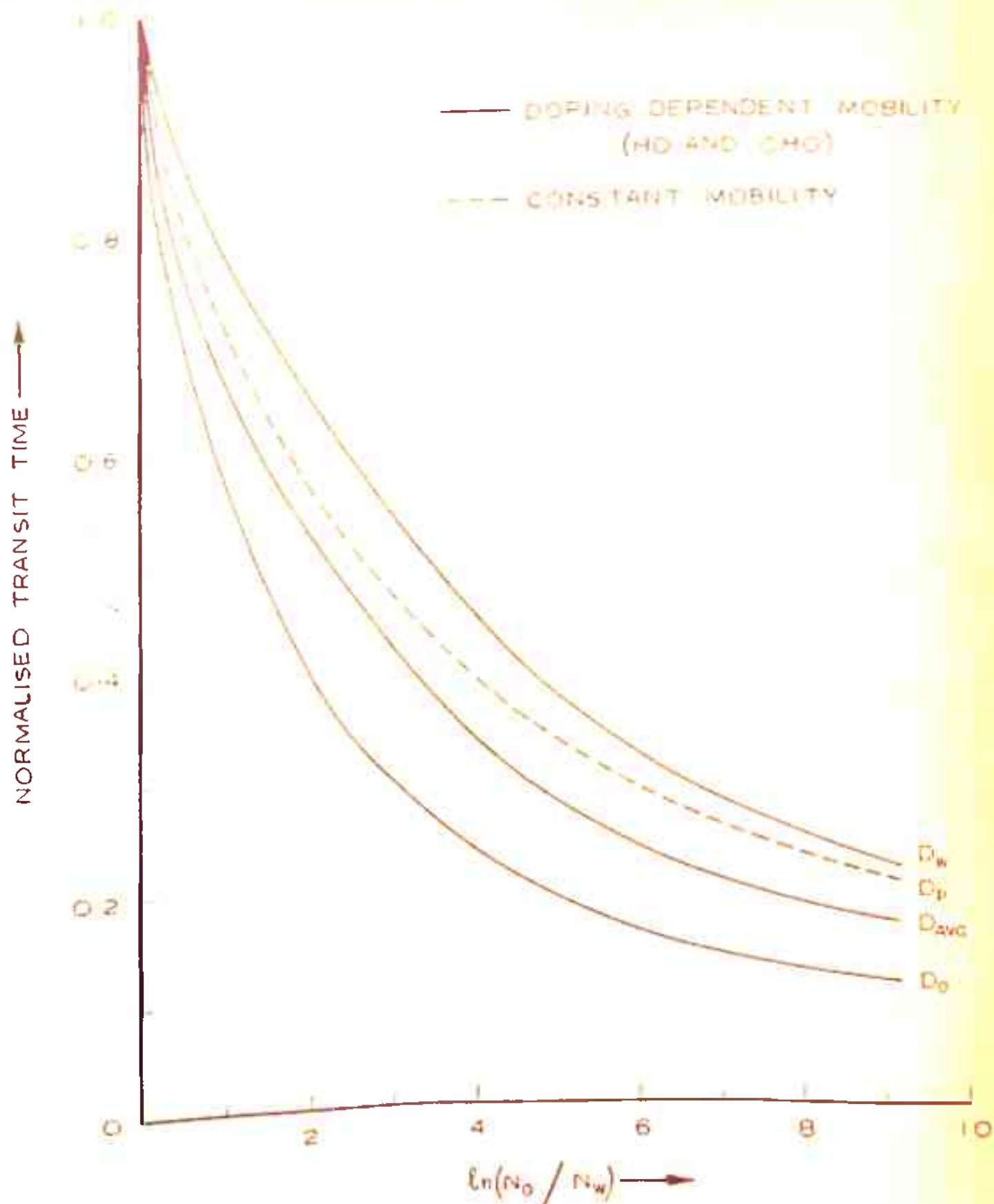


FIG.3.28 DEPENDENCE OF BASE TRANSIT TIME ON THE BUILT-IN ELECTRIC FIELD IN THE BASE—MARSHAK'S OPTIMUM DISTRIBUTION.

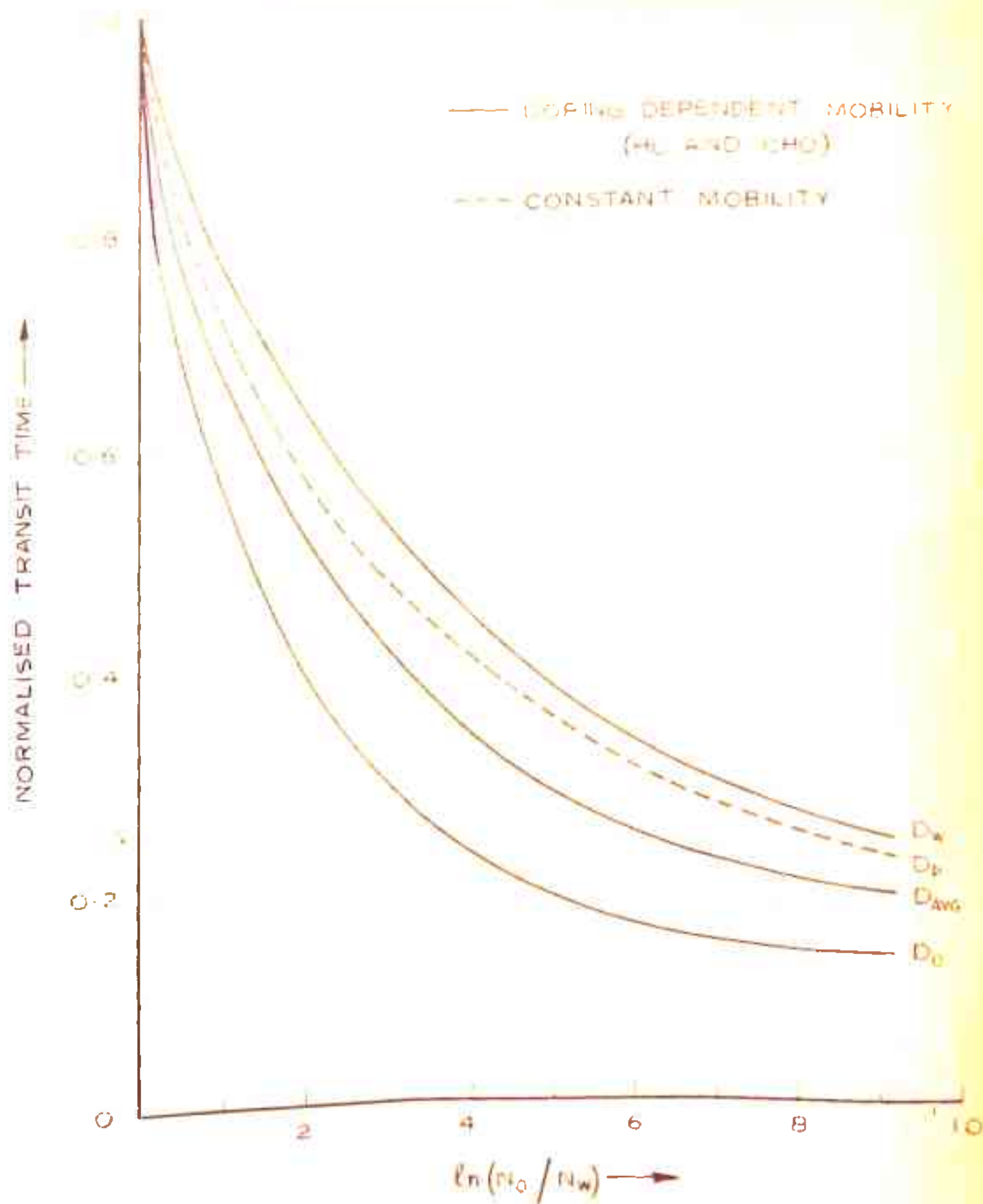


FIG.3.29 DEPENDENCE OF BASE TRANSIT TIME ON THE BUILT-IN ELECTRIC FIELD IN THE BASE—HYPERBOLIC DISTRIBUTION.

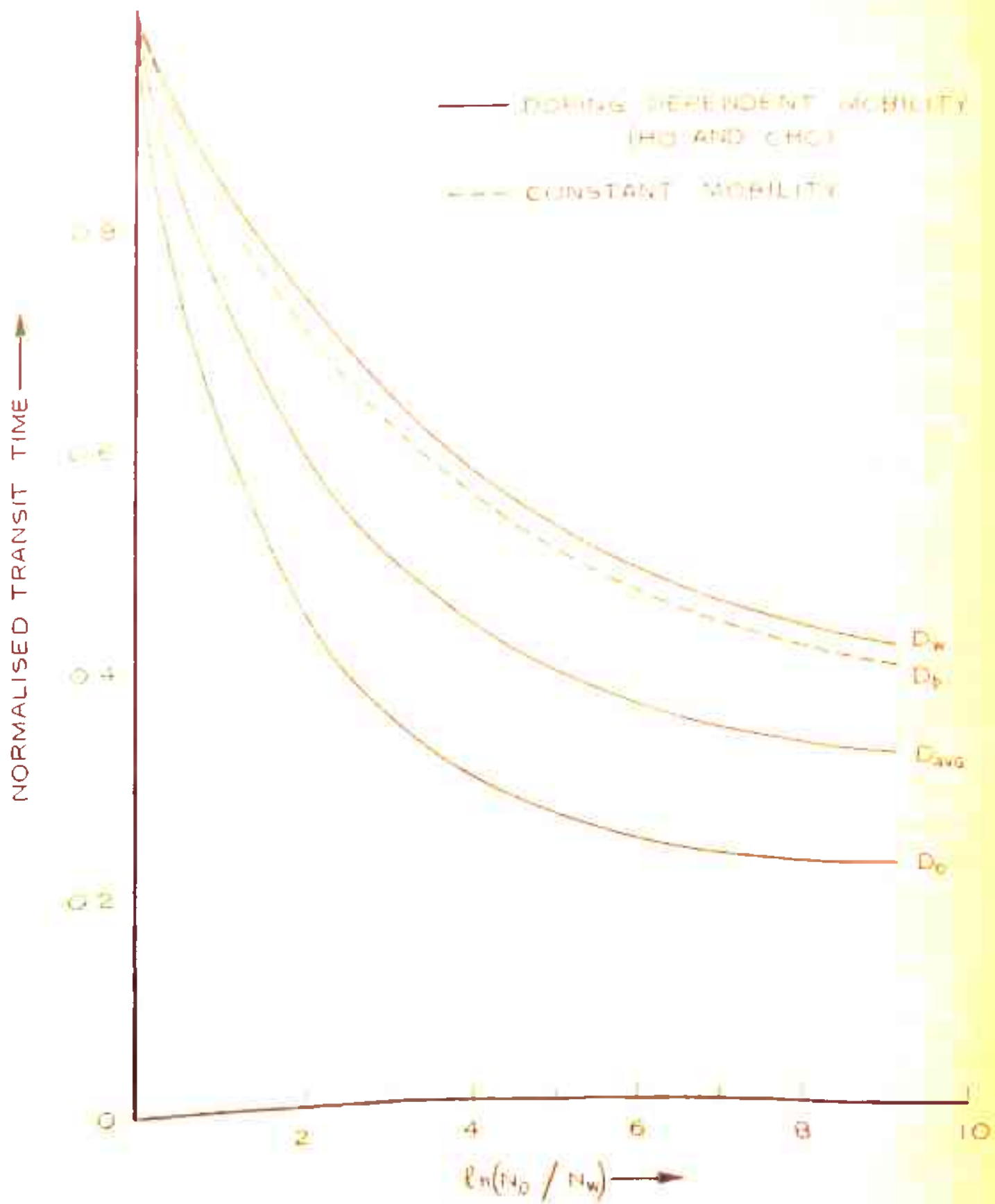


FIG 3-30 DEPENDENCE OF BASE TRANSIT TIME ON THE BUILT-IN ELECTRIC FIELD IN THE BASE—PARABOLIC-I DISTRIBUTION.

for impurity distributions which are concave down on $\ln N$ vs. X plot. This observation is true when either D_w or D_{avg} is taken as the reference value of diffusion coefficient. When D_0 is taken as reference, the transit time decreases monotonically with increase of N_0/N_w . But for doping distributions which are concave up, there is a monotonic decrease in transit time with increasing ratio of N_0/N_w . The normalised base transit time obtained for concave down impurity distributions and with the assumption of constant mobility, is smaller than the corresponding value of transit time obtained for doping dependent mobility case using D_{avg} as the reference value of the diffusion coefficient. For concave up distributions, the behaviour is just the reverse.

The physical explanation for the base transit time reduction in the case of optimum distributions lies in the fact that the injected minority carriers attain a higher drift velocity as they enter the base region. It is due to a large value of built-in electric field at the emitter end of the base region. The increase in drift velocity leads to a decrease in the base transit time of the injected minority carriers. The simultaneous effect of built-in electric field and doping dependent mobility results in a minimum in the curve showing the dependence of the base transit time on $\ln N_0/N_w$ for concave down impurity distributions.

The present investigation concerning the influence of mobility variation on base transit time has supplemented the results of a similar study previously made by Sugano and Koshiga¹⁰, and Bullis and Runyan¹¹.

3.7 SPECIAL FORM OF BASE IMPURITY DISTRIBUTION

In this section, a special form of base impurity distribution is considered, and computed results of built-in electric field, minority carrier concentration and base transit time are presented. The doping distributions considered so far are either concave up or concave down on a $\ln N$ vs. x plot. The present base impurity distribution is first concave down and then changes over to concave up. It is special in this sense only.

In a slightly different form, this impurity distribution has been first used by Hauser¹² for the channel doping in a Field Effect transistor. The original expression has been modified to take into account the following boundary conditions.

$$\begin{aligned} N &= N_0 \quad \text{at } x = 0 \\ N &= N_w \quad \text{at } x = 1 \end{aligned} \quad \dots (3.37)$$

The following mathematical expression describes the special impurity distribution

$$N(x) = N_0 \left[e^{-\eta} + (1 - e^{-\eta}) (1 - x)^m \right] \quad \dots (3.38)$$

where m is a constant.

Built-in Electric Field in the Base

The magnitude of the built-in electric field arising due to the special impurity doping distribution in the base region is calculated using equation 3.10. The following expression for the normalised electric field is obtained.

$$\left(\frac{qW}{KT}\right) E = \frac{mk'(1-X)^{m-1}}{1+k'(1-X)^m} \quad \dots (3.39)$$

where $k' = e^{\eta} - 1$

Minority Carrier Concentration in the Base

In the case of constant mobility, the excess minority carrier concentration is calculated using equation 3.11, and the following expression is obtained for normalised carrier concentration.

$$\left(\frac{q D_p}{J_p W}\right) p = \frac{(1-X)}{(1+m)} \left(1 + \frac{m}{N(X)/N_w}\right) \quad \dots (3.40)$$

$N(X)/N_w$ is substituted from equation 3.38.

Base Transit Time

The normalised transit time in the base region is computed by making use of eqn. 3.19. The following result is obtained.

$$\frac{t_B}{t_{BU}} = \frac{1}{1+m} + \frac{2m}{1+m} \int_0^1 \frac{1-X}{1+k'(1-X)^m} dx \quad \dots (3.41)$$

The transit time expression 3.41 is a function of m . It can be minimised to yield an optimum m value. Let

$$T = t_B/t_{BU}$$

Then the first derivative of T with respect to m i.e. $\frac{dT}{dm}$, when equated to zero yields the following relation.

$$\int_0^1 \frac{1-X}{1+k'(1-X)^m} dx - m(m+1)k' \int_0^1 \frac{(1-X)^{m+1} \log(1-X)}{(1+k'(1-X)^m)^2} dx - \frac{1}{2} = 0 \quad \dots (3.42)$$

The above equation is nonlinear in m having the functional form

$$f(m) = 0$$

The value of m can be obtained by applying Newton-Raphson's iterative method.

The plot of impurity distribution function $N(x)/N_0$ for $N_0/N_w = 10^3$, is given in Fig. 3.31. The optimum m value of 4.7 as calculated from eqn. 3.42 is used in this case. As is evident from this curve, the doping distribution curve is concave down over a major portion of the base and then it becomes concave up over rest of the base region.

The built-in electric field configuration in the base for this special distribution is sketched in Fig. 3.32 for different ratios of N_0/N_w . Fig. 3.33 shows the plot of excess minority carrier concentration. The optimum m values corresponding to different N_0/N_w ratios are derived from eqn. 3.42 and have been used in the calculation of the built-in electric field and excess carrier concentration in the base.

Table 3.6 gives the calculated value of normalised transit time for the special impurity distribution considered in this section. For comparison, the normalised base transit time values as obtained in the case of exponential distribution are also mentioned.

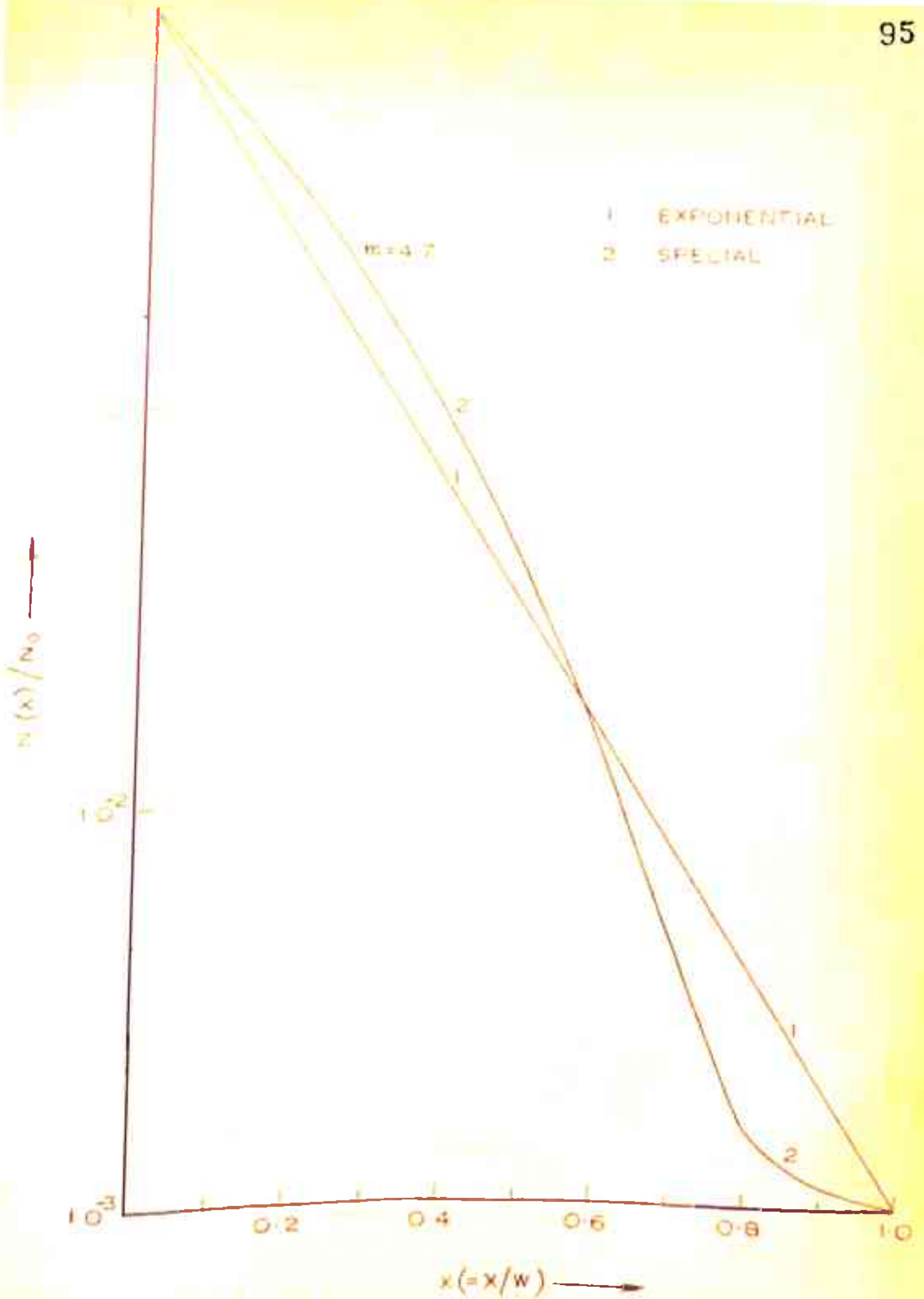


FIG. 331 SPECIAL FORM OF BASE IMPURITY DISTRIBUTION.

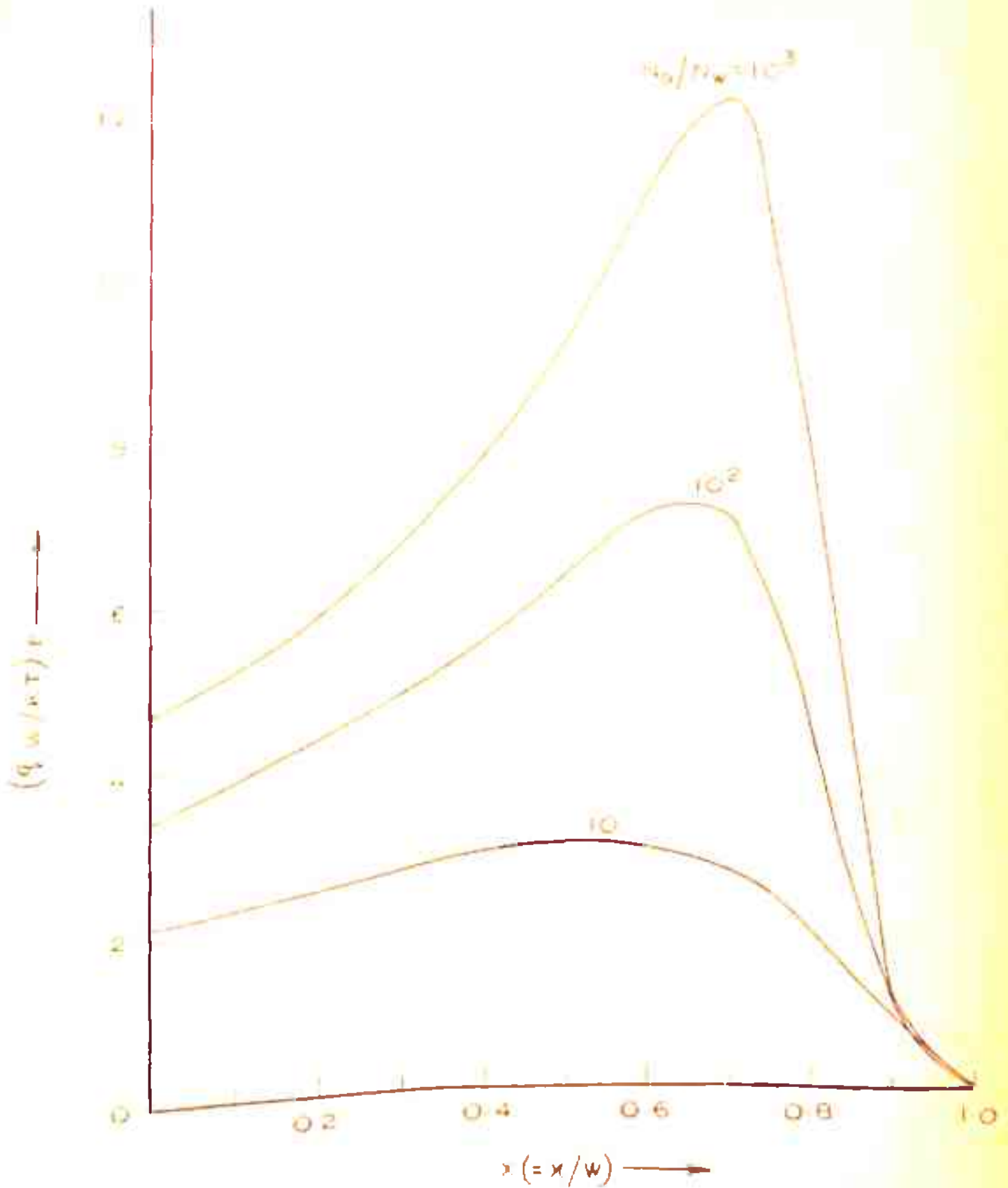


FIG. 3-3. BUILT-IN ELECTRIC FIELD IN THE BASE FOR IMPURITY DISTRIBUTION OF FIG. 3-31.

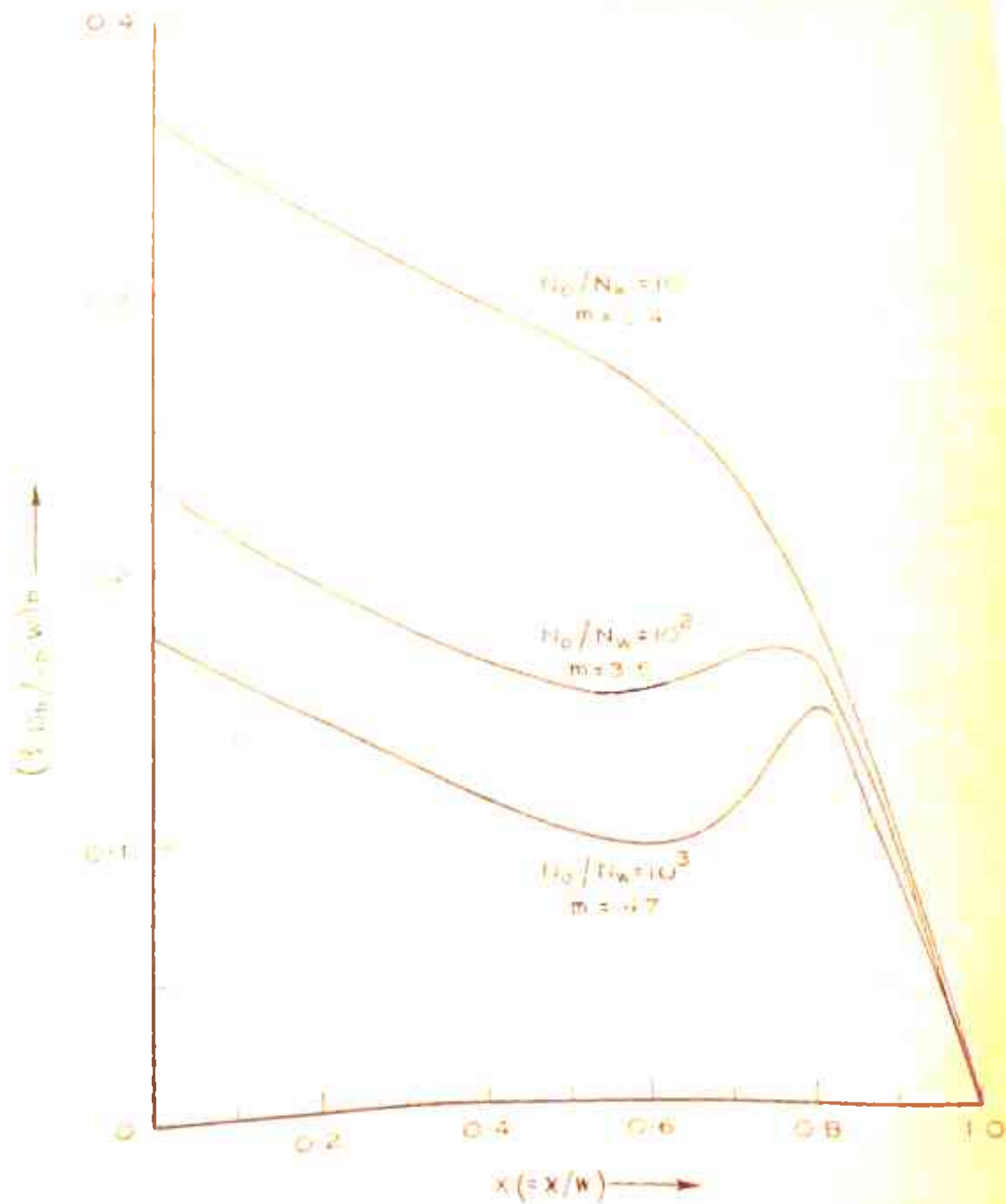


FIG. 333 MINORITY CARRIER CONCENTRATION IN THE BASE FOR IMPURITY DISTRIBUTIONS OF FIG. 331.

TABLE 3.6Calculation of Normalised Base Transit Time
for Special Form of Base Doping Distribution

(For comparison the transit times obtained in the case of exponential distribution are also given)

N_o/N_w	10	10^2	10^3	10^4
Optimum m	2.4	3.5	4.7	5.8
Special impurity distribution	0.50012	0.31544	0.23479	0.19068
Exponential distribution	0.52908	0.34093	0.24765	0.19357

A study of Table 3.6 shows that the transit times obtained in the case of special doping distribution are lower than the corresponding times obtained in the case of exponential distribution. The variational methods have proved analytically that it is the exponential distribution which should offer minimum base transit time in the case of constant mobility, but the results obtained in the case of special impurity distributions have established that the distributions obtained through variation^{al} method do not necessarily provide a unique minimum in transit time.

The behaviour of the impurity distribution and the electric field as plotted in Figs. 3.31 and 3.32 reveals that there is a point of inflection in these curves, whereas in the basic impurity distributions of Sec. 3.2 or the corresponding

electric field curves, there is no point of inflection. Hence, it can be concluded that the variational method of obtaining optimum impurity distribution for minimum base transit time fails for impurity distributions or electric field distributions having a point of inflection. Therefore, some other technique of optimising base impurity distributions should be used.

The base region minority carrier concentration (Fig. 3.33) shows the following behaviour. The concentration first decreases upto some point in the base, then it increases slightly and finally becomes zero at the collector end. For $N_0/N_w = 10$, there is no increase of excess concentration in the middle of the base.

3.8 SUMMARY AND DISCUSSION

The built-in electric field increases monotonically over the base region for impurity distributions which are concave down on a $\ln N$ vs. x plot. For other impurity distributions which are concave up, the electric field is maximum at the emitter end and decreases monotonically. This behaviour of the built-in electric field is a direct consequence of the nature of variation of the gradient of $\ln N$ since E is proportional to $\frac{d(\ln N)}{dx}$.

The excess minority carrier concentration profile in the base region shows that the current flow is due to a combination of drift and diffusion mechanisms in all cases of impurity distributions. For concave down doping

distributions, the carrier flow near emitter is both due to drift and diffusion. For impurity distributions which are concave up, the carrier flow is mainly due to drift near the emitter end. Further, there is a diffusive tendency of carriers towards the emitter from somewhere in the base. Near the collector, the carrier flow is mainly due to diffusion in all cases.

The typical nature of the minority carrier profile in the base depends on the electric field configuration. For concave up impurity distributions, the built-in electric field in the base is a monotonically decreasing function. Hence, the minority carrier concentration in the base is low at the emitter end and tends to increase towards the collector. Since the C-B junction is reverse biased, the carrier concentration at the collector end has to be zero. This causes a maximum in the carrier concentration profile somewhere in the base. In the case of concave down impurity distributions, the minority carrier concentration is maximum at the emitter end and monotonically decreases towards the collector end. This behaviour is due to the monotonically increasing electric field.

The calculated results indicate that for optimum impurity distributions the base transit time is minimum when corresponding empirical relations of doping dependent mobility are used. In the case of constant mobility, the exponential distribution yields a minimum value of base transit time. The higher values of the built-in electric

field at the emitter end of the base for optimum impurity distributions lead to a reduction in the emitter injected minority carriers. Further, the field gradient and the mobility gradient are such that the total stored base charge is less, and hence a lower value of transit time is obtained.

A study of the variation of transit time with the field factor ($\ln N_0/N_w$) reveals that for certain impurity profiles there is an optimum value of the field factor for which the transit time is minimum. Such an optimum value is observed for the exponential and all other impurity distributions which are concave down on a $\ln N$ vs. X plot when Sugano and Koshiga's relation for doping dependent mobility is used. The field gradient for concave down distributions increases monotonically from emitter to the collector. The mobility gradient increases to a maximum somewhere in the base and then decreases. The simultaneous effect of the two gradients leads to the existence of an optimum value of field factor which yields minimum transit time. For optimum distributions which are concave up, there is a monotonic decrease in the field gradient. Consequently, no optimum field factor is obtained. Since the mobility gradient depends very much upon the assumed empirical form of the doping dependence, mobility relations other than that of Sugano and Koshiga do not give rise to an optimum value for the field factor.

By considering a special impurity distribution which crosses over from concave down to concave up in the base region, it has been established that the optimum doping

distributions obtained by variational method do not necessarily offer minimum case transit time. The special doping distribution yields less transit time in the case of constant mobility. It is hence concluded that impurity distributions or electric field configurations having a point of inflection, a corner or discontinuity are not amenable to treatment by variational method which is applicable only to a restricted class of smooth curves.

In the next two Chapters - Chapters 4 and 5 - impurity distributions which are not smooth and built-in electric field configurations which have discontinuities are synthesised and studied for carrier transit behaviour.

+++++

REFERENCES

1. H. Kromer, 'The drift transistor' in Transistors I, RCA Lab. Princeton, N.J. 1956, pp. 202-220.
2. J.L. Moll and I.M. Ross, 'The dependence of transistor parameters on the distribution of base-layer resistivity', Proc. IRE, Vol. 44, pp. 72-78, 1956.
3. J. Lindmayer and C. Wrigley, 'Fundamentals of semiconductor devices', McGraw-Hill Book Co., New York, 1965, Ch. 4.
4. A.H. Marshak, 'Optimum doping distribution for minimum base transit time', IEEE Trans. Electron Devices, Vol. ED-14, pp. 190-194, 1967.
5. V.M. Bogachev, 'A calculation of cut-off frequency of a drift transistor by the stored charge method', Radio Engng. and Electronic Phys., Vol. 10, pp. 124-131, 1965.
6. McCracken and Dorn, 'Numerical methods and Fortran Programming', John Wiley, New York, 1964.
7. M.B. Das and A.R. Boothroyd, 'Determination of physical parameters of diffusion and drift transistors', IRE Trans. Electron Devices, Vol. ED-8, pp. 15-30, 1961.
8. J. Lindmayer and C. Wrigley, 'The high-injection-level operation of drift transistors', Solid State Electronics, Vol. 2, pp. 79-84, 1961.
9. T. Sugano and F. Koshiga, 'The calculation of cut-off frequencies of minority carrier transport factors in drift transistors when the mobilities are not constant', Proc. IRE, Vol. 49, p. 1218, 1961.
10. R.L. Pritchard, T. Sugano, and F. Koshiga, 'Cut-off frequencies of a junction transistor when mobilities are not constant', Proc. IRE, Vol. 52, pp. 91-93, 1962.

11. W.M. Bullis and W.R. Runyan, 'Influence of mobility and life time variations on drift-field effects in silicon-junction devices', IEEE Trans. Electron Devices, Vol. ED-14, pp. 75-81, 1967.
12. J.R. Hauser, 'Silicon semiconductor device technology, Vol. II', John Wiley and Sons, U.S.A., 1968, Ch. 3.

+++++

CHAPTER 4IMPURITY DISTRIBUTIONS FOR MINIMUM BASE
TRANSIT TIME THROUGH SEGMENTATION TECHNIQUE

- 4.1 INTRODUCTION
- 4.2 SYNTHESIS OF TYPICAL BASE IMPURITY DISTRIBUTIONS
 - 4.2.1 TYPE-A PROFILE: COMBINATION OF GAUSSIAN AND HYPERBOLIC
 - 4.2.2 TYPE-B PROFILE: COMBINATION OF EXPONENTIAL AND HYPERBOLIC
 - 4.2.3 TYPE-C PROFILE: COMBINATION OF GAUSSIAN AND EXPONENTIAL
 - 4.2.4 TYPE-D PROFILE: COMBINATION OF HYPERBOLIC AND EXPONENTIAL
 - 4.2.5 TYPE-E PROFILE: COMBINATION OF EXPONENTIAL AND GAUSSIAN
 - 4.2.6 TYPE-F PROFILE: COMBINATION OF HYPERBOLIC AND GAUSSIAN
- 4.3 BUILT-IN ELECTRIC FIELD IN THE BASE
- 4.4 EXCESS MINORITY CARRIER CONCENTRATION IN THE BASE
- 4.5 BASE TRANSIT TIME
- 4.6 SUMMARY AND DISCUSSION

CHAPTER 4IMPURITY DISTRIBUTIONS FOR MINIMUM BASE
TRANSIT TIME THROUGH SEGMENTATION TECHNIQUE4.1 INTRODUCTION

A special form of base impurity distribution which offers lower transit time than that obtained for the exponential profile has been discussed in the previous chapter. In this chapter, an attempt has been made to synthesise other impurity distributions which yield low base transit times. For the purpose of such a synthesis a new technique called 'the Segmentation Technique' is suggested. The built-in electric field, excess minority carrier concentration and base transit time are evaluated and the results are compared with those obtained in the cases of exponential and special base doping distributions. The synthesised impurity distributions and the corresponding base transit times yielded by these distributions confirm that such distributions having a point of inflection or a corner are not amenable to treatment by variational method. It is further established that suitable combinations of segments of standard distributions yield much lower base transit time than that obtained by employing the optimum distributions predicted by variational method.

4.2 SYNTHESIS OF TYPICAL BASE IMPURITY DISTRIBUTIONS

In the segmentation technique of synthesising base doping distributions, the base region is divided into two or more regions and each region has a segment of a different impurity distribution. The complete base distribution has a corner. For the present, only two segment impurity distributions are synthesised. The base region is divided into two regions (0 to s, and s to 1).

4.2.1 Type-A Profile: Combination of Gaussian and Hyperbolic

This profile is made up of a segment of Gaussian distribution and a segment of Hyperbolic distribution. The profile is

$$N_I(x) = N_0 e^{-\eta \frac{x^2}{s}} \quad (0 \leq x \leq s) \quad \dots (4.1a)$$

$$N_{II}(x) = N_0' (1 + (e^{.25\eta'} - 1) x)^{-4} \quad (s \leq x \leq 1) \quad \dots (4.1b)$$

where

$$\eta' = \ln N_0' / N_w$$

N_0' = impurity concentration at $x = 0$ for the projected hyperbolic distribution

s = x -coordinate of the intersection point (corner) of the two segments in the base.

At $x = s$, $N(x)$ given by eqns. 4.1a and 4.1b should be matched. This condition yields the following non-linear relation in s .

$$\left(\frac{N_o'}{N_o}\right)^{.25} e^{\eta s/4} - (e^{.25\eta'} - 1) s - 1 = 0 \quad \dots (4.2)$$

For given values of N_o'/N_w and N_o/N_w , s is unique and is obtained by solving the above equation as follows. The equation is written in the functional form as

$$f(s) = 0 \quad \dots (4.3)$$

Differentiating eqn. 4.2, we get

$$f'(s) = \left(\frac{N_o'}{N_o}\right)^{.25} \frac{\eta}{4} e^{\eta s/4} - (e^{\eta'/4} - 1) \quad \dots (4.4)$$

Applying Newton-Raphson's method, s can be obtained from the relation,

$$s = s - \frac{f(s)}{f'(s)} \quad \dots (4.5)$$

where the right hand side s is the initially guessed value of this variable.

4.2.2 Type-B Profile: Combination of Exponential and Hyperbolic

This profile is made up of a combination of two distributions - a segment of exponential and a segment of hyperbolic distribution. The mathematical relation is

$$N_I(x) = N_o \cdot e^{-\eta x} \quad (0 \leq x \leq s) \quad \dots (4.6a)$$

$$N_{II}(x) = N_o' (1 + (e^{.25\eta'} - 1) x)^{-4} \quad (s \leq x \leq 1) \quad \dots (4.6b)$$

The value of s for this distribution is also unique and is

the same as that obtained by solving the non-linear eqn. 4.2. N_0'/N_0 ratio is as given below.

$$\frac{N_0'}{N_0} = \frac{(1 + (e^{\eta'/4} - 1) s)^4}{e^{\eta s}} \quad \dots (4.7)$$

4.2.3 Type-C Profile: Combination of Gaussian and Exponential

Here a combination of segments of Gaussian and exponential distributions is considered. The analytical expression for the profile is

$$N_{I}(X) = N_0 e^{-\eta \frac{x^2}{s}} \quad (0 \leq x \leq s) \quad \dots (4.8a)$$

$$N_{II}(X) = N_0 e^{-\eta x} \quad (s \leq x \leq 1) \quad \dots (4.8b)$$

In this case s can assume any arbitrary value between 0 and 1.

4.2.4 Type-D Profile: Combination of Hyperbolic and Exponential

In this case the profile is made up of a combination of segments of hyperbolic and exponential distributions. The expression is

$$N_{I}(X) = N_0 (1 + (e^{\eta \frac{s}{4}} - 1) \frac{x}{s})^{-4} \quad (0 \leq x \leq s) \quad \dots (4.9a)$$

$$N_{II}(X) = N_0 e^{-\eta x} \quad (s \leq x \leq 1) \quad \dots (4.9b)$$

For this distribution also, s can take any arbitrary value between 0 and 1.

4.2.5 Type-E Profile: Combination of Exponential and Gaussian

The mathematical expression for this distribution is

$$N_I(x) = N_o e^{-\eta x} \quad (0 \leq x \leq p_1) \quad \dots (4.10a)$$

$$N_{II}(x) = N_{o_1} e^{-\eta_1 x} \quad (p_1 \leq x \leq 1) \quad \dots (4.10b)$$

where $\eta_1 = \ln N_o / N_{o_1}$

N_o = impurity concentration at $x = 0$, for the projected Gaussian distribution

p_1 = x -coordinate of the intersection point in the base region.

The condition that at $x = p_1$, the concentrations given by eqns. 4.10a and b should be matched yields the following quadratic relation in p_1

$$\eta_1 p_1^2 - \eta p_1 + \ln \frac{N_o}{N_{o_1}} = 0 \quad \dots (4.11)$$

The following root for p_1 is selected,

$$p_1 = (\eta - \sqrt{\eta^2 - 4\eta_1 \ln N_o / N_{o_1}}) / 2\eta_1 \quad \dots (4.12)$$

4.2.6 Type-F Profile: Combination of Hyperbolic and Gaussian

This distribution is a combination of two segments - a segment of hyperbolic distribution and a segment of Gaussian distribution. The following relation describes the distribution

$$N_I(x) = N_o \left(1 + (e^{\eta p_1 / 4} - 1) \frac{x}{p_1} \right) \quad (0 \leq x \leq p_1) \quad \dots (4.13a)$$

$$N_{II}(x) = N_{o_1} e^{-\eta_1 x^2} \quad (p_1 \leq x \leq 1) \quad \dots (4.13b)$$

In this case also, p_1 is the solution of the quadratic equation 4.11.

The following constants have been commonly used in the synthesised distributions.

$$\eta = \ln N_o / N_w \quad \dots (4.14)$$

$x = x/W$, normalised distance

N_o , N_w represent the base impurity concentration at $x = 0$, and $x = 1$, respectively.

Fig. 4.1 shows the plot of all the synthesised impurity distributions. The following numerical constants have been assumed.

$$N_o / N_w = 10^3; \quad N_{o_1} / N_w = 10^9; \quad N_{o_1} / N_o = 2 \times 10^2$$

4.3 BUILT-IN ELECTRIC FIELD IN THE BASE

At low injection, the strength of the base region built-in electric field resulting from an arbitrary impurity distribution $N(x)$ is given by the relation (Sec. 2.2, Ch. 2)

$$E = - \frac{KT}{qW} \frac{1}{N} \frac{dN}{dx} \quad \dots (4.15)$$

For impurity distributions of Sec. 4.2, the field is evaluated from the above relation. The analytical expressions are given

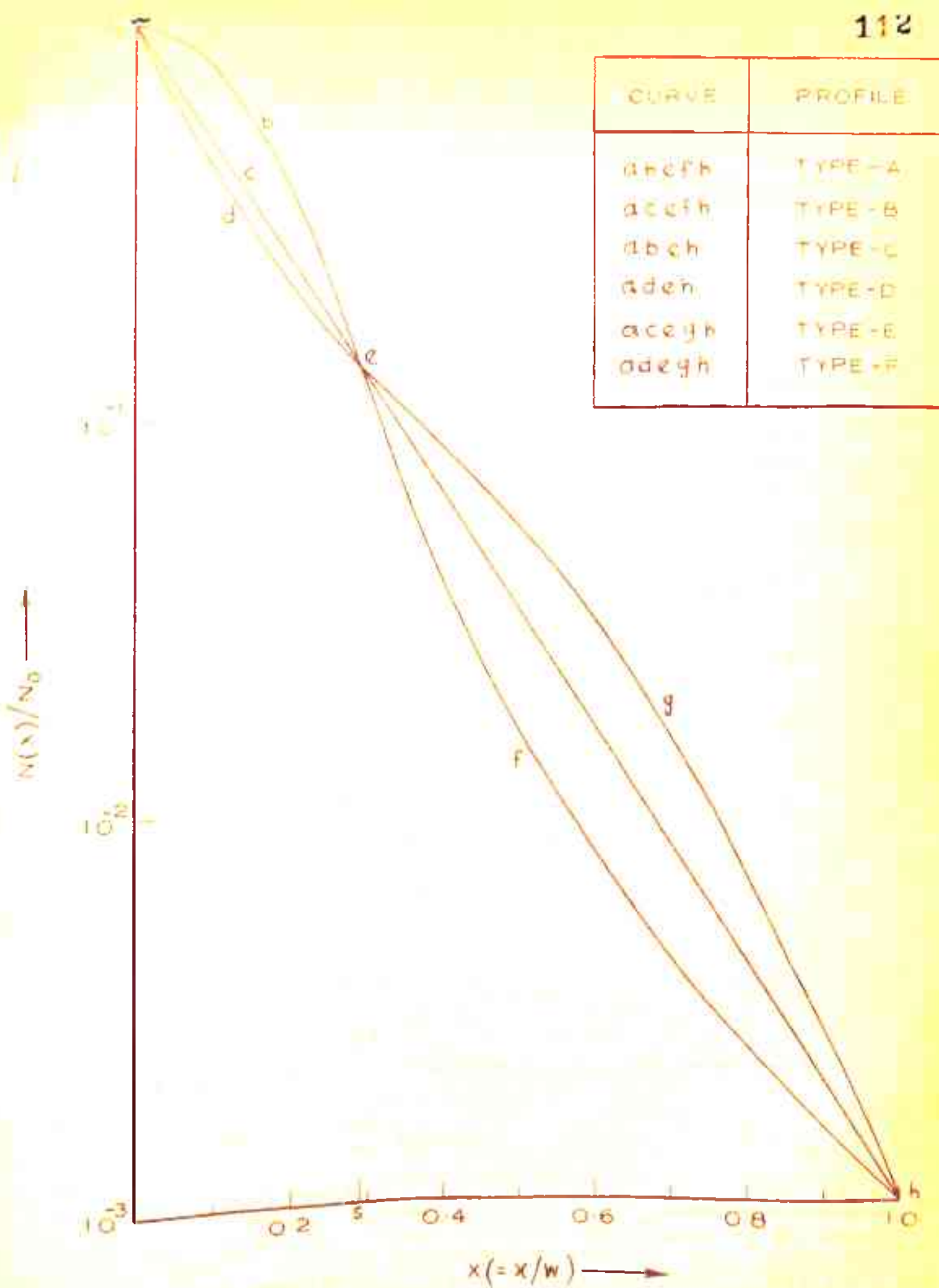


FIG. 4.1 SYNTHESISED TWO SEGMENT IMPURITY DISTRIBUTIONS IN THE BASE.

in Table 4.1. Fig. 4.2 shows the plot of normalised built-in field in the base region.

TABLE 4.1

Analytical Expressions of Normalised Built-in Electric Field for Two Segment Impurity Distributions

Impurity Distribution	Normalised built-in field, $(q W/KT) E$	
	Region I	Region II
Type-A	$2\eta x/s$	$\frac{4(e^{.25\eta'} - 1)}{1 + (e^{.25\eta'} - 1) x}$
Type-B	η	-do-
Type-C	$2\eta x/s$	η
Type-D	$\frac{4(e^{\eta s/4} - 1)}{1 + (e^{\eta s/4} - 1) x}$	η
Type-E	η	$2\eta_1 x$
Type-F	$\frac{4(e^{\eta p_1/4} - 1)}{1 + (e^{\eta p_1/4} - 1) x}$	$2\eta_1 x$

4.4 EXCESS MINORITY CARRIER CONCENTRATION IN THE BASE

Since the doping distributions are expressed as combinations of two different distribution functions, the excess minority carrier (hole) concentration in the base is expressed as below.

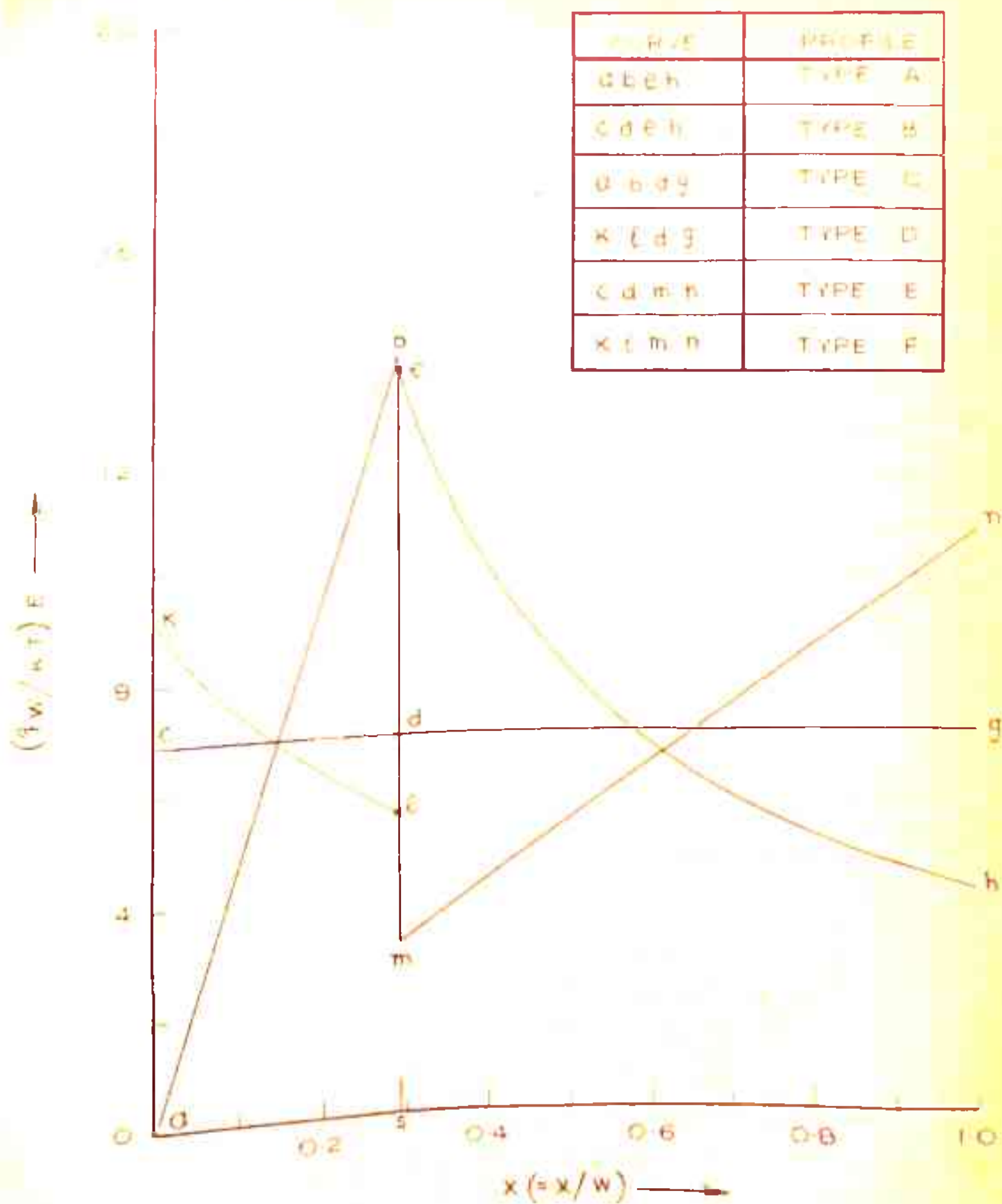


FIG. 4-2 BUILT-IN ELECTRIC FIELD IN THE BASE FOR IMPURITY DISTRIBUTIONS OF FIG. 4-1.

Region-I ($0 \leq x \leq s$)

$$\left(\frac{q D_p}{J_p}\right) P = \frac{1}{N_I(x)} \left[\int_x^s N_I(x) dx + \int_s^1 N_{II}(x) dx \right] \quad \dots (4.16a)$$

Region-II ($s \leq x \leq 1$)

$$\left(\frac{q D_p}{J_p}\right) P = \frac{1}{N_{II}(x)} \int_x^1 N_{II}(x) dx \quad \dots (4.16b)$$

These expressions are used to calculate the minority carrier concentrations for all assumed combinations of impurity distributions discussed in Sec. 4.2. Figs. 4.3 and 4.4 show the plots of minority carrier concentration in the base. For profiles E and F, s is replaced by P_1 in the above relation.

4.5 BASE TRANSIT TIME

In the present case of two segment impurity distributions, the normalised base transit time is expressed as

$$\frac{t_B}{t_{BU}} = 2 \int_0^s \frac{\int_x^s N_I(x) dx + \int_s^1 N_{II}(x) dx}{N_I(x)} dx + 2 \int_s^1 \frac{\int_x^1 N_{II}(x) dx}{N_{II}(x)} dx \quad \dots (4.17)$$

where $t_{BU} = w^2/2 D_p$

The above relation is obtained by calculating the total stored charge in the base.

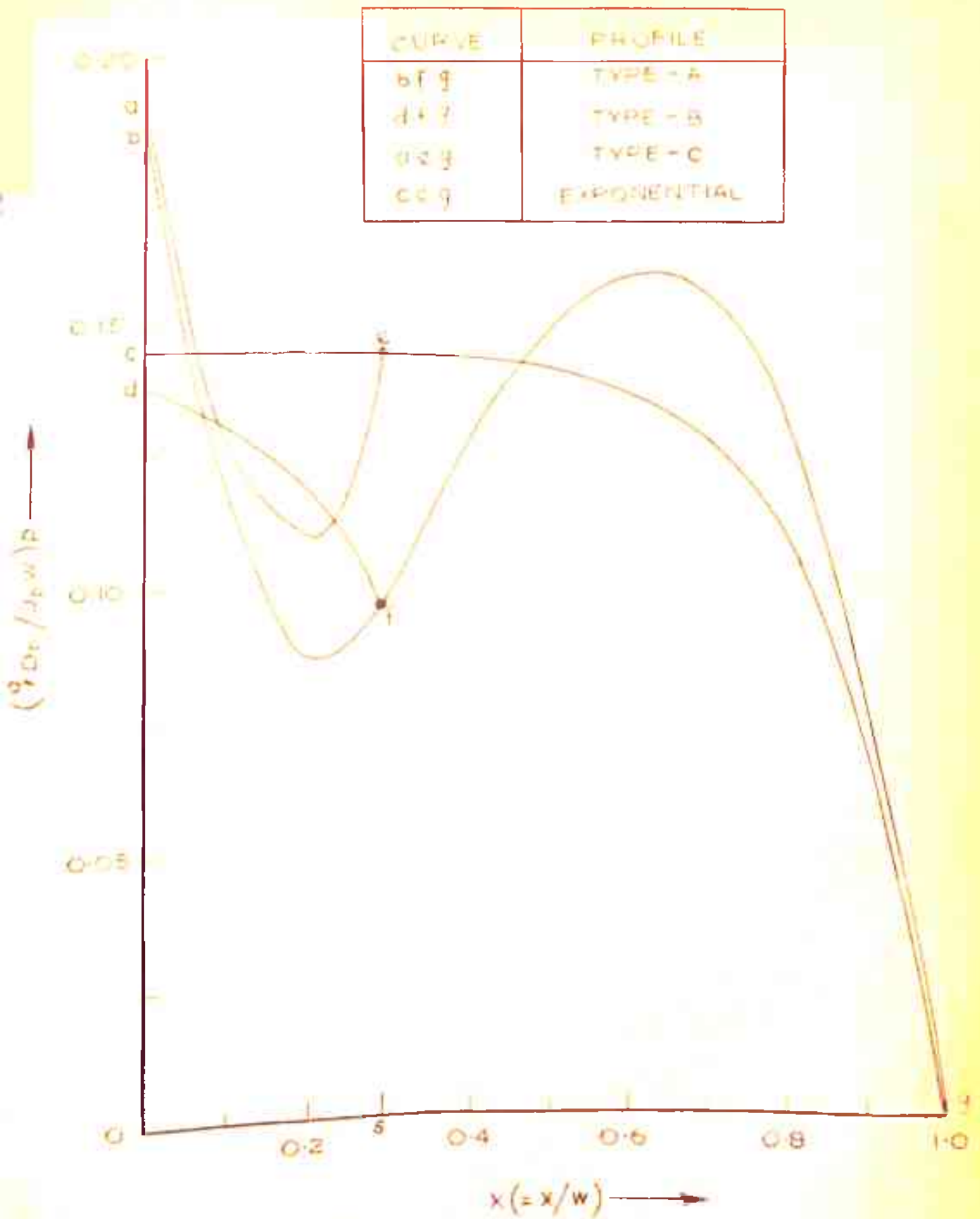


FIG 4.3 MINORITY CARRIER CONCENTRATION IN THE BASE FOR IMPURITY DISTRIBUTIONS OF FIG. 4.1 (TYPES: A-C).

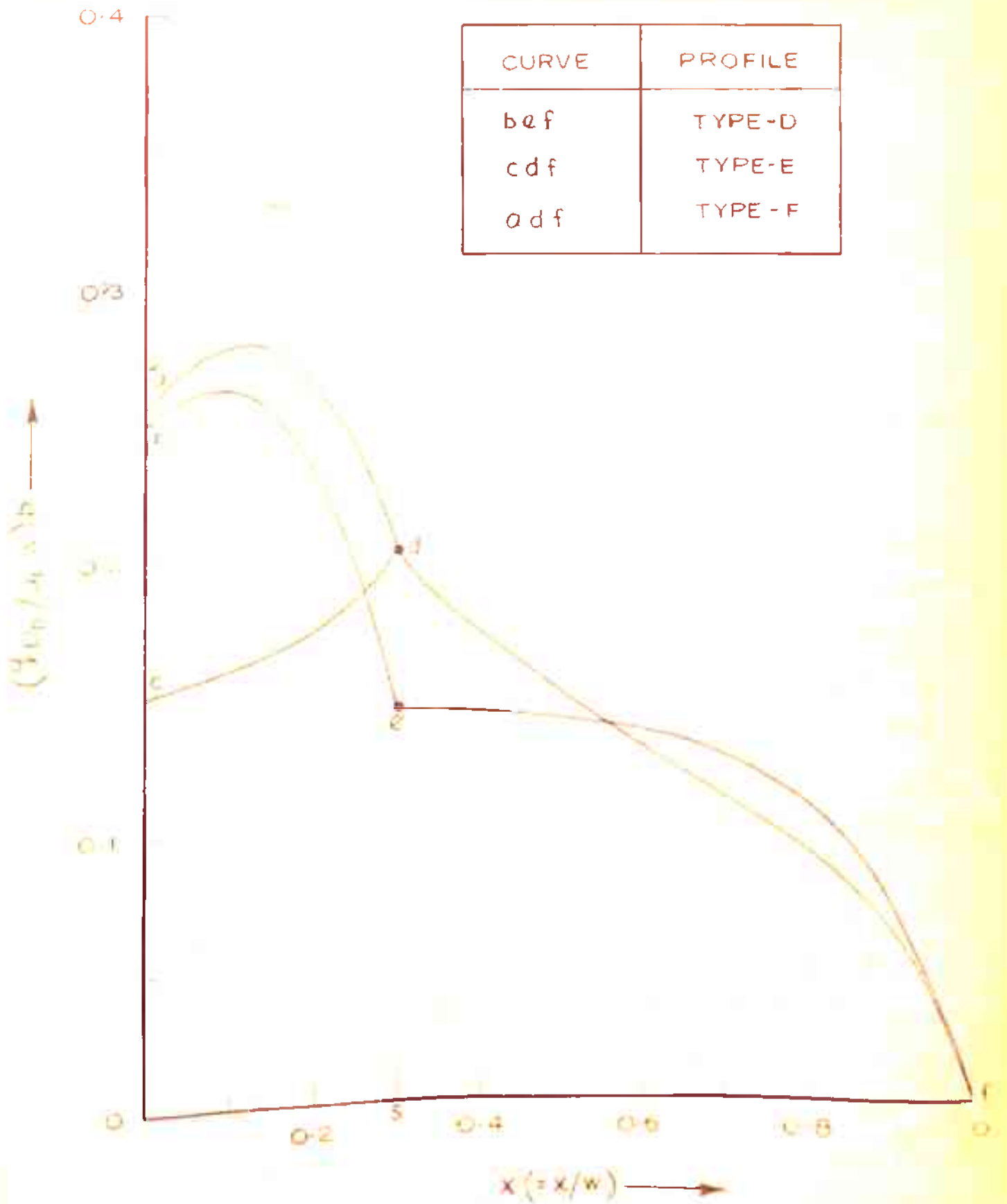


FIG. 4.4 MINORITY CARRIER CONCENTRATION IN THE BASE FOR IMPURITY DISTRIBUTIONS OF FIG. 4.1 (TYPES: D-F)

For the doping distributions of Sec. 4.2, the base transit time is computed numerically by evaluating eqn. 4.17. Different ratios of $N_{O'}/N_W$ and hence s , N_{O_1}/N_W and hence p_1 are assumed and transit time is evaluated. N_O/N_W is kept fixed at 10^3 .

Tables 4.2 and 4.3 give the results of transit time computations for distributions A to D and E to F, respectively. The value of transit time obtained in the case of the special form of the impurity distribution (Chapter 3) is also mentioned for comparison.

A study of the results given in Tables 4.2 and 4.3 reveals that with the increase of $N_{O'}/N_W$ ratio, and hence s value, the base transit time decreases in the case of profiles A, B and C. It is smaller as compared with the transit time obtained for exponentially doped base. For types E and F profiles, the base transit time increases with increase of N_{O_1}/N_W and is always greater than that obtained for exponential distribution. For profile-D, there is no improvement. The base transit times obtained for special and two segment impurity distributions establish the fact that the method of calculus of variations does not necessarily yield impurity distributions which give the minimum base transit time. Only a restricted class of impurity distributions which do not have any point of inflection or which are smooth are covered by this method.

TABLE 4.2

Calculation of Normalised Transit Time (t_B/t_{BU})
for Impurity Distributions obtained by Segmen-
tation Technique

Normalised transit time (Exponential distribution) = .24765

Normalised transit time (special impurity distri-
 bution) = .23479

$$N_o/N_w = 10^3$$

N_o/N_w	s	Normalised Transit Time for			
		Profile-A	Profile-B	Profile-C	Profile-D
10^4	0.141	0.25341	0.25551	0.24394	0.24817
10^5	0.212	0.24536	0.24913	0.24136	0.24911
10^6	0.250	0.24218	0.24679	0.24018	0.24983
10^7	0.271	0.24073	0.24576	0.23961	0.25029
10^8	0.282	0.24001	0.24526	0.23932	0.25056
10^9	0.290	0.23963	0.24500	0.23917	0.25072

TABLE 4.3

Calculation of Normalised Transit Time (τ_B/τ_{BU})
for Impurity Distributions obtained by Segmen-
tation Technique

N_{O_1}/N_w	P_1	Normalised Transit time for	
		Profile-E	Profile-F
5.00×10^2	0.111	0.27993	0.28044
4.00×10^2	0.153	0.27723	0.27831
3.33×10^2	0.189	0.27442	0.27618
2.00×10^2	0.303	0.26564	0.27038
1.66×10^2	0.350	0.26259	0.26886

4.6 SUMMARY AND DISCUSSION

Impurity distributions which are not smooth and which are combinations of segments of standard distributions have been synthesised through segmentation technique. A study of the built-in electric field, excess carrier concentration and base transit time for these distributions has confirmed the fact that the variational method of deducing optimum impurity distribution for minimum base transit time is not applicable to all classes of impurity distributions. Some of the synthesised distributions yield much lower base transit time as compared with the optimum profiles based on the variational method. Hence, the variational method does not lead to a unique solution for the optimum base impurity distribution. The physical explanation for the decrease in base transit time for some of the synthesised base impurity distributions can be given as follows. The first segment of these impurity distributions helps in increasing the drift velocity of the minority carriers upto some point in the base. This segment corresponds to a faster transit in the base region. The second segment which corresponds to a slow transit leads to a decrease in the drift velocity of the carriers. Hence a judicious combination of faster and slower segments of impurity distributions results in an overall decrease of base transit time. It is also noticed that the impurity distributions having typical built-in electric field configurations yield low values of transit time. Hence typical built-in field configurations can be synthesised in order to achieve low values of base transit time. This approach is dealt with in the next chapter.

+++++

CHAPTER 5

BUILT-IN ELECTRIC FIELD CONFIGURATIONS FOR MINIMUM BASE TRANSIT TIME THROUGH SEGMENTATION TECHNIQUE

- 5.1 INTRODUCTION
- 5.2 SYNTHESIS OF ELECTRIC FIELD CONFIGURATIONS - TWO SEGMENTS
 - 5.2.1 DERIVATION OF IMPURITY DISTRIBUTION
 - 5.2.2 EXCESS MINORITY CARRIER CONCENTRATION IN THE BASE
 - 5.2.3 BASE TRANSIT TIME
- 5.3 SYNTHESIS OF ELECTRIC FIELD CONFIGURATIONS - THREE SEGMENTS
 - 5.3.1 DERIVATION OF IMPURITY DISTRIBUTION
 - 5.3.2 EXCESS MINORITY CARRIER CONCENTRATION IN THE BASE
 - 5.3.3 BASE TRANSIT TIME
- 5.4 SUMMARY AND DISCUSSION

Chapter 5

BUILT-IN ELECTRIC FIELD CONFIGURATIONS FOR MINIMUM BASE TRANSIT TIME THROUGH SEGMENTATION TECHNIQUE

5.1 INTRODUCTION

The segmentation technique has been used earlier in the synthesis of impurity distributions for minimum base transit time. In this chapter, this technique is applied to obtain built-in electric field configurations for minimum transit time. Two segment and three segment configurations are synthesised and the corresponding impurity distributions are also deduced at low injection levels. Using these impurity distributions, the excess minority carrier concentration and the base transit time are calculated. The influence of doping dependent mobility on the minority carrier base transit time is studied for two segment distributions. The base transit times are compared with the times obtained for the exponential distribution. It is shown that the base region transit time improves when retarding field ($\frac{dN}{dx} > 0$) is present over a small portion of the whole base. Improvement in base transit time upto the extent of 20% is achieved as compared with the exponential distribution.

5.2 SYNTHESIS OF ELECTRIC FIELD CONFIGURATIONS - TWO SEGMENTS

To synthesise two segment electric field configurations, the base region is divided into two regions. Each region contains a constant built-in electric field. The magnitude of

the field differs in the two regions. The analytical expressions are given below.

Region I ($0 \leq x \leq s$)

$$E = \frac{KT}{q s W} \eta_1 \quad \dots (5.1a)$$

where s is the width of the first region in the base.

$\eta_1 > 0$ for aiding fields, and $\eta_1 < 0$ for retarding fields.

Region II ($s \leq x \leq 1$)

$$E = \frac{KT}{q(1-s)W} \eta_2 \quad \dots (5.1b)$$

η_1 and η_2 are constants specifying the strength of the built-in electric field in the two regions.

Fig. 5.1 shows a typical plot of synthesised electric field configurations.

5.2.1 Derivation of Impurity Distribution

The base region impurity distribution corresponding to the two segment field configuration is obtained from the following low inject^{ion} level expression of built-in electric field.

$$E = - \frac{KT}{qW} \frac{1}{N} \frac{dN}{dx} \quad \dots (5.2)$$

Integrating this relation the following expression for the impurity distribution is obtained.

$$N(x) = A \exp\left(- \frac{qW}{KT} \int_0^x E dx\right)$$

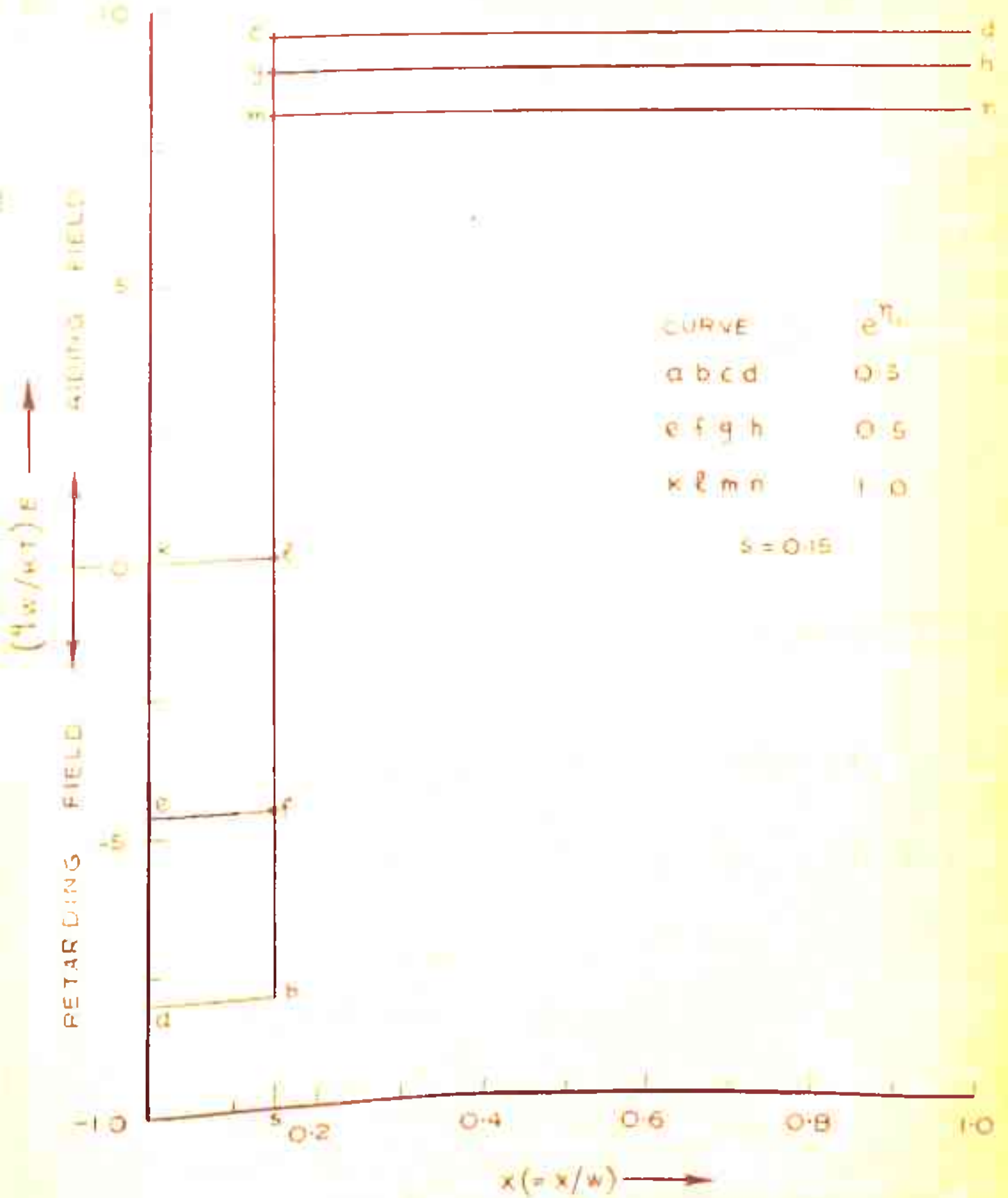


FIG. 5-1 SYNTHESISED TWO SEGMENT FIELD CONFIGURATIONS IN THE BASE.

Using the electric field expressions 5.1a and 5.1b, the two segment impurity distributions are given by:

$$N_I(x) = A \exp(-\eta_1 \frac{x}{s}) \quad (0 \leq x \leq s) \quad \dots (5.3a)$$

$$N_{II}(x) = A_1 \exp(-\eta_2 \frac{x-s}{1-s}) \quad (s \leq x \leq 1) \quad \dots (5.3b)$$

The constant A and A_1 can be determined from the following boundary conditions for $N(x)$.

$$N_I = N_0 \quad \text{at } x = 0$$

$$N_I = N_{II} = N_s \quad \text{at } x = s$$

$$N_{II} = N_w \quad \text{at } x = 1$$

Substituting the above boundary conditions, eqn. 5.3 yields the following result.

$$N_I(x) = N_0 \exp(-\frac{\eta_1}{s} x) \quad (0 \leq x \leq s) \quad \dots (5.4a)$$

$$N_{II}(x) = N_s \exp(-\frac{\eta_2}{1-s} (x-s)) \quad (s \leq x \leq 1) \quad \dots (5.4b)$$

where $\eta_1 = \ln N_0/N_s$

$$\eta_2 = \ln N_s/N_w$$

Eqs. 5.4a and 5.4b describe the segments of the impurity distributions in the two regions respectively.

Using this distribution, the minority carrier concentration and base transit time are evaluated in the ensuing sections. Fig. 5.2 shows a plot of two segment impurity

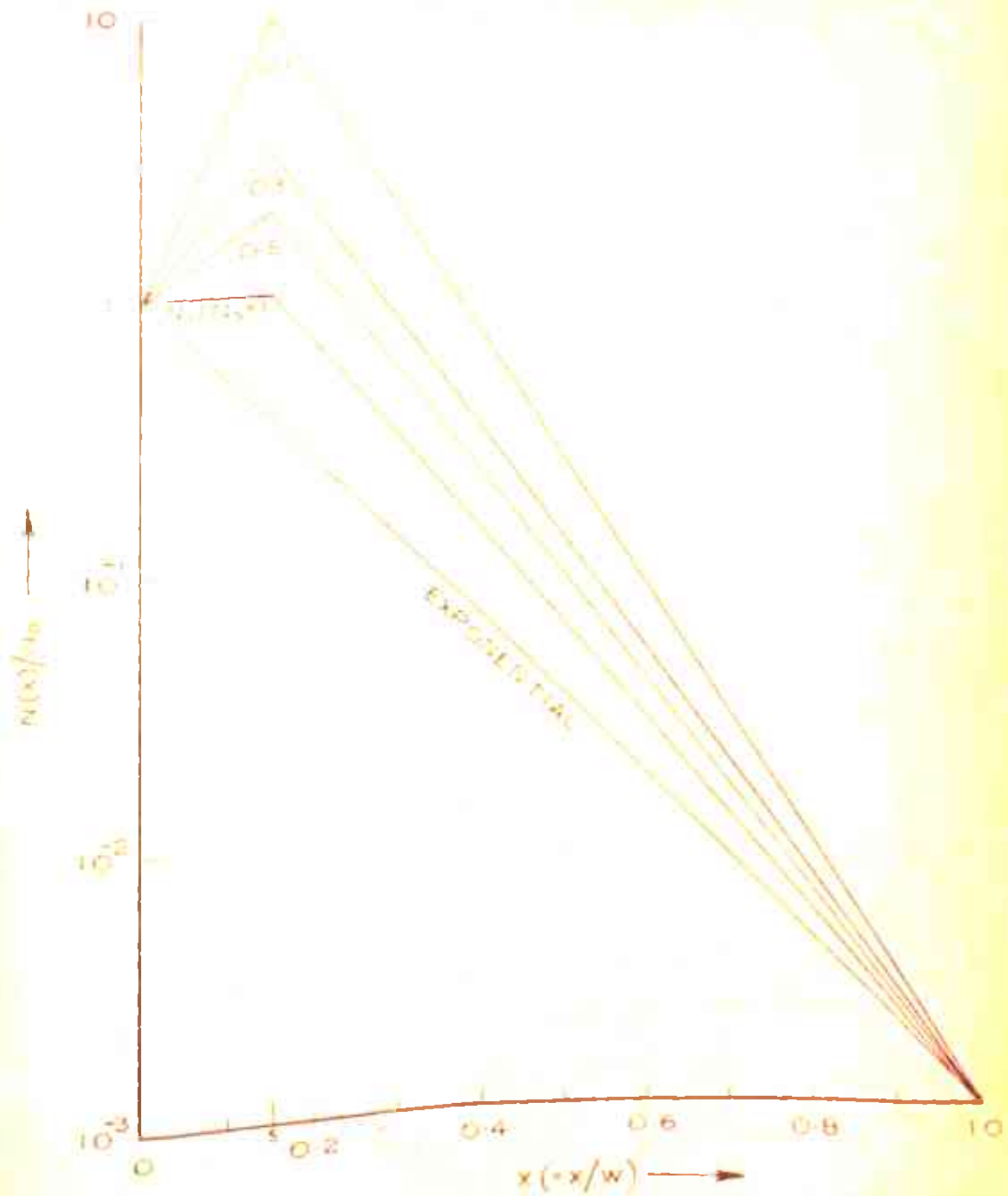


FIG 5.2. BASE IMPURITY DISTRIBUTIONS FOR TWO SEGMENT FIELD CONFIGURATIONS.

distributions. In the first segment, a retarding or a zero field is present.

5.2.2 Excess Minority Carrier Concentration in the Base

Making use of the basic relations obtained in Chapter 2, the minority carrier concentration in the case of two segment impurity distributions can be expressed as follows.

Region - I ($0 \leq x \leq s$)

$$\left(\frac{q D_p}{J_p W}\right) p = \frac{\int_0^s N_I(x) dx + \int_s^1 N_{II}(x) dx}{N_I(x)} \quad \dots (5.5a)$$

Region - II ($s \leq x \leq 1$)

$$\left(\frac{q D_p}{J_p W}\right) p = \frac{\int_s^1 N_{II}(x) dx}{N_{II}(x)} \quad \dots (5.5b)$$

When N_I and N_{II} from eqns. 5.4a and 5.4b are substituted in the above expression, the following relation is obtained.

$$\left(\frac{q D_p}{J_p W}\right) p = \frac{s}{\eta_1} (1 - e^{-\eta_1 + \eta_1 \frac{x}{s}}) + \frac{1-s}{\eta_2} (1 - e^{-\eta_2}) e^{-\eta_1 + \eta_1 \frac{x}{s}} \quad (0 \leq x \leq s) \quad \dots (5.6a)$$

$$\left(\frac{q D_p}{J_p W}\right) p = \frac{1-s}{\eta_2} \left(1 - e^{-\eta_2 x} + \eta_2 \frac{x-s}{1-s}\right) \quad (0 \leq x \leq 1) \quad \dots (5.6b)$$

Using this relation, the minority carrier concentration is evaluated and the results are plotted in Fig. 5.3.

5.2.3 Base Transit Time

Constant mobility case

In the case of constant mobility, the base transit time is obtained by integrating eqns. 5.6a and 5.6b between the limits 0 to s , and s to 1, respectively. Varnerin's stored base charge definition is then used and the following normalised base transit time expression is derived.

$$\frac{t_B}{t_{BU}} = 2s(1-s)A + 2s^2B + 2(1-s)^2C \quad \dots (5.7)$$

where

$$A = \frac{1 - e^{-\eta_1}}{\eta_1} \cdot \frac{1 - e^{-\eta_2}}{\eta_2}$$

$$B = \frac{\eta_1 - 1 + e^{-\eta_1}}{\eta_1^2}$$

$$C = \frac{\eta_2 - 1 + e^{-\eta_2}}{\eta_2^2}$$

$t_{BU} (= W^2/2 D_p)$ is the transit time of a uniform base transistor.

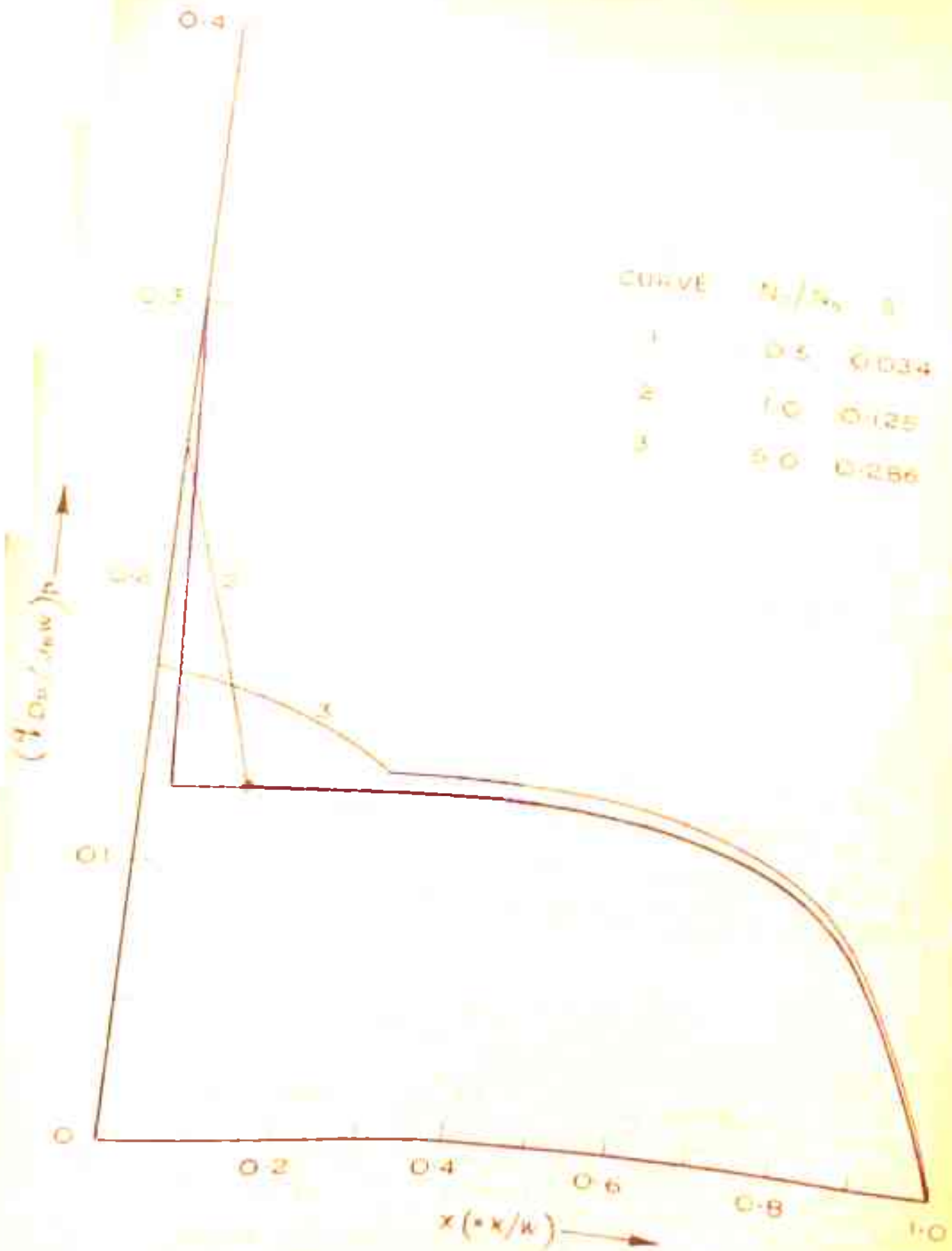


FIG 5.3 MINORITY CARRIER CONCENTRATION IN THE BASE FOR TWO SEGMENT DISTRIBUTIONS.

Let us define

$$T = t_B/t_{BU} \quad \dots (5.8)$$

Then the application of the condition

$$\frac{dT}{ds} = 0 \quad \dots (5.9)$$

yields the following unique value of s for minimum base transit time.

$$s = \frac{1}{2} \left(\frac{A - 2C}{A - B - C} \right) \quad \dots (5.10)$$

For different ratios of N_0/N_B , the base transit time is calculated from eqn. 5.7. The value of $N_0/N_W = 10^3$ is kept fixed.

Doping dependent mobility case

The mobility variation with doping affects the transit time in the base region. This effect is studied in this section for two segment impurity distributions. Sugano and Koshiga's following relation of the diffusion coefficient is used.

$$D = D_0 (N/N_0)^{-6} \quad \dots (5.11)$$

In order to evaluate base transit time for the two segment impurity distributions, the basic relation derived in Chapter 2 is used. The following general expression for the normalised base transit time is obtained. ($\theta = 0.25$ is assumed.)

$$\frac{t_d}{t_{B0}} = 2 \int_0^s \frac{\left(\int_x^s (N_I(x)/N_0)^{1.25} dx + \int_s^1 (N_{II}(x)/N_0)^{1.25} dx \right)}{N_I(x)/N_0} dx + 2 \int_s^1 \frac{\left(\int_x^1 (N_{II}(x)/N_0)^{1.25} dx \right)}{N_{II}(x)} dx \quad \dots (5.12)$$

where $t_{B0} = W^2/2 D_0$.

Substituting N_I and N_{II} from eqns. 5.4a and 5.4b in the above relation, the following expression is obtained.

$$\frac{t_B}{t_{B0}} = 1.6 s(1-s) W' + 1.6 s^2 T' + 1.6 (1-s)^2 U' \quad \dots (5.13)$$

where

$$W' = \frac{1 - e^{-\eta_1}}{\eta_1} \cdot \frac{1 - e^{-1.25 \eta_2}}{\eta_2} \cdot e^{-.25 \eta_1}$$

$$T' = \frac{e^{-1.25 \eta_1} + 4 - 5e^{-.25 \eta_1}}{\eta_1^2}$$

$$U' = \frac{e^{-1.25 \eta_2} + 4 - 5e^{-.25 \eta_2}}{\eta_2^2} \cdot e^{-.25 \eta_1}$$

Defining $T = t_B/t_{B0}$ and applying the condition

$$\frac{dT}{ds} = 0, \quad \dots (5.14)$$

the following s value is obtained.

$$s = \frac{1}{2} \left(\frac{W' - 2U'}{W' - T' - U'} \right) \quad \dots (5.15)$$

In this case, base transit time is computed for different values of N_0/N_B from eqn. 5.13. The results are compared with those obtained in the case of exponential distribution.

In both the cases of constant and doping dependent mobility, the transit time results are presented as percentage decrease in transit time, defined below.

$$\text{Percentage decrease in transit time} = \frac{t_B(\text{exp}) - t_B(N)}{t_B(\text{exp})} \times 100 \quad \dots (5.16)$$

where $t_B(\text{exp})$ and $t_B(N)$ denote transit times for exponential and general impurity distribution $N(x)$, respectively.

For retarding field structures, the percentage decrease in transit time as a function of s - the width of the first region - is plotted in Fig. 5.4. The ratio N_0/N_B serves as parameter. The transit time values are given in Table 5.1. A study of the results indicates that the decrease in transit time is maximum for smaller values of s and N_0/N_B . The above observation is made for the case of constant mobility.

For structures providing zero or aiding built-in electric field in region-I, the transit time and its percentage decrease are given in Table 5.2 for both constant and doping dependent mobility. Optimum s values as obtained from eqns. 5.9 and 5.15 are used. When constant mobility is assumed, the transit time is found to be minimum for zero electric field ($N_0/N_B = 1$) in region I. Upto some value of N_0/N_B ratio, the transit time increases. Further increase in this ratio results in a decrease in transit time. When

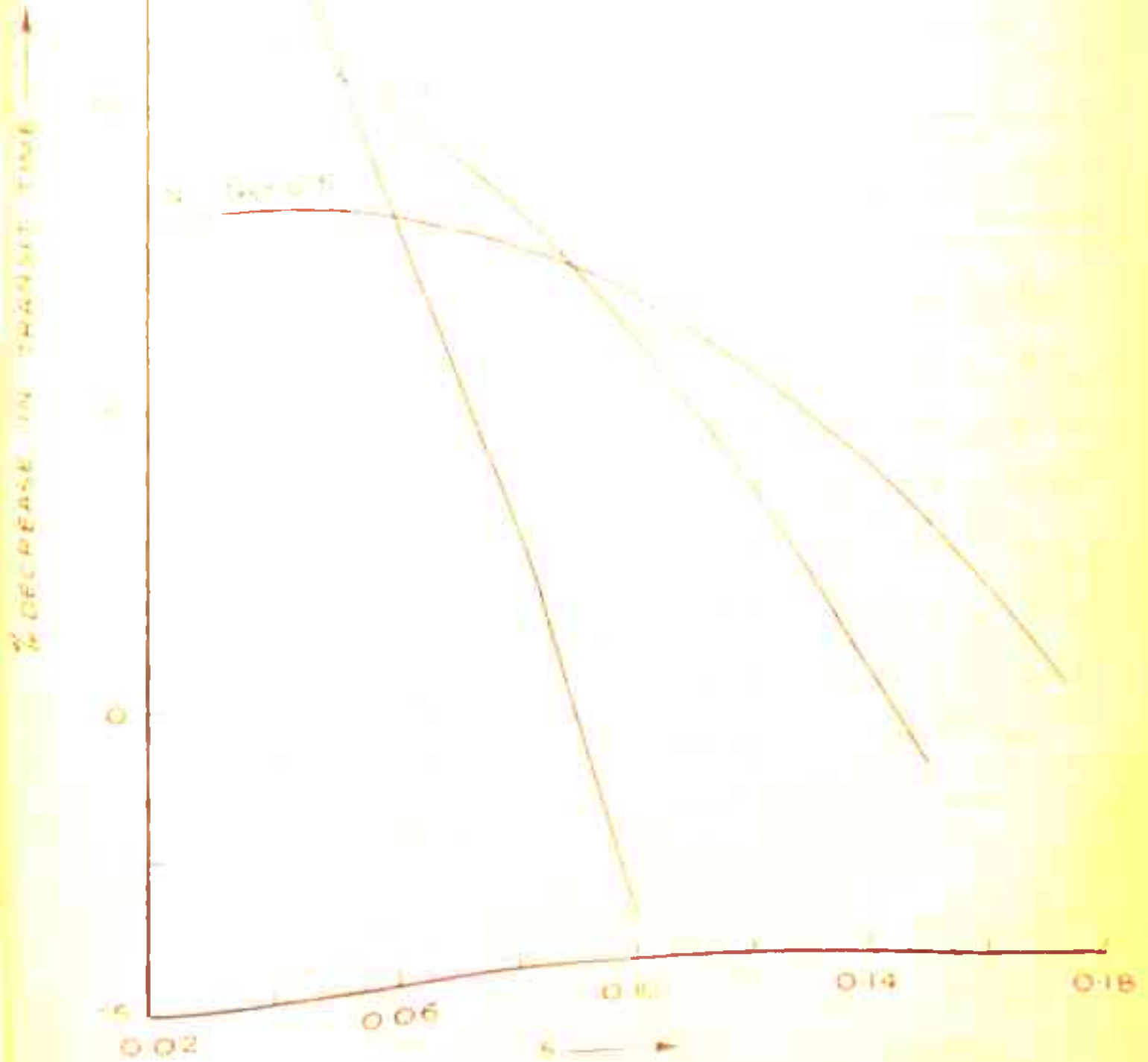


FIG. 5.4 PERCENTAGE DECREASE IN BASE TRANSIT TIME VS. WIDTH OF LOADING FIELD REGION S

TABLE 5.1

Calculation of Normalised Transit Time (t_B/t_{BU})
and Percentage Decrease in Transit Time for
Two Segment Retarding Field Configurations.

s	N_0/N_s					
	0.1		0.3		0.5	
	Transit Time	% Decrease	Transit Time	% Decrease	Transit Time	% Decrease
0.02	0.20355	17.8	0.21759	12.1	0.22742	8.10
0.03	0.20910	15.5	0.21869	11.6	0.22721	8.24
0.05	0.22132	10.6	0.22168	10.4	0.22746	8.10
0.07	0.23505	5.0	0.22570	8.8	0.22861	7.60
0.09	0.25026	-1.05	0.23075	6.8	0.23066	6.80
0.10	0.25843	-4.30	0.23367	5.6	0.23202	6.30
0.15	0.30490	-23.00	0.25215	-1.8	0.24222	2.20

($N_0/N_w = 10^3$ is kept constant in the above calculations)

Normalised Transit Time for
 Exponential Distribution
 (constant mobility) - = 0.24765

mobility depends on doping, the decrease in transit time is monotonic with increasing N_0/N_s ratio. As much as 25% improvement in transit time is obtained in this case.

TABLE 5.2

Calculation of Normalised Transit Time and Percentage Decrease in Transit Time for Two Segment Aiding Field Configurations

Normalised Transit Time for Exponential Distribution

- Constant Mobility = 0.24765
- Doping Dependent Mobility (Sugano and Koshiga) = 0.10431

$\frac{N_0}{N_s}$	Constant mobility			Doping dependent mobility		
	α	t_B/t_{B0}	% decrease	α	t_B/t_{B0}	% decrease
1.0	0.125	0.23473	5.2	-	-	-
5.0	0.286	0.24554	0.8	0.105	0.09637	7.7
10.0	0.366	0.24690	0.3	0.160	0.09235	11.5
100.0	0.634	0.24690	0.3	0.375	0.08253	21.0
500.0	0.817	0.24180	2.4	0.566	0.07886	24.4

$(N_0/N_w = 10^3)$ is kept constant in the above calculations)

5.3 SYNTHESIS OF ELECTRIC FIELD CONFIGURATIONS - THREE SEGMENTS

In this section, three segment built-in electric field configurations are synthesised through segmentation technique. Apart from other factors like improvement in base transit time, etc., the important factor in introducing the three segment approach is to show that any complicated structure of field or impurity distribution can be simulated by considering three or more segments for the complete profile.

In the present case, the total base region is divided into three regions. In each region, there is a constant built-in field of different magnitude. The analytical expression of the field is described below.

Region - I ($0 \leq x \leq p_1$)

$$E = \frac{KT}{q p_1 W} \eta_1 \quad \dots (5.17a)$$

Region - II ($p_1 \leq x \leq p_2$)

$$E = \frac{KT}{q(p_2 - p_1) W} \eta_2 \quad \dots (5.17b)$$

Region - III ($p_2 \leq x \leq 1$)

$$E = \frac{KT}{q(1 - p_2) W} \eta_3 \quad \dots (5.17c)$$

where p_1 , $(p_2 - p_1)$ and $(1 - p_2)$ are the normalised widths of the three regions of the base. η_1 , η_2 , η_3 are field parameters for regions I, II and III, respectively.

Fig. 5.5 shows a plot of the synthesised three segment field configurations.

5.3.1 Derivation of Impurity Distribution

Given the above field configuration, the corresponding impurity distribution is derived from eqn. 5.2. The following boundary conditions for $N(x)$ are used

$$N_I = N_0 \quad \text{at } x = 0$$

$$N_I = N_{II} = N_1 \quad \text{at } x = p_1$$

$$N_{II} = N_{III} = N_2 \quad \text{at } x = p_2$$

$$N_{III} = N_w \quad \text{at } x = 1,$$

and the following relation for the impurity distribution is obtained.

$$N_I(x) = N_0 e^{-\eta_1 \frac{x}{p_1}} \quad (0 \leq x \leq p_1) \quad \dots (5.18a)$$

$$N_{II}(x) = N_1 e^{-\eta_2 \frac{x - p_1}{p_2 - p_1}} \quad (p_1 \leq x \leq p_2) \quad \dots (5.18b)$$

$$N_{III}(x) = N_2 e^{-\eta_3 \frac{x - p_2}{1 - p_2}} \quad (p_2 \leq x \leq 1) \quad \dots (5.18c)$$

where

$$\eta_1 = \ln N_0/N_1,$$

$$\eta_2 = \ln N_1/N_2,$$

$$\eta_3 = \ln N_2/N_w,$$

$$\text{and } \eta = \ln N_0/N_w = \eta_1 + \eta_2 + \eta_3$$

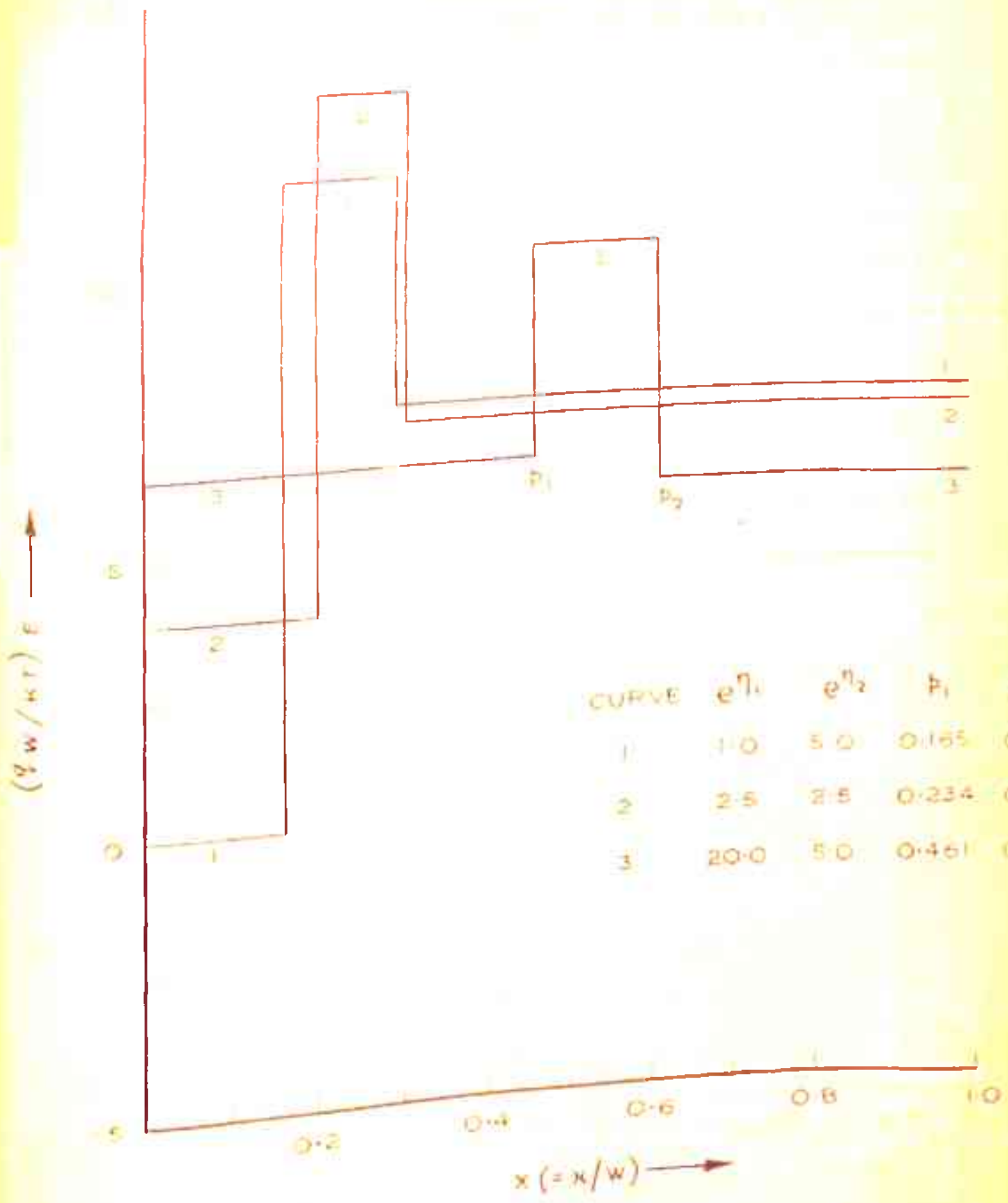


FIG. 5.5 SYNTHESISED THREE SEGMENT FIELD CONFIGURATIONS IN THE BASE.

For $n_1 < 0$, retarding field occurs while for $n_1 > 0$, aiding field occurs in region I of the base. The three segment impurity distributions are sketched in Fig. 5.6.

5.3.2 Excess Minority Carrier Concentration in the Base

The excess minority carrier concentration in this case is calculated by using the basic relation obtained in Chapter 2. The following expression is obtained.

$$\text{Region - I} \\ \left(\frac{q D_p}{J_p}\right) p = \frac{\int_x^{P_1} N_I(x) dx + \int_{P_1}^{P_2} N_{II}(x) dx + \int_{P_2}^1 N_{III}(x) dx}{N_I(x)} \quad \dots (5.19a)$$

$$\text{Region - II} \\ \left(\frac{q D_p}{J_p}\right) p = \frac{\int_x^{P_2} N_{II}(x) dx + \int_{P_2}^1 N_{III}(x) dx}{N_{II}(x)} \quad \dots (5.19b)$$

$$\text{Region-III} \\ \left(\frac{q D_p}{J_p}\right) p = \frac{\int_x^1 N_{III}(x) dx}{N_{III}(x)} \quad \dots (5.19c)$$

Eqns. 5.18a, b and c are substituted in the above relation and the carrier concentration is obtained as follows.

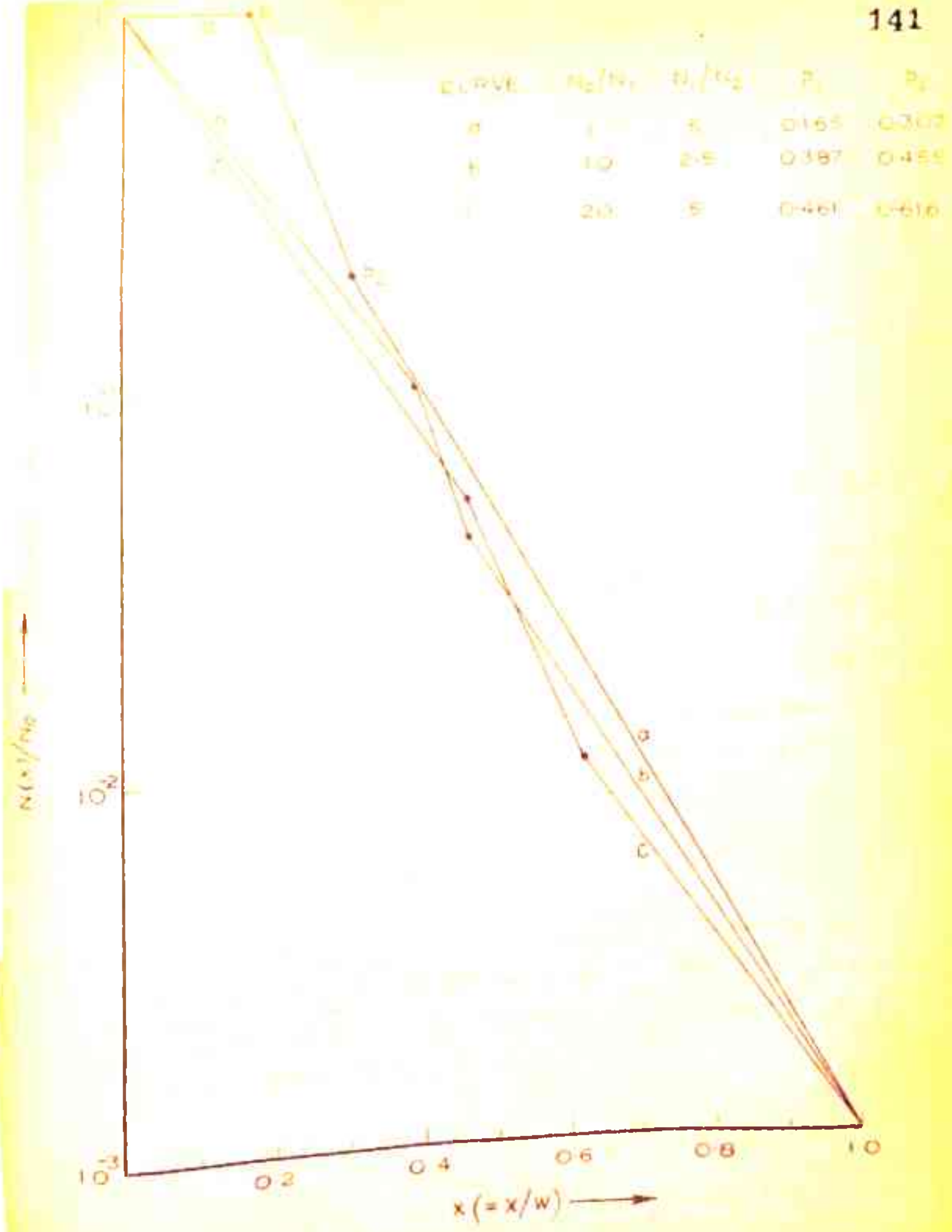


FIG. 5.6 BASE IMPURITY DISTRIBUTIONS FOR THREE SEGMENT FIELD CONFIGURATIONS

$$\begin{aligned} \left(\frac{q D_B}{J_p W}\right) P &= \frac{p_1}{\eta_1} (1 - e^{-\eta_1 x} + \eta_1 \frac{x}{p_1}) + \frac{p_2 - p_1}{\eta_2} (1 - e^{-\eta_2 x}) \\ &\quad e^{-\eta_1 x} + \eta_1 \frac{x}{p_1} + \frac{1 - p_2}{\eta_3} (1 - e^{-\eta_3 x}) e^{-\eta_1 x - \eta_2 x - \eta_1 \frac{x}{p_1}} \\ &\quad (0 \leq x \leq p_1) \end{aligned} \quad \dots (5.20a)$$

$$\begin{aligned} \left(\frac{q D_B}{J_p W}\right) P &= \frac{p_2 - p_1}{\eta_2} (1 - e^{-\eta_2 x} + \eta_2 \frac{x - p_1}{p_2 - p_1}) \\ &\quad + \frac{1 - p_2}{\eta_3} (1 - e^{-\eta_3 x}) e^{-\eta_2 x + \eta_2 \frac{x - p_1}{p_2 - p_1}} \quad (p_1 \leq x \leq p_2) \end{aligned} \quad \dots (5.20b)$$

$$\left(\frac{q D_B}{J_p W}\right) P = \frac{1 - p_2}{\eta_3} (1 - e^{-\eta_3 x} + \eta_3 \frac{x - p_2}{1 - p_2}) \quad (p_2 \leq x \leq 1) \quad \dots (5.20c)$$

For specific values of N_0/N_1 and N_1/N_2 ratios, the carrier concentration is calculated and the results are plotted in Fig. 5.7.

5.3.3 Base Transit Time

The base transit time is obtained by evaluating the total stored charge in the base. Varnerin's base transit time definition is used and the following expression for the normalized base transit time is obtained.

$$\begin{aligned} \frac{t_B}{t_{BU}} &= p_1^2 A' + (p_2 - p_1)^2 B' + (1 - p_2)^2 C' + p_1 (p_2 - p_1) D' \\ &\quad + (p_2 - p_1) (1 - p_2) E' + p_1 (1 - p_2) F' \quad \dots (5.21) \end{aligned}$$

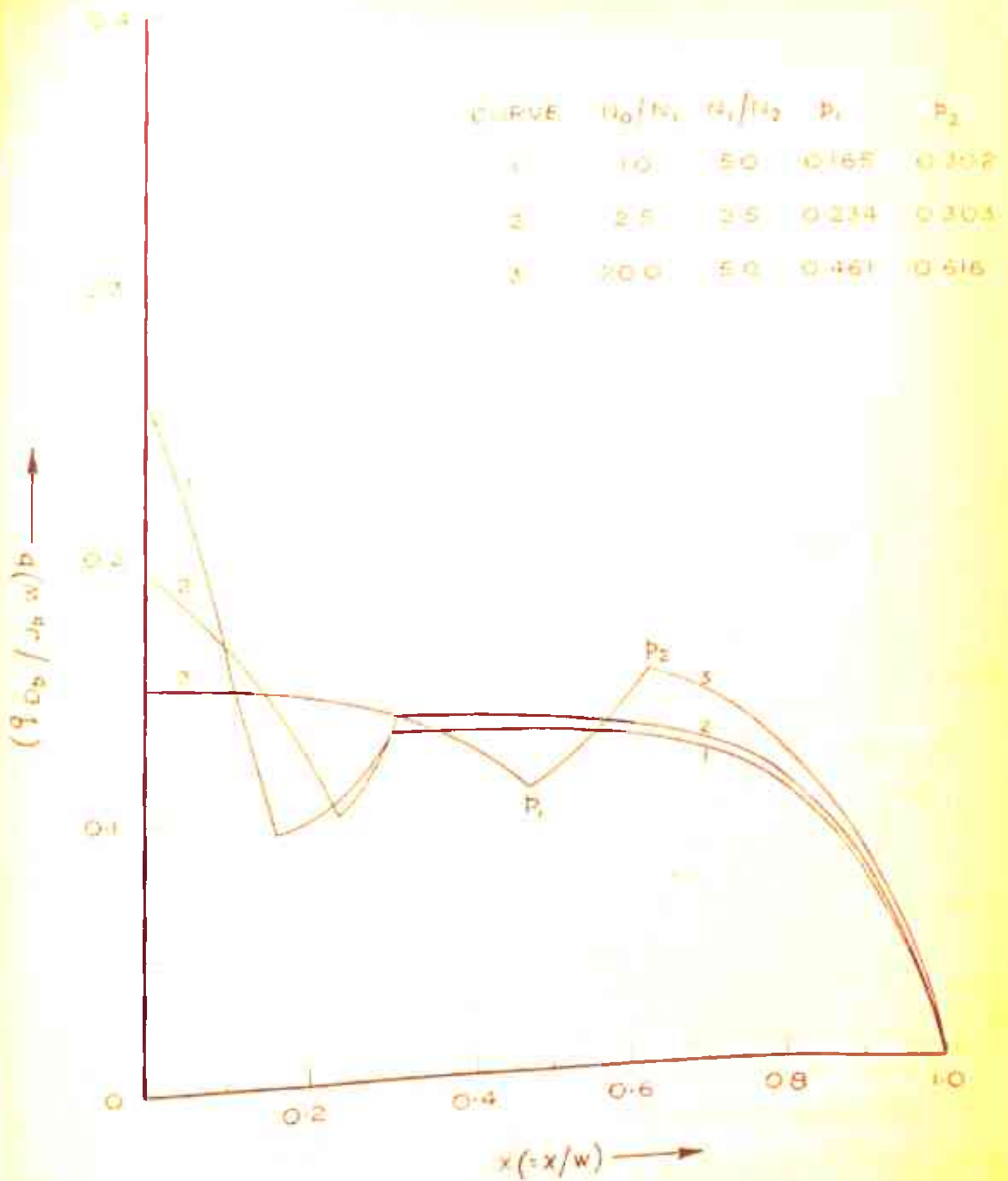


FIG. 5.7 MINORITY CARRIER CONCENTRATION IN THE BASE FOR THREE SEGMENT DISTRIBUTIONS.

where $t_{BU} = W^2/2 D_p$

$$A' = 2(\eta_1 - 1 + e^{-\eta_1})/\eta_1^2$$

$$B' = 2(\eta_2 - 1 + e^{-\eta_2})/\eta_2^2$$

$$C' = 2(\eta_3 - 1 + e^{-\eta_3})/\eta_3^2$$

$$D' = 2(1 - e^{-\eta_1})(1 - e^{-\eta_2})/\eta_1 \eta_2$$

$$E' = 2(1 - e^{-\eta_2})(1 - e^{-\eta_3})/\eta_2 \eta_3$$

$$F' = 2(1 - e^{-\eta_1})(1 - e^{-\eta_3})e^{-\eta_2}/\eta_1 \eta_3$$

Let us define

.. (5.22)

$$T = t_3/t_{BU}$$

For fixed values of N_0/N_1 and N_1/N_2 , the optimum values of p_1 and p_2 for minimum transit time can be obtained by the application of the following condition.

.. (5.23)

$$\frac{\partial T}{\partial p_1} = 0$$

.. (5.24)

$$\frac{\partial T}{\partial p_2} = 0$$

For $N_0/N_w = 10^3$, the transit time is evaluated from eqn. 5.20. The results of normalised transit time and its percentage decrease are presented in Table 5.3. Some specific combinations of N_0/N_1 and N_1/N_2 are considered and the values of p_1 and p_2 as obtained from eqns. 5.23 and 5.24 are used. The transit times are found to be less than those obtained for exponential distribution.

TABLE 5.2

Calculation of Normalised Transit Time
(t_B/t_{BU}) and Percentage Decrease in
Transit Time for Three Segment Distributions

N_0/N_1	N_1/N_2	P_1	P_2	t_B/t_{BU}	% Decrease in Transit Time
0.5	5.0	0.0025	0.2645	0.22643	8.5
1.0	5.0	0.1654	0.3023	0.23290	5.9
2.5	2.5	0.2341	0.3030	0.24171	2.4
10.0	2.5	0.3873	0.4558	0.24493	1.1
20.0	5.0	0.4613	0.6168	0.24435	1.3

($N_0/N_w = 10^3$ is kept constant in the above calculations)

Normalised Transit Time for Exponential Distribution (Constant Mobility) = 0.24765

5.4 SUMMARY AND DISCUSSION

Through segmentation technique, two segment and three segment built-in electric field configurations have been synthesised and the corresponding impurity distributions have been obtained. Minority carrier concentration and base transit time have been evaluated. It is observed that minimum transit time occurs when retarding field is present over a small portion of the whole base width. For two segment distributions, the percentage decrease in transit time as compared with the time for the exponential distribution is as high as 20% when mobility is constant. It approaches 25% when doping dependent mobility is assumed.

The improvement in the base transit time can be explained as follows. In the case of constant mobility, both two and three segment distributions providing a retarding field in region I of the base show an improvement in base transit time. Though the retarding field of the first region opposes the carrier flow, yet the large aiding field offered by the distributions of the subsequent regions speeds up the carrier flow resulting in a net improvement in the overall transit time. Such distributions can be expected to yield much better figure of merit for the transistor without adversely affecting the E-B transition capacitance. In the next chapter, the figure of merit for such distributions is evaluated.

CHAPTER 6

EFFECT OF BASE IMPURITY DISTRIBUTION ON THE FIGURE OF MERIT OF TRANSISTORS

- 6.1 INTRODUCTION
- 6.2 GENERAL EXPRESSION FOR FIGURE OF MERIT
- 6.3 EVALUATION OF FIGURE OF MERIT FOR BASIC IMPURITY DISTRIBUTIONS
 - 6.3.1 CONSTANT MOBILITY CASE
 - 6.3.2 DOPING DEPENDENT MOBILITY CASE
- 6.4 EVALUATION OF FIGURE OF MERIT FOR IMPURITY DISTRIBUTIONS SYNTHESISED THROUGH SEGMENTATION TECHNIQUE
- 6.5 EVALUATION OF FIGURE OF MERIT FOR IMPURITY DISTRIBUTIONS DERIVED FROM SYNTHESISED BASE REGION ELECTRIC FIELD CONFIGURATIONS
 - 6.5.1 TWO SEGMENT DISTRIBUTIONS
 - 6.5.2 THREE SEGMENT DISTRIBUTIONS
- 6.6 REMARKS ABOUT THE VALIDITY OF f_T APPROXIMATION
- 6.7 SUMMARY AND DISCUSSION

REFERENCES

CHAPTER 6

EFFECT OF BASE IMPURITY DISTRIBUTION ON THE FIGURE OF MERIT OF TRANSISTORS

6.1 INTRODUCTION

Figure of merit of a device is an important parameter as it is a true index of the performance capability of the device. Any quantitative expression used to define the figure of merit should fulfil the following conditions.

- a. The figure of merit should characterise only the property of the device and should not depend on the parameters of the circuit elements external to the device.
- b. The figure of merit should have a clear physical significance.

Based on the above requirements, an expression for figure of merit of high-frequency transistors is deduced. The effect of base doping distribution on the figure of merit is studied in detail. Some typical base impurity distributions which yield much higher device figure of merit than that obtained with conventional doping distributions are suggested. In particular, considerable improvement in figure of merit is achieved by using impurity distributions which give rise to retarding fields over a portion of the base region. This improvement is achieved without adversely

affecting the E-B barrier capacitance. It is also established that the optimum impurity distributions for minimum base transit time do not yield improved figure of merit.

6.2 GENERAL EXPRESSION FOR FIGURE OF MERIT

There are two high-frequency figures of merit which have received wide acceptance for describing the high frequency performance of transistors. These are the unity current gain frequency f_T , and the maximum frequency of oscillation f_{max} . A simple expression relating the cut-off frequency f_T to the reciprocal of a sum of time constants is the following^{1,2,3}.

$$\frac{1}{2\pi f_T} = t_E + t_B + t_D \quad \dots (6.1)$$

where $t_E = \frac{KT}{qI_e} C_e$: the emitter time constant

t_B = base transit time (expression given in Chapter 2)

$t_D = \frac{x_m}{2v_{sc}}$: collector depletion layer transit time.

C_e is the emitter transition capacitance and x_m is the width of the collector depletion layer. v_{sc} is the scatter limited drift velocity for carriers passing through the reverse biased collector depletion region. I_e is the d.c. emitter current.

In addition to the above three delays, the current carriers encounter a fourth delay also⁴. This is the collector charging time t_C defined as below.

$$t_C = r_{sc} C_c$$

where r_{sc} is the collector series resistance and C_c is collector transition region capacitance. But this delay is mainly important at intermediate or high emitter currents⁵ or in integrated circuit transistors⁶.

The maximum frequency of oscillation is the frequency at which the maximum available power gain is unity. In terms of the device parameters it is described as⁷⁻⁹

$$f_{max} = \sqrt{\frac{f_T}{8\pi r_b' C_c}} \quad \dots(6.2)$$

where r_b' is the base resistance.

Maeda, Imai and Furumoto¹⁰ investigated the following figure of merit which is equivalent to f_{max} .

$$F = \frac{f_T}{r_b' C_c} \quad \dots(6.3)$$

The above definition was later on modified by the same authors and the modified expression has been used to present design consideration of base impurity distribution for high frequency figure of merit. The modified expression is given below¹¹.

$$F' = \frac{f_T}{r_b'} \quad \dots(6.4)$$

In the present study, the figure of merit definition as given by eqn. 6.3 has been used. The computations of the figure of merit for different base doping distributions are presented. The results are compared with those obtained

in the case of exponential doping distribution. The comparison with the exponential distribution is made due to the fact that this distribution has been found through variational method to be the optimum for minimum base transit time when mobility is constant. Moreover, the exponential profile is often used as an approximation in the analytical treatment of the conventional base doping distributions such as, Gaussian and erfc. The following assumptions have been made in the derivation of the normalised figure of merit expression.

- (a) The contribution to the cut-off frequency f_T is mainly from the base transit time t_B i.e.

$$f_T \approx \frac{1}{2\pi t_B} \quad \dots(6.5)$$

This approximation is valid for the example considered in this Chapter. It has been used earlier by Kromer¹² also. The justification for this assumption is also evident when actual calculations of the magnitude of the other time delays, such as, t_E and t_D are made.

- (b) The collector transition capacitance C_c is evaluated by assuming that the collector-base junction is linearly graded for lower values of C-B reverse bias voltage. This assumption is substantiated by actually solving the Poisson's equation for several impurity distributions (Appendix-V). Within 10-20% accuracy, it has been observed that the linear grading approximation is quite suited for most of the impurity distributions except a few cases where abrupt approximation proves to be better.

Gandhi¹³ has also shown the validity of this assumption for graded-base transistors operating at low C-B reverse bias.

Based on the above assumptions and eqn. 6.3, the new figure of merit is obtained as

$$FM = \frac{1}{t_B r_b' C_c} \quad \dots(6.6)$$

Using the above relation, the normalised figure of merit can be expressed in the following manner.

$$\frac{FM(N)}{FM(\text{exp})} = \frac{t_B(\text{exp})}{t_B(N)} \cdot \frac{r_b'(\text{exp})}{r_b'(N)} \cdot \frac{C_c(\text{exp})}{C_c(N)} \quad \dots(6.7)$$

where the normalisation is done with respect to the exponential doping distribution in the base. The subscripted variables in the above equation either refer to the arbitrary distribution N or the exponential distribution (exp).

The case transit time expressions have already been obtained in Chapter 2. The same results are used here. The relation for normalised base transit time in the case of constant mobility, can be expressed as

$$\frac{t_B(\text{exp})}{t_B(N)} = \left(\frac{\eta - 1 + e^{-\eta}}{\eta^2} \right) \left[\int_0^1 \frac{N_N(x) dx}{N_N(x)} \right]^{-1} \quad \dots(6.8)$$

where $N_N(x)$ represents any arbitrary impurity distribution in the base.

The base resistance r_b' is given by the relation²

$$r_b'(N) \propto \left(q \int_0^W \mu_n(x) N_N(x) dx \right)^{-1} \quad \dots(6.9)$$

In constant mobility case, use of the above relation yields the normalised base resistance as

$$\frac{r_b'(\text{exp})}{r_b'(N)} = \frac{\int_0^1 N_N(X) dX}{\int_0^1 N_{\text{exp}}(X) dX} \quad \dots (6.10)$$

where N_{exp} represents exponential doping distribution.

The capacitance of a linearly graded junction is given by the relation¹³

$$\frac{C_c}{A} = \left[\frac{k^2 \epsilon_0^2 q a}{12 V} \right]^{1/3}$$

where a is the grade constant and V is the applied reverse bias C-B voltage.

For same C-B junction voltage in the cases of exponential and arbitrary impurity distributions, the normalised capacitance can be written as

$$\frac{C_c(\text{exp})}{C_c(N)} = \left(\frac{a_{\text{exp}}}{a_N} \right)^{1/3} \quad \dots (6.11)$$

where a_{exp} and a_N denote the grade constants for exponential and arbitrary distributions in the base, respectively.

The grade constant is evaluated from the following relation

$$a = \left. \frac{dN}{dx} \right|_{x=x_j}$$

x_j is the location of the C-B junction. If the impurity distribution is described in the manner,

$$N = N_N(x) - N_B \quad \dots (6.12)$$

at $x = x_j$, $N_N(x_j)$ will be equal to the background collector region concentration N_B .

In cases where step junction approximation proves to be the better one, the junction capacitance is calculated from the following relation¹³.

$$\frac{C_c}{A} = \left(\frac{q k \epsilon_0}{2V} \frac{N_w N_B}{N_w + N_B} \right)^{1/2} \quad \dots (6.13)$$

where N_w is the impurity concentration at the collector^{end} of the base region. A reverse bias of 5 volts is assumed for the purpose of calculating capacitance from the above relation.

Substituting expressions 6.8, 6.10 and 6.11 into eqn. 6.7, the complete figure of merit as a function of the impurity concentration N is obtained as

$$\frac{FM(N)}{FM(\text{exp})} = \frac{\eta - 1 + e^{-\eta}}{\eta^2} \left[\int_0^1 \frac{\int_0^x N_N(x) dx}{N_N(x)} dx \right]^{-1} \times \frac{\eta}{1 - e^{-\eta}} \int_0^1 N_N(x) dx \left(\frac{a_{\text{exp}}}{a_N} \right)^{1/3} \quad \dots (6.14)$$

This is the general expression for the normalised figure of merit and is valid in the case of constant mobility.

6.3 EVALUATION OF FIGURES OF MERIT FOR BASIC IMPURITY DISTRIBUTIONS

The basic impurity doping distributions in the base have been treated earlier in Chapter 3 for the evaluation of minority carrier base transit time, built-in electric field and excess carrier concentration. In this section, the normalised figure of merit is calculated for these impurity distributions. Both the cases of constant and doping dependent carrier mobility are considered. The base impurity distributions are modified such that eqn. 6.12 is applicable. This modification is necessary since it is used to calculate the junction capacitance. This does not affect either the base transit time or the base resistance because $N_w > N_B$.

Gaussian, Erfc., Ho and Cho's optimum, Marshak's optimum and Hyperbolic distributions are considered in the base. Only in the case of hyperbolic distribution, a step junction approximation in the calculation of collector capacitance is ^{found} to be necessary; otherwise for all other distributions, the linear grading has been assumed. For step junction capacitance calculation, eqn. 6.13 is used. The impurity concentration is assumed to change abruptly from N_w to N_B . A C-B reverse bias voltage of 5 volts is assumed for this calculation.

The expressions for the impurity distributions and the corresponding grade constants at the C-B junction are given in Table 6.1. For numerical evaluations, the following constants are used wherever necessary.

TABLE 0.1

Basic Impurity Distributions and their
Corresponding Grade Constants

Impurity Distribution	Analytical Expression for $N(x)$	Grade Constant $\phi = \left. \frac{dN}{dx} \right _{x=x_j}$
Gaussian	$N_0 e^{-\eta x^2} - N_B$	$\frac{N_B}{W} \cdot 2\eta \sqrt{\frac{1}{\eta} \ln N_0/N_B}$
Erfc.	$N_0 \operatorname{erfc}(\beta x) - N_B$	$\frac{2}{\sqrt{\pi}} \frac{N_B}{W} \beta \frac{e^{-(\beta x_j)^2}}{\operatorname{erfc}(\beta x_j)}$
Exponential	$N_0 e^{-\eta x} - N_B$	$\frac{N_B}{W} \eta$
Ho and Cho's optimum	$N_0 e^{a_1 x + a_2 x^2 + a_3 x^3} - N_B$ (Valid for $N_0/N_B = 10^3$)	$\frac{N_B}{W} (a_1 + 2a_2 x_j + 3a_3 x_j^2)$
Marshak's optimum	$N_0 \exp(\gamma \sqrt{x} - \sqrt{\gamma B + \gamma x}) - N_B$	$\frac{N_B}{W} \cdot \frac{\gamma}{2(\ln \frac{N_0}{N_B} + \sqrt{\gamma B})}$
Hyperbolic	$N_0 \left(1 + \left(e^{\eta/4} - 1\right) x\right)^{-4} - N_B$	Capacitance is evaluated from step junction approximation

Here $\eta = \ln N_0/N_B$

$$\operatorname{erfc}(\beta) = e^{-\eta}, \quad x_j = x_j/W$$

N_B = Background impurity concentration

W = Electrical base width

$$a_1 = -8.71435; \quad a_2 = 3.6408; \quad a_3 = -1.80724$$

Other constants are described in Chapter 3.

$$\begin{aligned}
 N_0/N_W &= 10^3; & N_0 &= 10^{10} \text{ cm}^{-3}, \\
 N_B &= 5 \times 10^{14} \text{ cm}^{-3}, & W &= 5 \times 10^{-4} \text{ cm}.
 \end{aligned}$$

6.3.1 Constant Mobility Case

In the case of constant mobility, the normalised figure of merit is given by eqn. 6.14. For the above mentioned distributions, evaluation of the figure of merit is made by using numerical methods. The results of such calculations are presented in Table 6.2. The evaluation reveals that in the case of constant mobility, impurity distributions which are concave down on a $\ln N$ vs. X plot, such as, Gaussian and erfc, show an improvement in the device figure of merit over the exponential base doping distribution, while there is a deterioration when concave up distributions are used in the base.

6.3.2 Doping Dependent Mobility Case

When the carrier mobility in the base region depends on doping and is expressed by Sugano and Koshiga's¹⁴ empirical relation

$$\mu = \mu_0 \left(\frac{N}{N_0} \right)^{-\theta}$$

the normalised figure of merit expression 6.14 assumes a different form. In the derivation of this expression it is assumed that the minority and majority carrier mobility in the base follow the same doping dependence. In fact, the

exponent θ in the above relation should differ in the two cases. But to a first degree approximation this assumption holds good without introducing a large error¹¹. The base transit time has been computed earlier in Chapter 3, and base resistance can be calculated with the help of eqn. 6.9. Collector base capacitance does not change. Under these conditions, the normalised figure of merit in the case of doping dependent mobility assumes the following analytical form.

$$\frac{FM(N)}{FM(exp)} = \frac{\int_0^1 \left(\frac{N_{exp}}{N_0} \right)^{1+\theta} dx}{\int_0^1 \frac{dx}{N_{exp}/N_0}} \times \frac{\int_0^1 \left(N_N/N_0 \right)^{1-\theta} dx}{\int_0^1 \frac{dx}{N_N/N_0}} \times \left(\frac{a_{exp}}{a_N} \right)^{1/3} \quad \dots (6.15)$$

Using the above relation, normalised Figure of Merit is evaluated for the doping distributions described in Table 6.1. The calculated results are given in Table 6.2. For Mershak's and Ho and Cho's optimum distributions, the corresponding expressions of mobility (Chapter 2) are also used and the normalised figure of merit is calculated. These results are also tabulated in Table 6.2.

A study of the results shows that in the case of doping dependent mobility (Sugano and Koshiga's relation) there is no

TABLE 6.2

Calculation of Normalised Figure of Merit
for Basic Impurity Distributions

Impurity Distribution	$\tau_B(\text{exp})/\tau_B(N)$		$r_b'(\text{exp})/r_b'(N)$		$C_c(\text{exp})/C_c(N)$		$F_M(N)/F_M(\text{exp})$	
	Constant Mobility	Doping Dependent Mobility	Constant Mobility	Doping Dependent Mobility	Constant Mobility	Doping Dependent Mobility	Constant Mobility	Doping Dependent Mobility
Gaussian	0.8974	0.5751	2.3311	2.0259	0.7811	1.6342	0.9102	0.9102
Erfc.	0.9489	0.7073	2.0646	1.5556	0.8238	1.6139	0.9065	0.9065
Ho and Cho's optimum	0.9767	1.0143	0.8707	0.8918	0.9833	0.8363	0.9146	0.9146
Ho and Cho's optimum*	0.9767	1.0014	0.8707	0.8844	0.9833	0.8363	0.8710	0.8710
Marshak's optimum	0.9619	1.1603	0.7076	0.7431	1.1431	0.7781	0.9856	0.9856
Marshak's optimum**	0.9619	1.0563	0.7076	0.7280	1.1431	0.7781	0.8791	0.8791
Hyperbolic	0.8835	1.2745	0.4978	0.5465	1.1552	0.5001	0.8034	0.8034

* $\mu = a/(1+bN^c)$,** $\mu = a - b \ln N$

improvement in the device figure of merit over the exponential distribution. This is also true for empirical relations of carrier mobility other than Sugano and Koshiga's. But as compared to the constant mobility case, there is an improvement in the figure of merit for impurity distributions which are concave up on a $\ln N$ vs. X plot, whereas for concave down impurity distributions in the base, the figure of merit decreases. The calculated results of figure of merit reveal that the concave down distributions, such as, Gaussian and Erfc., exhibit an improvement in the case of constant mobility, while there is no improvement in the figure of merit when doping dependent mobility is considered.

A possible explanation to the above observations is given below. The concave down impurity distributions accommodate a larger amount of base impurities. This increase in the amount of impurity atoms results in a decrease in the base resistance. Consequently there is an improvement in the figure of merit over that of the exponential distribution when mobility is constant. But in the case of doping dependent mobility, the net decrease in the base resistance is less because of the decrease in mobility at higher impurity densities. Hence, the overall figure of merit is reduced in this case as compared with that of the exponential. However, the decrease in carrier mobility helps in relatively improving the figure of merit for concave up impurity distributions.

6.4 EVALUATION OF FIGURE OF MERIT FOR IMPURITY DISTRIBUTIONS SYNTHESISED THROUGH SEGMENTATION TECHNIQUE

In this section, impurity distributions synthesised through segmentation technique (Chapter 4) are considered and the normalised figure of merit is evaluated. The special form of impurity distribution, described in Chapter 3, is also treated for comparison. The synthesised impurity distributions are modified so as to include the effect of the background concentration N_B . This is done in order to make capacitance calculations feasible. The corresponding transit time and base resistance are not influenced by this change since $N_w > N_B$. The modified expressions are given in Table 6.3. In the evaluation of figure of merit the transit time results obtained earlier in Chapter 4 are used. The normalised base resistance is calculated from the following relation (constant mobility case).

$$\frac{r_{b'}(\text{exp})}{r_{b'}(N)} = \frac{\eta}{1 - e^{-\eta}} \left(\int_0^s \frac{N_I(x)}{N_0} dx + \int_s^1 \frac{N_{II}(x)}{N_0} dx \right) \quad \dots (6.16)$$

The capacitance calculations are based on a linear grading approximation. Only for the cases of segment of hyperbolic distribution in region II and special distributions, the step junction approximation is used; the impurity concentration in the base is assumed to change abruptly from N_w to N_B . The grade constant and hence the capacitance calculations are based on the second region impurity distribution in the base. The normalised figure of merit is obtained by making use of eqn. 6.7. The figure of merit is evaluated for different ratios

TABLE 6.3

Analytical Expressions for Two Segment Impurity Distributions

Impurity Distribution	Region I Distribution : $N_I(x)$	Region II Distribution : $N_{II}(x)$
Type-A : Combination of Gaussian and Hyperbolic	$N_0 e^{-\eta \frac{x^2}{s}} - N_B$	$N_0 (1 + (e^{-\eta x^2/s} - 1) x)^{-4} - N_B$
Type-B : Combination of Exponential and Hyperbolic	$N_0 e^{-\eta x} - N_B$	-do-
Type-C : Combination of Gaussian and Exponential	$N_0 e^{-\eta \frac{x^2}{s}} - N_B$	$N_0 e^{-\eta x} - N_B$
Type-D : Combination of Hyperbolic and Exponential	$N_0 (1 + (e^{\eta x/s} - 1) \frac{x}{s})^{-4} - N_B$	-do-
Type-E : Combination of Exponential and Gaussian	$N_0 e^{-\eta x} - N_B$	$N_0 e^{-\eta_1 x^2} - N_B$
Type-F : Combination of Hyperbolic and Gaussian	$N_0 (1 + (e^{\eta p_1/x} - 1) \frac{x}{p_1})^{-4} - N_B$	-do-
Special form of Distribution		$N_0 (e^{-\eta} + (1 - e^{-\eta}) (1 - x)^m) - N_B$

of N_{O1}/N_W and N_{O2}/N_W (symbols are same as used in Chapter 4). The computed results for different doping distributions are given in Tables 6.4 and 6.5. A study of the results indicates that an improvement in the figure of merit over the exponential distribution is possible when either the special form of distribution or the distributions which are concave down in the first region and then cross over to concave up in the second region are used for base doping (Types A to C). There is no improvement when other combinations of base impurity distributions such as types D, E and F are used.

The improvement in the figure of merit can be explained on the basis of a decrease in the base resistance. For types A to C and special impurity distributions, the calculations made in Chapter 4 record a decrease in transit time as compared with exponential distribution. Thus both transit time and the base resistance components of figure of merit are improved and lead to an overall increase in the device figure of merit.

6.5 EVALUATION OF FIGURE OF MERIT FOR IMPURITY DISTRIBUTIONS DERIVED FROM SYNTHESISED BASE REGION ELECTRIC FIELD CONFIGURATIONS

In Chapter 5, two and three segment base region built-in electric field configurations for minimum base transit time have been synthesised through segmentation technique. The corresponding base region impurity distributions have also been derived at low injection levels. In this section, normalised figure of merit is evaluated for these impurity distributions. Both constant and doping dependent mobilities are considered.

TABLE 6.4

Calculation of Normalised Figure of Merit for Impurity Distributions Synthesised through Segmentation Technique (Distribution Types - A to D)

Normalised figure of merit for special form of doping distribution = 1.4851

N_o / N_w	FM(N)/FM (exp)			
	Type-A	Type-B	Type-C	Type-D
10^5	1.3096	1.0474	1.2425	0.9614
10^6	1.4250	1.0858	1.3091	0.9435
10^7	1.4850	1.1026	1.3461	0.9326
10^8	1.5173	1.1107	1.3666	0.9262
10^9	1.5350	1.1150	1.3780	0.9225

TABLE 6.5

Calculation of Normalised Figure of Merit for Impurity Distributions Synthesised through Segmentation Technique (Distribution Types - E and F)

N_o / N_w	FM(N)/FM (exp)	
	Type-E	Type-F
5.0×10^2	0.9936	0.9871
4.0×10^2	0.9124	0.8980
3.3×10^2	0.8708	0.8468
2.0×10^2	0.8311	0.7593
1.6×10^2	0.8342	0.7366

($N_o/N_w = 10^3$ is kept constant in the above calculations)

It is shown that impurity distributions which present a retarding electric field in region I of the base, yield a much better improvement in device figure of merit.

6.5.1 Two Segment Distributions

The analytical expression for the two segment impurity distribution is given below. It has been modified to take into account the effect of N_B .

Region I ($0 \leq X \leq s$)

$$N_I(X) = N_0 e^{-\eta_1 \frac{X}{s}} - N_B \quad \dots(6.17a)$$

Region II ($s \leq X \leq 1$)

$$N_{II}(X) = N_s e^{-\eta_2 \frac{X-s}{1-s}} - N_B \quad \dots(6.17b)$$

where $\eta_1 = \ln N_0/N_s$

$$\eta_2 = \ln N_s/N_w$$

N_s = impurity concentration at $X = s$ in the base region

The base transit time has already been calculated for these distributions in Chapter 5. The same results are used here in the calculation of figure of merit. The expression of normalised base resistance, when constant mobility is assumed, is achieved by using eqn. 6.16. The following relation is obtained.

$$\frac{r_b'(\text{exp})}{r_b'(N)} = \frac{\eta}{1 - e^{-\eta}} \left(\frac{s}{\eta_1} (1 - e^{-\eta_1}) + \frac{1-s}{\eta_2} (e^{-\eta_1} - e^{-\eta}) \right) \quad \dots (6.18)$$

When mobility is not constant but depends upon the doping density, the above relation assumes the following form (using Sugano and Koshiga's mobility relation).

$$\frac{r_b'(\text{exp})}{r_b'(N)} = \frac{\eta}{(1 - e^{-.75\eta})} \left(\frac{s}{\eta_1} (1 - e^{-.75\eta_1}) + \frac{1-s}{\eta_2} (e^{-.75\eta_1} - e^{-.75\eta}) \right) \quad \dots (6.19)$$

To calculate the normalised C-B junction capacitance, the linear grading approximation is made and the following expression is obtained.

$$\frac{C_c(\text{exp})}{C_c(N)} = \left[\frac{\eta_2}{(1-s)\eta} \right]^{-1/3} \quad \dots (6.20)$$

Using the above relations of base resistance, collector capacitance and the corresponding transit time results, the normalised figure of merit is obtained by making use of eqns. 6.14 and 6.15. The evaluation is made for different values of s and η_1 (or N_o/N_s). Both constant and doping dependent mobility cases are analysed.

The results are presented in Tables 6.6 to 6.9 for different values of s . For a fixed value of s , the ratio N_o/N_s is varied. A study of the results reveals that for smaller widths of the retarding field region, the improvement in the figures of merit over that of the exponential

TABLE 6.6

Calculation of Normalized Figure of Merit for Two Segment Impurity Distributions ($s = 0.05$)

$\frac{N_0}{N_s}$	$\frac{N_a}{N_w}$	Constant Mobility			Doping dependent mobility			
		$\frac{t_B(\text{exp})}{t_B(N)}$	$\frac{r_b'(\text{exp})}{r_b'(N)}$	$\frac{C_c(\text{exp})}{C_c(N)}$	$\frac{FM(N)}{FM(\text{exp})}$	$\frac{t_B(\text{exp})}{t_B(N)}$	$\frac{r_b'(\text{exp})}{r_b'(N)}$	$\frac{FM(N)}{FM(\text{exp})}$
0.05	2×10^4	1.060	15.458	0.871	14.286	0.452	7.279	2.874
0.10	1×10^4	1.118	8.482	0.893	6.477	0.602	4.722	4.542
0.20	5×10^3	1.128	4.714	0.916	4.879	0.741	3.092	2.101
0.40	2.5×10^3	1.102	2.664	0.943	2.770	0.856	2.046	1.653
0.50	2×10^3	1.088	2.226	0.952	2.308	0.888	1.796	1.519
0.80	1.25×10^3	1.052	1.537	0.972	1.574	0.945	1.372	1.262
1.00	1×10^3	1.033	1.296	0.983	1.316	0.969	1.211	1.153

(N_0/N_w is kept fixed in the above calculations at 10^3)

TABLE 6.7

Calculation of Normalised Figure of Merit
For Two Segment Impurity Distributions ($s = 0.10$)

$\frac{N_0}{N_a}$	$\frac{N_a}{N_w}$	Constant Mobility			Doping dependent mobility			
		$\frac{t_B(\text{exp})}{t_B(N)}$	$\frac{r_b'(\text{exp})}{r_b'(N)}$	$\frac{C_c(\text{exp})}{C_c(N)}$	$\frac{FM(N)}{FM(\text{exp})}$	$\frac{t_B(\text{exp})}{t_B(N)}$	$\frac{r_b'(\text{exp})}{r_b'(N)}$	$\frac{FM(N)}{FM(\text{exp})}$
0.05	2.0×10^4	0.831	16.952	0.856	12.063	0.290	7.928	1.973
0.10	1.0×10^4	0.958	9.458	0.677	7.951	0.429	5.208	1.963
0.20	5.0×10^3	1.036	5.371	0.900	5.014	0.584	3.461	1.621
0.40	2.5×10^3	1.066	3.119	0.926	3.082	0.735	2.333	1.589
0.50	2.0×10^3	1.067	2.634	0.935	2.629	0.780	2.062	1.504
0.80	1.25×10^3	1.056	1.864	0.955	1.882	0.867	1.598	1.324
1.00	1.0×10^3	1.046	1.592	0.965	1.609	0.905	1.421	1.242

($N_0/N_w = 10^3$ is kept fixed in the above calculations)

TABLE 6.8

Calculation of Normalized Figure of Merit
For Two Segment Immobility Distributions ($\alpha = 0.15$)

$\frac{M_0}{M_0}$	$\frac{M_0}{M_w}$	Constant Mobility			Doping Dependent Mobility			
		$\frac{t_B(\text{exp})}{t_B(N)}$	$\frac{r_b'(\text{exp})}{r_b'(N)}$	$\frac{C_c(\text{exp})}{C_c(N)}$	$\frac{FM(N)}{FM(\text{exp})}$	$\frac{t_B(\text{exp})}{t_B(N)}$	$\frac{r_b'(\text{exp})}{r_b'(N)}$	$\frac{FM(N)}{FM(\text{exp})}$
0.05	2.0×10^4	0.660	18.447	0.840	10.242	0.205	8.577	1.477
0.10	1.0×10^4	0.812	10.434	0.860	7.294	0.319	5.693	1.566
0.20	5.0×10^3	0.932	6.027	0.883	4.963	0.462	3.831	1.563
0.40	2.5×10^3	1.007	3.575	0.908	3.274	0.618	2.620	1.473
0.50	2.0×10^3	1.022	3.042	0.917	2.853	0.669	2.327	1.429
0.80	1.25×10^3	1.038	2.191	0.937	2.132	0.772	1.824	1.321
1.00	1.0×10^3	1.039	1.888	0.947	1.858	0.820	1.632	1.268

($N_0/N_w = 10^3$ is kept fixed in the above calculations)

TABLE 6.9

Calculation of Normalised Figure of Merit
For Two Segment Impurity Distributions ($a = 0.20$)

$\frac{N_0}{N_B}$	$\frac{N_A}{N_W}$	Constant Mobility			Doping Dependent Mobility			
		$\frac{t_B(\text{exp})}{t_B(N)}$	$\frac{r_b'(\text{exp})}{r_b'(N)}$	$\frac{C(\text{exp})}{C(N)}$	$\frac{FM(N)}{FM(\text{exp})}$	$\frac{t_2(\text{exp})}{t_2(N)}$	$\frac{r_b'(\text{exp})}{r_b'(N)}$	$\frac{FM(N)}{FM(\text{exp})}$
0.05	2.0×10^4	0.533	19.941	0.823	8.766	0.153	9.226	1.164
0.10	1.0×10^4	0.686	11.410	0.843	6.607	0.246	6.179	1.282
0.20	5.0×10^3	0.825	6.683	0.865	4.779	0.369	4.201	1.343
0.40	2.5×10^3	0.933	4.030	0.890	3.351	0.516	2.906	1.337
0.50	2.0×10^3	0.959	3.449	0.899	2.977	0.567	2.592	1.321
0.80	1.25×10^3	0.999	2.518	0.916	2.312	0.674	2.051	1.271
1.00	1.0×10^3	1.011	2.184	0.928	2.051	0.727	1.842	1.244

($N_0/N_W = 10^3$ is kept fixed in the above calculations)

distribution is maximum. As the strength of the retarding field is reduced the improvement in figure of merit also diminishes monotonically. This is true for both the cases of constant and doping dependent mobility, provided the width of the retarding field region is restricted to smaller values. When this width is more, there exists an optimum value for the strength of the retarding field for which the figure of merit improvement is maximum if mobility is doping dependent. Figs. 6.1 and 6.2 show the variation of the normalised figure of merit with N_0/N_B in the cases of constant and doping dependent mobility. The width of the retarding field region, s , serves as the parameter.

6.5.2 Three Segment Distributions

The analytical expression for the three segment distribution, after taking into consideration the effect of N_B , is given below.

Region-I ($0 \leq x \leq p_1$)

$$N_I(x) = N_0 \cdot e^{-\eta_1 \frac{x}{p_1}} - N_B$$

.. (6.21a)

Region-II ($p_1 \leq x \leq p_2$)

$$N_{II}(x) = N_1 \cdot e^{-\eta_2 \frac{x - p_1}{p_2 - p_1}} - N_B$$

.. (6.21b)

Region-III ($p_2 \leq x \leq 1$)

$$N_{III}(x) = N_2 \cdot e^{-\eta_3 \frac{x - p_2}{1 - p_2}} - N_B$$

.. (6.21c)

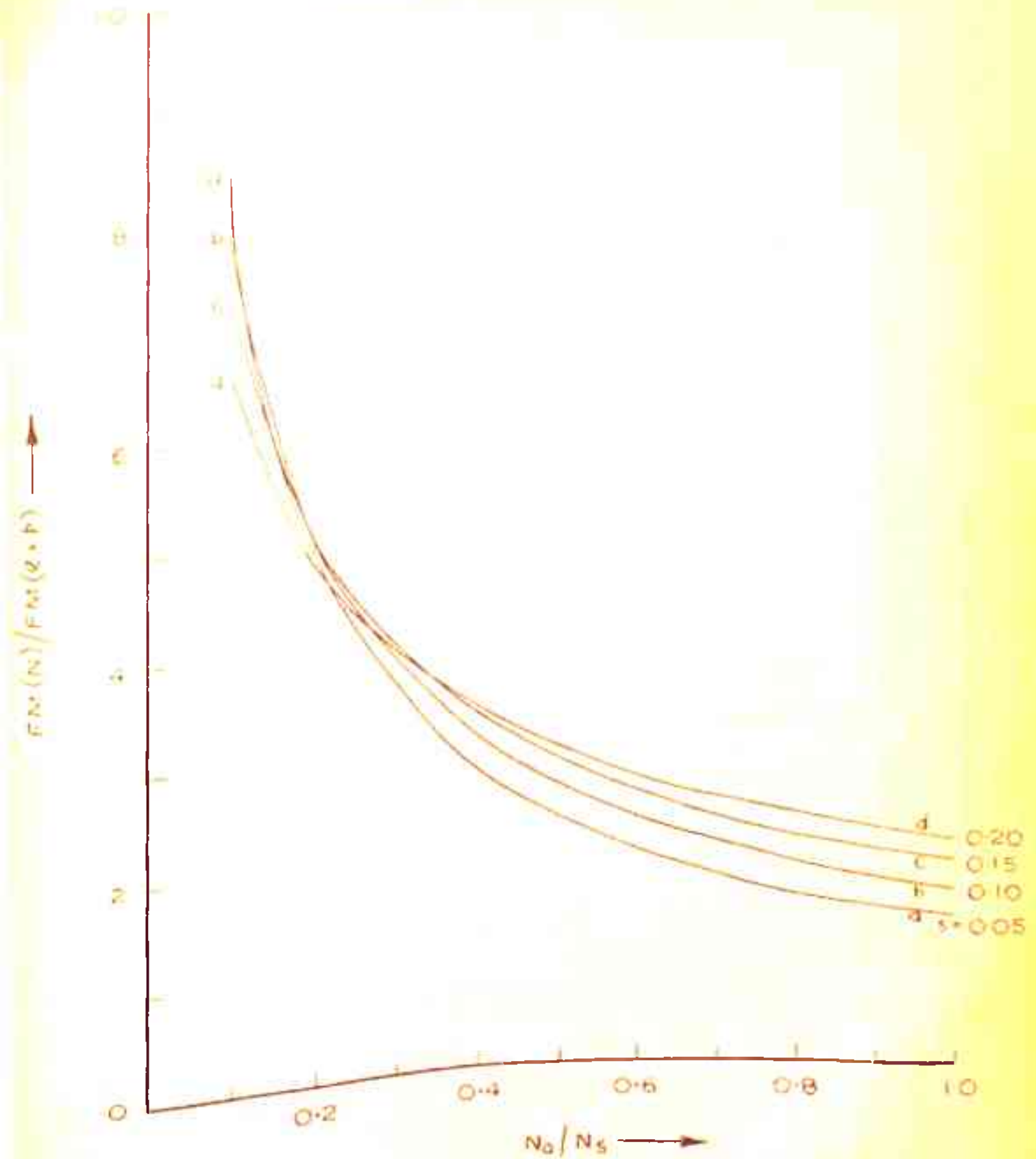


FIG 6.1 VARIATION OF NORMALISED FIGURE OF MERIT WITH CONCENTRATION RATIO, N_0/N_s —CONSTANT MOBILITY CASE.

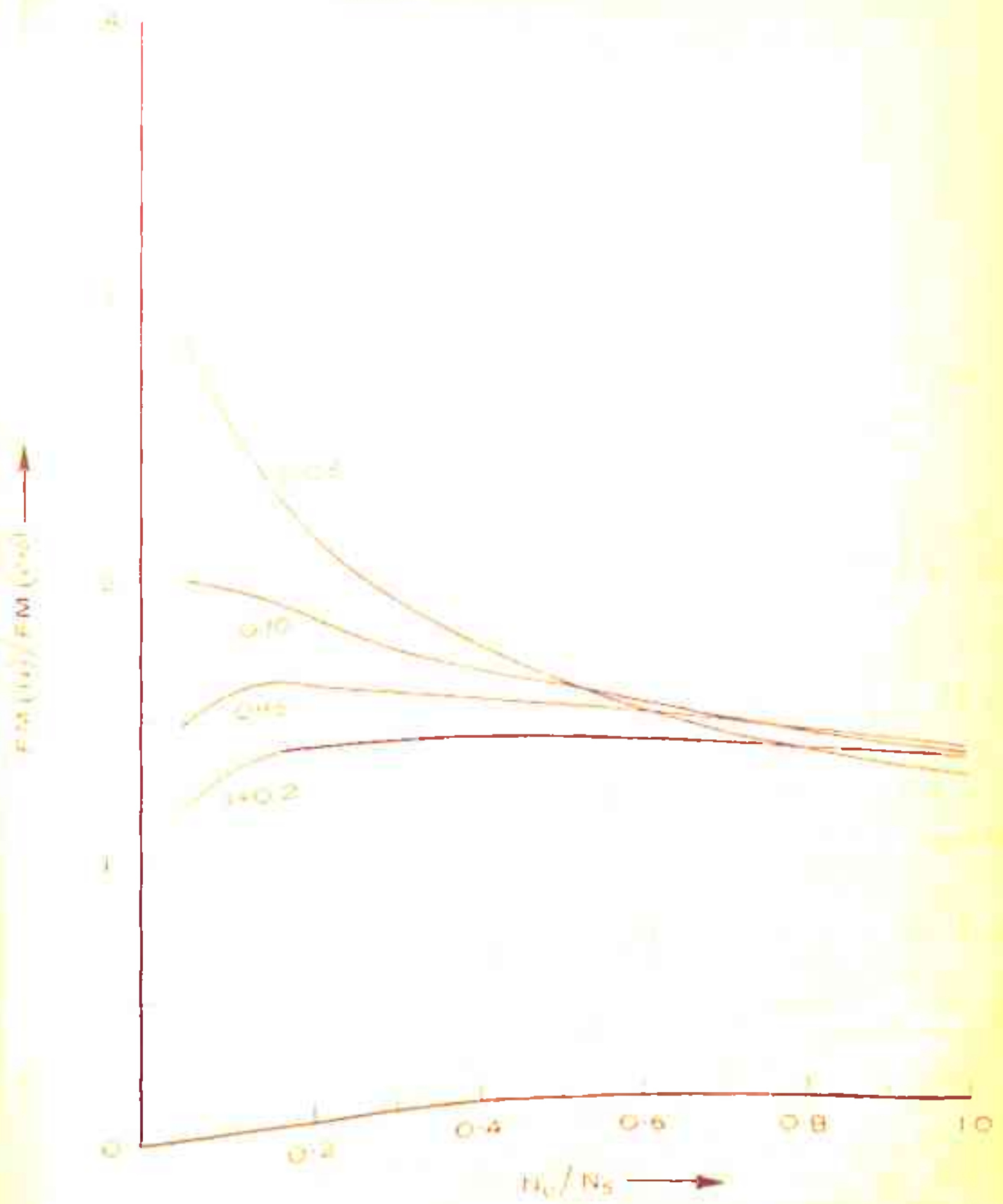


FIG. 6.2 VARIATION OF NORMALISED FIGURE OF MERIT WITH CONCENTRATION RATIO, N_0/N_s —DOPING DEPENDENT MOBILITY CASE

$$N_I(x) = N_{II}(x) = N_1 \text{ at } x = p_1, \quad N_{II}(x) = N_{III}(x) = N_2 \text{ at } x = p_2$$

$$\text{where } \eta_1 = \ln N_0/N_1$$

$$\eta_2 = \ln N_1/N_2$$

$$\eta_3 = \ln N_2/N_w$$

$$\eta = \ln N_0/N_w = \eta_1 + \eta_2 + \eta_3$$

Here also the transit time results obtained in Chapter 5 are used. The normalised base resistance is derived with the help of eqn. 6.9. The following expression is obtained

$$\frac{r_b'(\text{exp})}{r_b'(N)} = \frac{\eta}{1 - e^{-\eta}} \left[p_1 \frac{1 - e^{-\eta_1}}{\eta_1} + (p_2 - p_1) \frac{e^{-\eta_1} (1 - e^{-\eta_2})}{\eta_2} + (1 - p_2) \frac{e^{-(\eta_1 + \eta_2)} (1 - e^{-\eta_3})}{\eta_3} \right] \dots (6.22)$$

The normalised capacitance is obtained by using the linear grading approximation. The following result is obtained.

$$\frac{C_c(\text{exp})}{C_c(N)} = \left[\frac{\eta_3}{(1 - p_2)\eta} \right]^{-1/3} \dots (6.23)$$

The normalised figure of merit is evaluated by multiplying eqns. 6.22, 6.23 and the normalised base transit time results.

The computed results are given in Table 6.10. A study of the results reveals that there is an improvement in the device figure of merit over the exponential distribution in the base. Thus it is concluded that impurity distributions providing retarding fields in a small portion of the base yield

better device figure of merit.

TABLE 6.10
Calculation of Normalised Figure of Merit
for Three Segment Impurity Distributions.

$N_0/N_1 = 0.5,$

$N_0/N_w = 10^3$

N_1/N_2	P_1	P_2	Normalised			
			t_B	r_b'	C_c	FM
10	0.0282	0.333	1.0904	2.1132	0.9534	2.1900
20	0.0372	0.410	1.0902	2.0932	0.9601	2.1910
50	0.0424	0.509	1.0918	2.0780	0.9719	2.2050
100	0.0445	0.585	1.0942	2.0685	0.9855	2.2308
500	0.0460	0.755	1.1077	2.0387	1.0679	2.4117

P_1 - width of the first segment

P_2 - total width upto the second segment

$(N_0/N_1) < 1$ corresponds to retarding fields in the first segment of the base

6.6 REMARKS ABOUT THE VALIDITY OF f_T APPROXIMATION

The characteristic frequency f_T has been defined to be reciprocal of the different time delays. Here, actual calculations of the different time delays are made and it is stressed that the approximation

$$f_T = \frac{1}{2\pi t_B}$$

is quite valid. As mentioned earlier, Kromer has also used this approximation.

Let us consider the following typical data

$$N_0/N_w = 10^3, \quad W = 5 \times 10^{-4} \text{ cm (5 microns)}, \quad I_e = 5 \text{ mA}$$

$$C_e = 20 \text{ pF.}; \quad D_p = 12.5 \text{ cm}^2/\text{sec.}$$

Using these constants, the time delays are calculated below.

Emitter delay time (t_E)

$$t_E = \frac{KT}{q I_e} C_e = \frac{26}{5} \times 20 \times 10^{-12}$$

$$= 10^{-10} \text{ sec.}$$

Base transit delay time (t_B)

For an exponential doping in the base

$$t_B = \frac{W^2}{D_p} \frac{\eta - 1 + e^{-\eta}}{\eta^2}$$

$$= 24.75 \times 10^{-10} \text{ sec.}$$

Collector depletion layer delay time (t_D)

t_D is expressed by the following relation

$$t_D = \frac{x_m}{2 v_{sc}}$$

From the solution of Poisson's equation, the depletion layer width x_m for an exponential distribution has been found to be $x_m = 3.86 \times 10^{-4}$ cms. The numerical constants used earlier in this chapter are used for this purpose.

Substituting the value of scatter limited velocity $v_{sc} = 10^7$ cm/sec., we obtain

$$t_D = 0.193 \times 10^{-10} \text{ sec.}$$

Collector charging delay t_C is not very important at low injection levels and it mainly depends upon the resistivity of the collector region. Hence, it is neglected. The above calculation shows that the base transit delay is many times greater than the sum of other delays, and hence the approximate relation for f_T is quite justified.

N_0 is kept same for all the distributions. This amounts to obtaining same value of the emitter transition capacitance C_0 . Hence, the emitter time constant will add a constant term if its effect is considered¹¹. In that case, f_T can be written as

$$\frac{1}{2\pi f_T} = t_E + t_B$$

Since the time delay addition is going to be constant for all the distributions, the relative effect will not be very significant.

The above discussion leads to the conclusion that the approximation used for f_T is quite justified. The collector depletion layer delay time can be significant if the operation at high currents is considered³, and the base widths are much narrower.

6.7 SUMMARY AND DISCUSSION

The figure of merit of transistors having different types of base impurity distributions has been calculated. It has been shown that the optimum impurity distributions for minimum base transit time do not yield improved figure of merit. This is due to the fact that the criterion for optimum figure of merit include factors other than the base transit time, namely, the total impurity content in the base and C-B capacitance. The Gaussian, erfc., two segment (types A to C) and the special form of the impurity distributions are found to yield an improvement in the figure of merit in the case of constant mobility. When doping dependent mobility is considered, the figure of merit for these distributions is found to be no better than the exponential. The above behaviour can be explained as follows. The concave down impurity distributions and the two segment distributions which are concave down in the first segment accommodate larger amount of base impurities giving rise to a lower base resistance. Consequently there is a considerable improvement in the figure of merit as compared with the exponential profile. When mobility variation is taken into account, the reduction in base resistance is much less because of the decrease of the mobility value at higher impurity concentration. Hence the figure of merit is no better than that of the exponential.

A much higher figure of merit can be achieved by combinations of retarding and accelerating fields in the base

region. The impurity distributions which present a retarding field over a small portion of the base are able to accommodate a larger amount of base impurity. This results in a decrease of base resistance. The transit time also improves for such distributions. Further, the emitter end impurity concentration N_0 is not changed in such impurity profiles. Hence, the E-B capacitance is not adversely affected. Thus a much higher device figure of merit is achieved if the impurity distribution presents a retarding field over a small portion of the base.

+++++

REFERENCES

1. J.M. Early, 'Structure-Determined Gain-Band Product of Junction Triode Transistors', Proc. IRE, Vol. 46, pp. 1924-1927, 1958.
2. J.L. Moll, 'Physics of Semiconductors', McGraw-Hill Book Co., New York, 1964, Ch. 8.
3. R.J. Whittier and D.A. Tremere, 'Current gain and cut-off frequency fall off at high currents', IEEE Trans., Vol. ED-16, pp. 39-57, 1969.
4. C.T. Kirk, 'A Theory of Transistor Cut-off Frequency (f_T) fall off at high current densities', Trans. IRE, Vol. ED-9, pp. 164-174, 1962.
5. B.K. Petrov and V.F. Synorov, 'Maximum oscillation frequency of a drift triode', Radio Engng. Electronic Phys., Vol. 15, pp. 944-945, 1970.
6. R.M. Warner, et al., 'Integrated Circuits - Design Principles and Fabrication', McGraw-Hill Book Co., N.Y., 1965.
7. J. Lindmayer and C. Wrigley, 'Fundamentals of Semiconductor Devices', Van Nostrand, New York, 1965, Ch. 5.
8. R.L. Pritchard, 'Electrical Characteristics of Transistors', McGraw-Hill Book Co., New York, 1967, Ch. 8.
9. Ya. A. Fedotov, 'Frequency Characteristics of Junction Transistors', Radio Tekh. i. Elektr., Vol. 2, pp. 1189-1199, 1957.
10. M. Maeda, et al., 'Figure of Merit of High-Frequency Transistors', Electronics and Comm. in Japan, Vol. 48, pp. 60-67, 1965.

11. M. Maeda, et al., 'Design Consideration of Base Impurity Distribution for Figure of Merit of High-Frequency Transistors', Electronics and Comm. in Japan, Vol. 49, pp. 59-66, 1966.
12. H. Krömer, 'The Drift Transistors' in Transistors I, RCA Labs., Princeton, N.J., pp. 202-220, 1956.
13. S.K. Gandhi, 'The Theory and Practice of Micro-Electronics', John Wiley and Sons, 1968, Ch. 13.
14. T. Sugano and F. Koshige, 'The calculation of cut-off frequencies of minority carrier transport factors in drift transistors when the mobilities are not constant', Proc. IRE, Vol. 49, p. 1218, 1961.

+++++

CHAPTER 7

SUMMARY, CONCLUDING REMARKS AND SCOPE FOR FURTHER WORK

- 7.1 SUMMARY
- 7.2 CONCLUDING REMARKS - FEASIBILITY
OF OBTAINING GENERAL IMPURITY
DISTRIBUTIONS
- 7.3 SCOPE FOR FURTHER WORK

REFERENCES

CHAPTER 7SUMMARY, CONCLUDING REMARKS
AND SCOPE FOR FURTHER WORK7.1 SUMMARY

Optimum impurity distributions for minimum base transit time have been derived through variational method. A new approach based on electric field configuration has been proposed besides the conventional stored charge approach for deriving the optimum distribution. It is found that both the approaches are equivalent under low injection levels. When carrier mobility in the base is assumed to be constant, the exponential doping distribution is found to be the optimum. For typical empirical relations of doping dependent mobility, optimum impurity distributions have been derived through calculus of variations. It is observed that the optimum impurity distribution profiles are concave up on a $\ln N$ vs. x plot while the conventional base doping distributions such as Gaussian and Erfc. are concave down on such a plot. It has also been shown that for a given empirical relation of doping dependent mobility, the optimum doping distribution for minimum base transit time is unique. It is suggested that the electric field approach of deducing optimum impurity distribution should be adopted when field-dependent mobility is important, as may be the case in modern shallow junction devices, and when the device operation at intermediate injection levels is considered.

Using the stored charge definition, base transit time has been evaluated for both constant and doping dependent mobility. Optimum as well as conventional doping distributions are studied and different empirical relations of mobility are considered. It has been verified that the optimum distributions offer minimum base transit time when the corresponding empirical relation of mobility is used. The excess minority carrier concentration and the built-in electric field have also been calculated. It is found that the built-in electric field either increases or decreases monotonically over the base region depending upon the gradient of $\ln N$ i.e., $\frac{d(\ln N)}{dx}$. The minority carrier concentration profile in the base region exhibits an interesting property. For concave down distributions, the carrier flow is due to both diffusion and drift towards the collector while for concave up distributions, the carriers show a slight diffusive tendency towards the emitter from somewhere in the base. A special form of base impurity distribution having a point of inflection is also synthesised and it has been established that this distribution yields a lower value of transit time as compared to that obtained in the case of optimum distributions.

The synthesis and study of the special base impurity distribution has revealed that impurity distributions or electric field configurations showing a point of inflection yield low value of transit time. Some more typical impurity distributions which are not smooth and which have a corner are synthesised through a new technique named as segmentation

technique. These two segment distributions are combinations of segments of standard distributions. The evaluation of transit time and built-in electric field for such distributions has established that impurity distributions and electric field configurations having a point of inflection, a corner, or a discontinuity are not amenable to treatment by variational method. Some of these impurity distributions offer a smaller value of base transit time as compared to the optimum distributions. Hence, a proper combination of faster and slower segments of impurity distributions can lead to low values of base transit time.

The segmentation technique has also been employed to obtain built-in electric field configurations for minimum base transit time. The corresponding impurity distributions are synthesised at low injection levels. It has been found that base region transit time improves when a retarding field is present over a small portion of the whole base. In the case of constant mobility, approximately 20% improvement in base transit time is possible when these impurity distributions rather than the conventional (particularly exponential) distributions are used for base doping. The improvement has been feasible due to the presence of a large value of aiding field in a portion of the base. However, the large aiding field does not adversely affect other parameters, such as, emitter base capacitance.

The effect of base impurity distribution on the high-frequency figure of merit of bipolar transistors has been

investigated. Some typical base impurity distributions, which offer much better device figure of merit than that obtained with exponential distribution, are suggested. It is observed that the frequency properties of the transistors are affected by base transit-time, base resistance, and collector capacitance. The influence of all these parameters on the figure of merit has been studied.

The computation of figure of merit has revealed that optimum distributions which offer minimum base transit time need not necessarily yield improved device figure of merit. For example, with Sugano and Koshiga's mobility relation, the hyperbolic impurity distribution is optimum for minimum base transit time, but the figure of merit worsens for this distribution. In the case of constant mobility, the concave down impurity distributions, such as, Gaussian and Erfc., and the two segment distributions which are concave down over part of the base, yield an improvement in the device figure of merit as compared to the figure of merit of a transistor having exponential doping distribution in the base. It has also been observed that the use of two segment base impurity distributions providing retarding field over the first segment of the base results in a much better improvement in the device figure of merit. This improvement is mainly due to a decrease in base resistance. Hence, both from the point of view of minimum transit time and maximum figure of merit, the retarding field distributions are to be preferred. This is an interesting conclusion contrary to the general impression that base

profiles having retarding field segment will cause a deterioration in transit time and figure of merit of the device.

7.2 CONCLUDING REMARKS - FEASIBILITY OF OBTAINING GENERAL IMPURITY DISTRIBUTIONS

The investigations presented in this thesis have established that the proper control of impurity profile in the base region of a transistor leads to minimum minority carrier transit time and maximum figure of merit of the device. However, the present methods used for fabricating semiconductor devices by diffusion techniques invariably produce profiles which are approximately either Gaussian or complementary error functions.^{1,2} In this section, the feasibility of realising typical impurity profiles, suggested to be the optimum ones for improved device performance at high frequencies, is examined.

If the amount of impurities flowing to the surface of the material through the gas stream is strictly controlled, a best-fit approximation to a given impurity profile can be obtained. The above suggestion has been made by Marzak and Hamilton³ after an interesting theoretical study. In this procedure of obtaining general impurity distributions, the standard diffusion furnace may not be used since the glass wells usually become saturated and thus act as a source of impurities independent of the gas stream concentration. Hence the design of a new reactor has also been suggested by these workers. It has been proposed that a reactor similar to that used for epitaxial growth can be constructed. The wafer is

heated by induction with an RF generator, and the walls of the reactor remain sufficiently cool so that negligible impurities are contributed by them. To achieve the required distribution profile, a proper control function which minimises the deviation of the actual impurity profile from the desired profile has to be determined. A computational routine using linear programming technique, can be developed, which, for a given diffusion time, determines the necessary control function producing a best-fit approximation to the desired profile over the spatial range of interest.

It is well-known that in double-diffused transistors formed by solid-state diffusion techniques, there is a retarding field over a small portion of the base^{4,5}. This can be used to an advantage if proper control on impurity concentration and process parameters such as temperature and time is exercised. Thus the two segment impurity distribution having a retarding field over a portion of the base can be synthesised in practice.

Finally, there are indications that the newly introduced technique of device fabrication - the Ion Implantation Technique - can be used to achieve a desired distribution for optimum device performance⁶.

7.3 SCOPE FOR FURTHER WORK

Amongst present day semiconductor devices, particularly transistors, shallow junction devices are finding an important place⁷. Due to small base widths, even for an order of change of two to three times in the doping level from emitter end to

the collector end in the base, the field is quite high. The high value of field affects the carrier mobility. Hence optimum electric field configurations for minimum base transit time could be derived through variational method taking into consideration the field-dependent mobility. The electric field approach suggested in Chapter 2 could be used for this purpose.

The present study has dealt with the device operation at low injection levels. The transit behaviour of carriers at high currents could form quite ^{an} interesting study. A similarity in the nature of minority carrier profiles obtained for impurity distributions which are concave up on a $\ln N$ vs x plot and the carrier profiles obtained by Lindmayer and Wrigley⁶ for an exponentially doped base region transistor operating under high current has been noticed. This could be investigated further for any possible correlation in the two situations by studying the electric field components due to high injection and due to impurity doping.

In the analysis of device figure of merit, it has been assumed that the characteristic frequency f_T is essentially decided by base transit time t_B . The contribution of the other delays could be considered. Particularly, at high currents the contribution due to C-B depletion layer transit time becomes important⁹. Hence the analysis at high currents can be carried out taking into consideration the above time delay so as to arrive at a correct estimate of f_T and the figure of merit.

+++++

REFERENCES

1. A.S. Grove, 'Physics and Technology of Semiconductor Devices', John Wiley, New York, 1966.
2. R.M. Burger and R.P. Donovan, 'Fundamentals of Silicon Integrated Device Technology' Vol. I, Prentice-Hall, New Jersey, 1967.
3. A.H. Marshak and D.J. Hamilton, 'The Feasibility of obtaining General Impurity Distributions of Diffusion', IEEE Trans. Electron Devices, Vol. ED-17, pp. 897-907, 1970.
4. N. Kawamura, 'Investigation of Current Gain of Drift Transistor having Retarding Field', NSC R and D reports, No.6, pp. 44-52, 1963.
5. I.I. Shagurin, 'Effect of the Retarding Field in the Base of a Drift Transistor on the Transfer Coefficient of Minority Carriers', IZV. V.U.Z., Radio Elektronika, Vol. 11, pp. 603-607, 1968.
6. L.P. Hunter, 'Handbook of Semiconductor Electronics', McGraw-Hill Book Co., New York, 1970, 3rd Edition, Sec.7.
7. V.A. Dhaka, 'Design and Fabrication of Subnanosecond Current Switch and Transistors', IBM Jour. Res. and Dev., Vol. 12, pp. 476-482, 1968.
8. J. Lindmayer and C. Wrigley, 'The High-Injection-Level Operation of Drift Transistors', Solid State Electronics, Vol. 2, pp. 79-84, 1961.
9. R.J. Whittier and D.A. Tremere, 'Current gain and cut-off frequency fall off at high currents', IEEE Trans. Electron Devices, Vol. ED-16, pp. 39-57, 1969.

APPENDICES

- APPENDIX-I DERIVATION OF THE FIRST INTEGRAL
OF EULER EQUATION
- APPENDIX-II EVALUATION OF NONLINEAR EQUATION
BY NEWTON-RAPHSON METHOD
- APPENDIX-III COMPUTER PROGRAM FOR THE EVALUA-
TION OF TRANSIT TIME - CONSTANT
MOBILITY CASE
- APPENDIX-IV COMPUTER PROGRAM FOR THE EVALUA-
TION OF TRANSIT TIME - DOPING
DEPENDENT MOBILITY CASE
- APPENDIX-V EVALUATION OF C-B JUNCTION
CAPACITANCE FOR ARBITRARY IMPURITY
DISTRIBUTION IN THE BASE

APPENDIX-I

DERIVATION OF THE FIRST INTEGRAL
OF EULER EQUATION

The Euler-Lagrange equation is given by the relation

$$\frac{\partial f}{\partial y} - \frac{d}{dx} \cdot \frac{\partial f}{\partial \dot{y}} = 0 \quad \dots (I.1)$$

This can be written more explicitly as

$$f_y - f_{xy} \dot{y} - f_{yy} \ddot{y} - f_{yy} \ddot{y} = 0 \quad \dots (I.2)$$

If the function f does not depend explicitly on x i.e. it depends on y and \dot{y} only, Euler equation (I.2) becomes

$$f_y - f_{yy} \dot{y} - f_{yy} \ddot{y} = 0, \quad \dots (I.3)$$

since $f_{xy} = 0$. Multiplying both sides of eqn. I.3 by \dot{y} , the left hand side of this equation turns into an exact derivative $\frac{d}{dx} (f - \dot{y} \frac{\partial f}{\partial \dot{y}})$.

In fact,

$$\begin{aligned} \frac{d}{dx} (f - \dot{y} \frac{\partial f}{\partial \dot{y}}) &= f_y \dot{y} + f_{\dot{y}} \ddot{y} - \ddot{y} f_{\dot{y}} - f_{y\dot{y}} \dot{y}^2 - f_{\dot{y}\dot{y}} \dot{y} \ddot{y} \\ &= \dot{y} (f_y - f_{y\dot{y}} \dot{y} - f_{\dot{y}\dot{y}} \ddot{y}) \end{aligned} \quad \dots (I.4)$$

Consequently, the Euler equation has a first integral

$$f - \dot{y} \frac{\partial f}{\partial \dot{y}} = C \quad \dots (I.5)$$

This first-order equation does not involve x explicitly and it can be solved for \dot{y} . Eqn. I.5 is the required condition which has been used to derive $N(x)$ for minimum base transit time.

APPENDIX-II

EVALUATION OF NONLINEAR EQUATION
BY NEWTON-RAPHSON METHOD

The nonlinear equation 2.00 is reproduced below.

$$\ln \frac{2}{\alpha} \left(1 + \frac{c + 2}{2} \alpha \right) + \frac{c}{1 + \frac{c + 2}{2} \alpha} = \frac{2c}{k^2} X - 2c, \quad \dots (II.1)$$

The solution of the above equation is obtained subject to the following boundary conditions.

$$\begin{aligned} \alpha &= \alpha_0 = b N_0^c & \text{at } X = 0 \\ \alpha &= \alpha_w = b N_w^c & \text{at } X = 1 \end{aligned} \quad \dots (II.2)$$

If we define

$$f(\alpha) = \ln \frac{2}{\alpha} \left(1 + \frac{c + 2}{2} \alpha \right) + \frac{c}{1 + \frac{c + 2}{2} \alpha}, \quad \dots (II.3)$$

then eqn. II.1 can be written as follows

$$f(\alpha) = f(\alpha_0) - (f(\alpha_0) - f(\alpha_w)) X \quad \dots (II.4)$$

For a defined value of X , eqn. II.4 can be solved by Newton-Raphson's iterative method.

Let us define

$$F(\alpha, X) = f(\alpha) + (f(\alpha_0) - f(\alpha_w)) X - f(\alpha_0) \quad \dots (II.5)$$

For a given value of X , a first guess for α can be made as follows.

$$\alpha = \alpha - \frac{F(\alpha, X)}{F'(\alpha, X)} \quad \dots (II.6)$$

where $F'(\alpha, X) = \frac{df}{d\alpha}$

The iteration for α continues till eqn. II.4 is satisfied. This value of α is the required solution of the nonlinear eqn. II.1.

+++++

APPENDIX-IIICOMPUTER PROGRAM FOR THE EVALUATION OF
TRANSIT TIME - CONSTANT MOBILITY CASE

In this appendix, the computer program for evaluating the transit time in the case of constant mobility is given. The expression for normalised transit time is

$$\frac{t_B}{t_{3U}} = 2 \int_0^1 \frac{\int_0^1 N(x) dx}{N(x)} dl, \quad \dots (III.1)$$

where t_{3U} is the transit time of a uniform base transistor and $N(x)$ is any arbitrary impurity distribution in the base. For illustration, the following Gaussian impurity distribution is treated.

$$\frac{N(x)}{N_0} = \exp(-\eta x^2) \quad \dots (III.2)$$

where $\eta = \ln N_0/N_w$.

N_0 = Impurity concentration at the emitter end of the base.

N_w = Impurity concentration at the collector end of the base.

COMPUTER PROGRAM

```

// JOB T
// FOR
* EXTENDED PRECISION
* ONE WORD INTEGERS
* LIST SOURCE PROGRAM
  SUBROUTINE SIMSE(A,B,N,F,XINT)
  DIMENSION Z(201)
  AB=B-A
  H=AB/N
  END=F(A)+F(B)
  DO 10 I=2,N
  U=I-1
  XI=A+H*U
  10 Z(I)=F(XI)
  EVEN=0.
  ODD=0.
  DO 11 I=2,N,2
  11 EVEN=EVEN+Z(I)
  NN=N-1
  DO 12 I=3,NN,2
  12 ODD=ODD+Z(I)
  XINT=(END+4.*EVEN+ODD+ODD)*H/3.
  RETURN
  END
// DUP
*STORE          WS UA SIMSE

```

```

// FOR
* EXTENDED PRECISION
* LIST SOURCE PROGRAM
* ONE WORD INTEGERS
  SUBROUTINE SIMSA(A,B,N,F,XINT)
  DIMENSION Z(201)
  AB=B-A
  H=AB/N
  END=F(A)+F(B)
  DO 10 I=2,N
  U=I-1
  XI=A+H*U
  10 Z(I)=F(XI)
  EVEN=0.
  ODD=0.
  DO 11 I=2,N,2
  11 EVEN=EVEN+Z(I)
  NN=N-1
  DO 12 I=3,NN,2
  12 ODD=ODD+Z(I)
  XINT=(END+4.*EVEN+ODD+ODD)*H/3.
  RETURN
  END
// DUP
*STORE          WS UA SIMSA

```

```

// FOR
* EXTENDED PRECISION
* ONE WORD INTEGERS
* LIST SOURCE PROGRAM
  FUNCTION FA (X)
  COMMON ETA
  FA=EXP(-ETA*X*X)
  RETURN
  END
// DUP
*STORE          WS  UA  FA

```

```

// FOR
* EXTENDED PRECISION
* ONE WORD INTEGERS
* LIST SOURCE PROGRAM
  FUNCTION FAA(X)
  EXTERNAL FA
  COMMON ETA
  CALL SIMSA(X,1.,40,FA,XINT)
  FAA=XINT/FA(X)
  RETURN
  END
// DUP
*STORE          WS  UA  FAA

```

```

// FOR
* EXTENDED PRECISION
* ONE WORD INTEGERS
* LIST SOURCE PROGRAM
* IOCS(DISK,2501 READER,1403 PRINTER)
  EXTERNAL FAA
  DIMENSION ETAA(5)
  COMMON ETA
  READ(8,100)(ETAA(I),I=1,5)
100 FORMAT(10F5.2)
  DO 10 I=1,5
  ETA=ETAA(I)
  CALL SIMSE(0.,1.,40,FAA,XINT)
  TB=XINT+XINT
  WRITE(5,101) ETA,TB
101 FORMAT(1X,2F20.6)
  10 CONTINUE
  CALL EXIT
  END
// 1BQ

```

DESCRIPTION OF COMPUTER PROGRAMSubroutine SIMSE and SIMSA

These subroutines are used to evaluate integrals. The method is based on Simpson's Integration formula. The following computer variables have been used.

- A = Lower limit of the integral
- B = Upper limit of the integral
- N = Even number of intervals in which the difference of upper and lower limits of the integral is divided
- F = Function to be integrated
- XINT = Result of the integration.

Functions FA(X) and FAA(X)

The function FA(X) expresses the normalised impurity distribution function $N(X)/N_0$. In the present case, FA(X) is the Gaussian distribution function (eqn. III.2). FAA(X) is defined as follows:

$$FAA(X) = \frac{\int_X^1 FA(X) dx}{(FA(X))} \quad \dots(III.3)$$

The integral in the above equation is evaluated by using SIMSA subroutine. The integration interval is divided into 40 intervals.

Main Program

In the main program, different values of the constant η are read and for each value of η , the function FAA(X)

is integrated to yield $T_B = t_B/t_{3U}$.

The program presented in this appendix can be used for any arbitrary distribution function $N(X)$ with suitable changes in the function subprogram $FA(X)$.

+++++

APPENDIX-IVCOMPUTER PROGRAM FOR THE EVALUATION OF
TRANSIT TIME - DOPING DEPENDENT MOBILITY CASE

In Appendix-III, the computer program for evaluating the transit time in the case of constant mobility has been presented. When the mobility is not constant and depends on doping density, the transit time integral assumes the following form

$$t_B = w^2 \int_0^1 \frac{\left(\frac{N(x)}{D_p(x)} \right) dx}{N(x)}$$

..(IV.1)

If Sugano and Koshiga's empirical relation of doping dependent diffusion coefficient, $D_p(x)$ is substituted in the above equation, the following expression of normalised base transit time is obtained.

$$\frac{t_B}{t_{B0}} = 2 \int_0^1 \frac{\left((N(x)/N_0) \right)^{1.25} dx}{N(x)/N_0}$$

.. (IV.2)

where $t_{B0} = w^2/2 D_0$, and D_0 is the value of the diffusion coefficient when $N(x) = N_0$.

In this appendix, the computer program for evaluating the above integral (eqn. IV.2), is presented. Ho and Cho's optimum distribution is considered for this illustration. This distribution is itself obtained by evaluating eqn. 2.60 (Chapter 2) through Newton-Raphson's iterative method (Appendix-II).

COMPUTER PROGRAM

```

// JOB T
// FOR
* ONE WORD INTEGERS
* EXTENDED PRECISION
* LIST SOURCE PROGRAM
  SUBROUTINE SIMSE(A,B,F,NI,N,EPS,XINT)
    N=NI
    AB=B-A
    K=1
    H=AB/N
    XINTS=1.E38
    END=F(A)+F(B)
    ODD=0.
    IF(N-4)3,1,1
1  NA=N-2
   DO 2 I=2,NA,2
     XI=A+H*I
2  ODD=ODD+F(XI)
3  EVEN=0.
   NA=N-1
   DO 4 I=1,NA,2
     XI=A+H*I
4  EVEN=EVEN+F(XI)
   XINT=.3333333333*H*(END+4.0*EVEN+ODD+ODD)
   GO TO (6,5).K
5  IF(ABS(XINT-XINTS)-EPS*ABS(XINT))8,8,7
6  K=2
7  ODD=EVEN+ODD
   XINTS=XINT
   N=N+N
   H=AB/N
   GO TO 3
8  XINT=(16.*XINT-XINTS)/15.
   RETURN
   END
// DUP      WS UA SIMSE
*STORE

```

```

// FOR
* EXTENDED PRECISION
* LIST SOURCE PROGRAM
* ONE WORD INTEGERS

```



```

SUBROUTINE SIMSA(A,B,F,NI,N,EPS,XINT)
  N=NI
  AB=B-A
  K=1
  H=AB/N
  XINTS=1.E+38
  END=F(A)+F(B)
  ODD=0.
  IF(N=4) 3,1,1
1  NA=N-2
  DO 2 I=2,NA,2
  XI=A+H*I
2  ODD=ODD+F(XI)
3  EVEN=0.
  NA=N-1
  DO 4 I=1,NA,2
  XI=A+H*I
4  EVEN=EVEN+F(XI)
  XINT=.3333333333*H*(END+4.0*EVEN+ODD+ODD)
  GO TO (6,5),K
5  IF(ABS(XINT-XINTS)-EPS*ABS(XINT))8,6,7
6  K=2
7  ODD=EVEN+ODD
  XINTS=XINT
  N=N+N
  H=AB/N
  GO TO 3
8  XINT=(16.*XINT-XINTS)/15.
  RETURN
END

```

```

// DUP
*STORE      WS  UA  SIMSA

```

```

// FOR
* EXTENDED PRECISION
* ONE WORD INTEGERS
* LIST SOURCE PROGRAM
  FUNCTION FA(X)
  ENO=1.E+18
  R=1.4E-14
  S=.77
  AL=.004
2  B=1.+1.385*AL
  DIFF=ALOG(B/AL)+S/B-3.1281*X-1.183516
  IF(ABS(DIFF)-.0001) 3,3,1
1  DFDAL=(B+1.385*S*AL)/(AL*B*B)
  DAL=DIFF/DFDAL
  AL=AL+DAL
  GO TO 2
3  FZ=AL
  FA=(FZ/R)**(1./S)
  FA=FA/ENO
  FA=FA**1.25
  RETURN
END

```

```

// DUP
*STORE      WS  UA  FA

```

```

// FOR
* EXTENDED PRECISION
* ONE WORD INTEGERS
* LIST SOURCE PROGRAM
  FUNCTION RA(X)
    ENO=1.E+16
    R=1.4E-14
    S=.77
    AL=.004
  2 B=1.+1.385*AL
    DIFF=ALOG(B/AL)+S/B-3.1281*X-1.183516
    IF(ABS(DIFF)-.0001) 3,3,1
  1 DFDAL=- (B+1.385*S*AL)/(AL*B*B)
    DAL=- DIFF/DFDAL
    AL=AL+DAL
    GO TO 2
  3 FZ=AL
    RA=(FZ/R)**(1./S)
    RA=RA/ENO
    RETURN
  END

// DUP      WS UA RA
*STORE

```

```

// FOR
* ONE WORD INTEGERS
* EXTENDED PRECISION
* LIST SOURCE PROGRAM
  FUNCTION FAA(X)
    EXTERNAL FA
    CALL SIMSA(X,1.,FA,20,N,.0001,XINT)
    FAA=XINT/RA(X)
    RETURN
  END

// DUP      WS UA FAA
*STORE

```

```

// FOR
* ONE WORD INTEGERS
* EXTENDED PRECISION
* LIST SOURCE PROGRAM
* IOCS(DISK,2501 READER,1403 PRINTER)
  EXTERNAL FAA
  ETA=ALOG(10.)
  CALL SIMSE(0.,1.,FAA,10,N,.0001,XINT)
  TB=XINT+XINT
  WRITE(5,101) TB,ETA
  101 FOR MAT(1X,2F20.5)
  CALL EXIT
  END

// IEQ

```

DESCRIPTION OF THE PROGRAMSubroutine SIMSA and SIMSE

These subroutines are different than the corresponding subroutines used in Appendix-III. In these cases, the function is integrated between the definite limits with defined initial value of the integration interval. The result is then compared with a predefined accuracy. If it is not satisfied, the interval is automatically doubled and the evaluation of the integral is made again. Thus the interval goes on doubling till the desired accuracy is reached. This method is also based on the Simpson's integration formulae. The following computer variables are used.

- A = Lower limit of the integral
- B = Upper limit of the integral
- F = Function to be integrated
- NI = Initial value of the number of intervals
- N = Final value of the number of intervals
- EPS = Degree of accuracy of the integrated results
- XINT = Result of integration

Functions PA(X), RA(X) and FAA(X)

The function RA(X) is the Ho and Cho's impurity distribution function. The function itself is expressed as solution of eqn. 2.60 (Chapter 2) through Newton-Raphson's method. The following computer variables are used.

$$N_0 = ENO$$

$$\frac{N(x)}{N_0} = RA(x)$$

$$\alpha = AL$$

$$\alpha x = DAL$$

$$\frac{\partial f}{\partial \alpha} = DFDAL$$

The function $FA(x)$ equals $RA(x)^{1.25}$ i.e.

$$FA(x) = N(x)^{1.25}$$

The function $FAA(x)$ is defined as follows.

.. (IV.3)

$$FAA(x) = \frac{\int_x^1 FA(x) dx}{RA(x)}$$

.. (IV.4)

The integration of $FA(x)$ is performed through SIMSA subroutines.

Main Program

The main program evaluates the transit time $T_B = t_B/t_{B0}$ by evaluating the integral of $FAA(x)$ between the limits 0 and 1. The values of T_B are printed.

The program given in this appendix can be used for any distribution function $N(x)$ and any relation for doping dependent diffusion coefficient, provided suitable changes are made in the functions $RA(x)$ and $FA(x)$.

+++++

APPENDIX-VEVALUATION OF C-B CAPACITANCE FOR
ARBITRARY IMPURITY DISTRIBUTION IN THE BASE

In this appendix, a brief introduction to the method of solving Poisson's equation for any arbitrary base impurity distribution function $N(x)$ is given. Such a solution leads to an exact information about the depletion layer properties of graded junctions. For the purpose of illustration, donor diffusion into a p-type semiconductor is considered and an exponential distribution is assumed. When reverse bias is applied at the junction, the following assumptions can be made.

- a. Ionisation of donors and acceptors is complete.
- b. The depletion region is completely free of mobile carriers.

The net charge density ρ within the depletion region can be written as

$$\rho = q(N(x) - N_B) \quad \dots (V.1)$$

where N_B is the background concentration.

Using eqn. V.1, Poisson's equation can be written as

$$\frac{dE}{dx} = \frac{q N_0}{k T_0} \left(\frac{N(x)}{N_0} - \frac{N_B}{N_0} \right) \quad \dots (V.2)$$

where N_0 is the surface concentration of the impurities.

The junction depth x_j is defined by

$$N(x) - N_B = 0$$

.. (V.3)

Integrating Poisson's eqn. V.2, the electric field on the two sides of the junction can be determined. If W is the electrical base width, then

$$x_j = W + a_1$$

.. (V.4)

where a_1 is the depletion layer width on the left side of the junction.

The electric field on the left side is

$$E_1 = \frac{q}{k \epsilon_0} \int_W^{W+a_1} N(x) dx + E \text{ (at } x = W) \quad \dots (V.5)$$

If a_2 is the depletion layer width on the R.H.S. of the junction, the electric field on the right is

$$E_2 = - \frac{q}{k \epsilon_0} \int_{W+a_1}^{W+a_1+a_2} N(x) dx \quad \dots (V.6)$$

In eqn. V.5, the field at $x = W$ is the result of graded impurity distribution. The expression is

$$E \text{ (at } x = W) = - \frac{KT}{q} \frac{d}{dx} (\ln N) \quad \dots (V.7)$$

But the field should be continuous at the junction x_j i.e.

$$E_1 = E_2 \quad \dots (V.8)$$

Equating eqns. V.5 and V.6, the following expression is obtained

$$\frac{q W N_0}{k \epsilon_0} \left(1 + \frac{a_1 + a_2}{W} \right) \int_0^1 N(X) dx + E \text{ (at } X = 1) = 0$$

.. (V.9)

where $X = x/W$.

Let us define

$$A = 1 + \frac{a_1 + a_2}{W}$$

Then the above equation can be written in the following functional form

$$f(A) = 0$$

.. (V.10)

This can be solved by applying Newton-Raphson's iterative method. A can be obtained from the relation

$$A = A - \frac{f(A)}{f'(A)}$$

.. (V.11)

where $f'(A) = \frac{q W N_0}{k \epsilon_0} N(A)/N_0$ (from eqn. V.9)

.. (V.12)

The voltage drops on the two sides of the junction are obtained by a second analytical integration of the Poisson's equation.

$$V_1 = - \int_0^{W+a_1} E_1(x) dx$$

.. (V.13)

$$V_2 = - \int_{W+a_1}^{W+a_1+a_2} E_2(x) dx$$

.. (V.14)

The total voltage at the junction can be obtained as

$$V_B = N_0 w^2 \frac{q}{k T_0} \left[\int_1^A x \frac{N(x)}{N_0} dx - \left(1 + \frac{a_1}{w}\right) \int_1^A \frac{N(x)}{N_0} dx \right] - E \text{ (at } x = 1) \quad \dots (V.15)$$

Eqns. V.9 and V.15 are the general relations valid for any arbitrary impurity distribution $N(x)$. The results obtained for the following exponential distribution are given below.

$$\frac{N(x)}{N_0} = e^{-\eta x} = \frac{N_B}{N_0} \quad \dots (V.16)$$

x_j is obtained from eqn. V.3. The following result is achieved.

$$\frac{x_j}{w} = \frac{1}{\eta} \ln \frac{N_0}{N_B} \quad \dots (V.17)$$

Hence a_1/w can be written as

$$\frac{a_1}{w} = \frac{x_j}{w} - 1 \quad \dots (V.18)$$

Eqn. V.9 yields the following non-linear relation

$$\eta \frac{N_B}{N_w} \left(\frac{a_1 + a_2}{w} \right) \cdot e^{-\eta \frac{a_1 + a_2}{w}} - 1 - \frac{KT}{q} \cdot \frac{\eta^2}{w^2} \frac{k T_0}{q N_w} = 0 \quad \dots (V.19)$$

Since a_1/w is known and $N_w = N_0 e^{-\eta}$, a_2/w can be obtained by solving the above equation for specified ratios of N_0/N_B .

The total voltage drop V_B can be obtained from eqn. V.15. The following expression is obtained

$$V_D = \frac{q W^2 n_D}{k \epsilon_0} \left[\frac{N_D}{N_A} \frac{1}{2} \left(\frac{a_1^2 - a_2^2}{W^2} \right) + \frac{1}{\eta^2} \left(1 - e^{-\eta \frac{a_1 + a_2}{W}} \right) - \frac{1}{\eta} \left(\frac{a_1}{W} + \frac{a_2}{W} e^{-\eta \frac{a_1 + a_2}{W}} \right) \right] - \frac{kT}{q} \eta \frac{a_1}{W} \quad \dots (V.20)$$

For given values of N_D , the junction capacitance is calculated from

$$C_c = \frac{k \epsilon_0}{a_1 + a_2} \quad \dots (V.21)$$

The method of evaluating junction capacitance presented here is similar to that of Lawrence and Warner[†].

The generalised relations have been used for different distributions mentioned in Chapter 6 and capacitance is evaluated. A comparison of the values obtained through eqn. V.21 with those obtained by assuming a linearly graded approximation, has shown that a linear grading can be assumed for the calculation of junction capacitance for most of the distributions.

+++++

† H. Lawrence, R.M. Warner, Jr., 'Diffused Junction Depletion Layer Calculations', BSTJ, V. 39, March 1960, pp. 389-403.